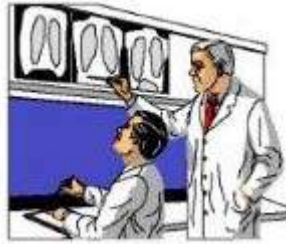


X-RAY FILM READING MADE EASY



WILLIAM F. HOOK, MD

Associate Clinical Professor of Radiology (retired) University of North Dakota School Of Medicine and Health Sciences. Diplomate American Board of Radiology. Diplomate American Board of Nuclear Medicine.

DEDICATION

TO MY SON WILLIAM CHARLES HOOK, MD, FORMER B52 PILOT AND MECHANICAL ENGINEER TURNED PHYSICIAN. *HOPEFULLY THE OLD MAN CAN STILL TEACH THE KID A FEW THINGS.*

ACKNOWLEDGEMENTS

Many thanks to my radiological colleagues Drs. Pablo Ramos, Al Hill, Keith Knepel, Bill Cain, John Doerner, Brad Meyer and Doug Winjum of Medcenter One, Bismarck, for help in picking the cases presented herein as well as for many years of peer review in my own practice. Also to former associates Drs. Norb O'Keefe, Bill Kozel, Lee Podoll, and Gene Kralicek who also contributed cases and similarly provided me with ongoing peer review and many hours of one on one education. All of these physicians are a joy with whom to work.

Also thanks to Drs. Dwight Hertz and Yat-Sun (Sam) Leung for providing photomicrographs of normal and diseased lung, and to my good friend Dr. Don Nelson for assistance in radiologic-pathologic correlation.

I should not be surprised at the skills demonstrated by my son, Paul Hook, computer whiz *extraordinaire*, who saved me many hours of frustration during computer glitches in the preparation of this manuscript. I am grateful!

Not to be excluded are those dedicated teachers of my past including the late Professors of Radiology Drs. Ben Felson, Lee Theros, Stew Imes, and Johan Eriksen as well as current star Mo Reeder. There are many more too numerous to list. You know who you are. *To all of you I give heartfelt gratitude for a lifetime of learning and fun.*

INTRODUCTION

After 30 plus years of teaching the fundamentals of film interpretation to radiology residents, and more recently, family practice residents and medical students, it is with some dismay that I see more and more pressure to provide quickie courses in a matter of days or even hours to nurse practitioners, physician's assistants, and interested others, who then, armed with a few simple rules, disappear.

I hope, (but suspect otherwise) they are not thrown upon an unsuspecting public as fully capable of rendering radiological opinions, but then, I've heard it said, everyone is an expert these days.

Teleradiology, a nearly fully developed reality, will someday ease the pressure from educators, ER physicians, and unavailability of immediate radiological consultation in rural settings. Teleradiology and/or Picture Archiving and Communication Systems (PACS) will also relieve the additional pressures from out patient satellite clinics, administrators and the demand for immediate answers in busy practices. I bemoan the current practice of unread films disappearing from the department because administrators, in an effort to keep service ahead of the competition, cater to the demands of clinicians who insist on a first look at studies, quality control often not included before the patient leaves the department. We have for the most part corrected this problem by having the films hand carried to a diagnostic radiologist before the patient is released. And this is one problem that will disappear with digital radiology and PACS.

I am also sad about some of the ever-changing aspects of the practice of medicine where technology has become a substitute for thinking. Some doctors no longer talk to, but even more important, no longer listen to their patients. Medical imaging studies should be used for confirmations of clinical impressions. Let's not get the x-ray and lab studies and then, if all else fails, do a history and physical! Most patients will tell you what is wrong with them if you will just ask the right questions, and a thorough PE will point you in the right direction. Yet, day after day we receive orders for imaging studies in the high tech modalities for patients who often have not only not been examined properly, but have not even had a simple plain film radiograph!

Oh well, I could expound for hours on what is wrong in medicine and medical education. (I guarantee if I ever become the czar of medical education, the rotating internship will return!) However, there is a lot of "what's right" in medicine too. I have always been of the "see one, do one, teach one" school, and have never felt that knowledge should not be shared with anyone interested, regardless of turf wars or other motives. For that reason we will proceed with this manual which my wife, Linda, an experienced RN, calls "Radiology for Dummies", and insert the disclaimer that the tips herein are not intended as a substitute for expertise.

William F. Hook, MD

Carefree, AZ. December 2000.

TABLE OF CONTENTS

CHAPTER ONE	BASICS	PAGE 1
CHAPTER TWO	CHEST	PAGE 6
CHAPTER THREE	ABDOMEN	PAGE 53
CHAPTER FOUR	SKULL	PAGE 73
CHAPTER FIVE	SPINE	PAGE 90
CHAPTER SIX	PELVIS, HIPS	PAGE 106
CHAPTER SEVEN	ELBOW, WRIST	PAGE 120
CHAPTER EIGHT	ANKLE, FOOT	PAGE 132
INDEX		PAGE 138
REFERENCES		PAGE 145

CHAPTER ONE BASICS

Although everyone understands what one means when it is said to “get an x-ray”, or refers to the image on film as “an x-ray”, the proper term for an image on x-ray film is a radiograph.

There are four densities on a radiograph. They are from black to white: **gas, fat, water** and **mineral**.

Gas, of course, is self-explanatory and includes air in the lungs and upper airway, gas in the intestines, and gas such as nitrogen in so called vacuum spaces. It becomes black on a radiograph because there are few molecules to stop or attenuate the x-ray beam as it passes through the body to darken the film. It won't take the student or practitioner long to recognize normal gas patterns on a radiograph, and as we start to program the computer that we call a brain between his or her ears, the student will begin to use pattern recognition as a means to correct interpretation.

Fat, on the other hand, is just a shade or two lighter than gas, a dark gray, and becomes important in specific locations, as we'll see later. Water density tissue makes up the majority of body parts and includes muscle and organs. Since we've all been made aware that the body is made up of 70+% water, it is no surprise to find it usually comprises most of the volume seen on a radiograph of, for instance, the abdomen in a healthy individual. Although water density tissue varies in its density even on plain film radiographs, it has a uniform appearance when compared to the other three densities of gas, fat and mineral. It is a lighter shade of gray than fat, but not as white as the mineral seen in bone or the really white appearance of metal, such as seen in an ingested foreign body like a coin. Now that you have the basics of the four densities down, let's review them on an actual radiograph. In figure # 1 we have appropriately labeled the four densities on a plain film of the abdomen.

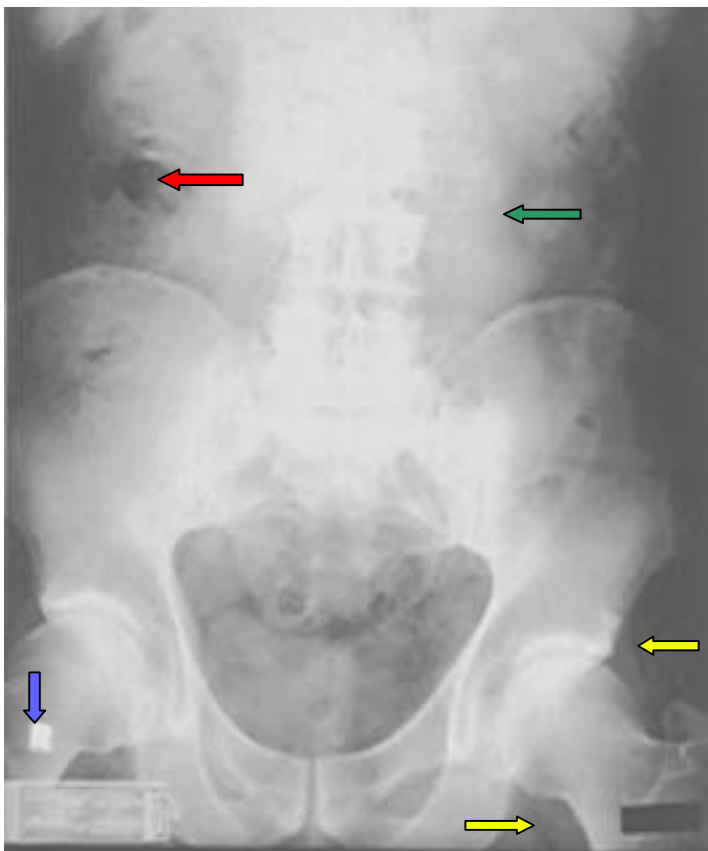


Figure #1(left). The red arrow points to the black density of gas seen in the right side of the colon. The yellow arrows indicate the slightly lighter density (than gas) of fat in the left hip joint capsule. The blue arrow shows the bright density of metal (mineral) in the “R” of the film marker. Mineral density, not quite as bright as the heavy metal marker, is also noted throughout the bones of the skeleton. The green arrow indicates the water density of the left psoas muscle.

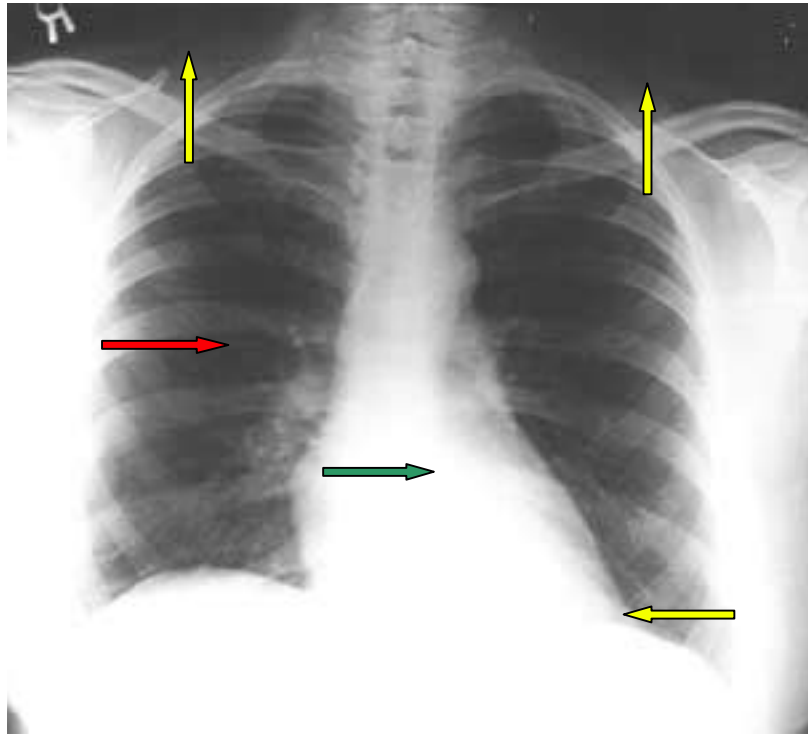
After you have studied the KUB (stands for **K**idneys, **U**reters, and **B**ladder, also called a Scout film of the abdomen) film, go to the next radiograph and identify the four basic densities in the chest. (Figure #2)



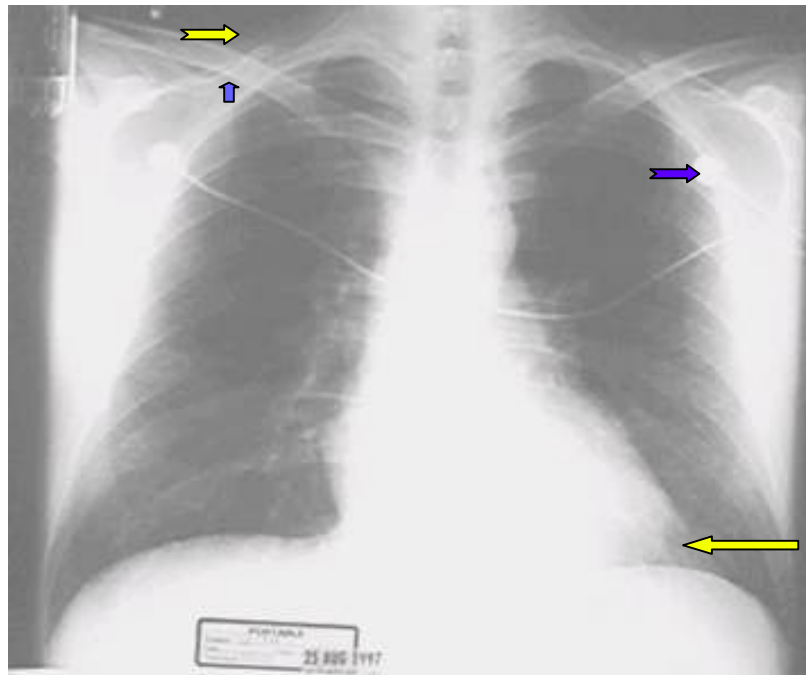
Figure # 2. Can you identify the four basic densities in this chest film? Clue: The tough one to see is fat. Where in the chest would you expect to see it? Check your answers in figures 3 and 3a on page 3.

One of the keys to successful film interpretation, like most diagnostics, is recognizing normals. Helpful aids to gaining experience include the use of standard references that depict variants of normal that one might see on a radiograph. Two of these include:

1. **Atlas of Normal Roentgen Variants that may Simulate Disease, 4th Edit. Theo. E. Keats, MD
Year Book Medical Publishers, Inc.
Chicago, London, Boca Raton.**
2. **Borderlands of the Normal and Early Pathologic in Skeletal Roentgenology, 3rd Edit. Prof. Dr. E.A. Zimmer-Berne, translated by Stefan P. Wilk, MD Los Angeles, Grune & Straton, New York, London.**



Figures # 3(above) & 3a(below). Yellow arrows indicate fat density in the cardiac fat pad and in the supraclavicular fossae. Blue arrowheads show mineral density in the bones of the skeleton and the metal of the EKG leads. The red arrows point to the black density of air (gas) in the lungs and the green arrow indicates the water density of the heart muscle.



It should be recognized that radiological diagnosis is made by the process of triangulation, a method stressed by the radiologic pathology division of the Armed Forces Institute of Pathology. The first part of the triangle is made up of the objective findings, which gives rise to the second side of the triangle, the differential diagnosis. I tell my students that if they learn nothing else during their short stay with us, they should learn to give the radiologist the third side of the triangle, which is history!

Differential diagnosis for groups or single objective findings have been compiled by Drs. Mo Reeder and the late Ben Felson, two of radiology's premier educators, into lists called gamuts. I consider their reference text an essential part of my library, and use it frequently. After awhile use of the gamuts becomes part of daily practice, and part of memory, so that the text needs to be referred to only in unusual cases or to refresh memory. The text is listed below for those interested, and I would advise diagnostic radiology residents to have a copy on hand.

3. Reeder and Felson's Gamuts in Radiology, 3rd edit. M. Reeder, Springer-Verlag 1993, NY, Berlin, Heidelberg, London, Paris, Tokyo, Barcelona, Budapest.

There are other things, which can aid the fledgling interpreter to gain confidence in seeing objective findings on the film. They include:

1. Turn off extraneous light. Lights overhead or empty adjacent lighted view boxes compromise what can be seen on the radiograph.
2. Use a magnifying glass, especially on small parts such as hands and feet. Magnification is also useful to see fine line detail in lungs and in other areas. The technologist can also magnify the film for you, e.g. one frequently used study is the magnified view of the carpal navicular.
3. Have a hot light available to see overexposed areas.
4. Have a darkroom technologist make light copies of overexposed films. Most darkrooms have that capability and it saves the patient another exposure. However never accept a technically unsatisfactory film in the fear of exposing the patient to too much radiation. To put it in perspective, a single view of the chest exposes the patient to about the same amount of radiation he or she would get by flying from Denver to San Francisco in an airliner.
5. Use rulers and calipers until your eye gets used to normal relationships. For example, in the chest, the heart should be about half the size of the width of the rib cage (C-T ratio).
6. It may sound too basic, but always check names and dates on the film. Even experienced radiologists get caught once in awhile comparing films from two different patients, or rendering an opinion on the wrong patient because someone mixed up the films. Later I'll give you some clues on how to be sure you're comparing studies on the same patient even if the labels are wrong. Also be sure the left-right markers are correct.
7. Always compare old vs. new studies when available. It is also helpful to compare left vs. right even in chest, skull and abdomen.

8. Get additional views if you think it might help. After awhile I'll tell you what views to ask for in certain common situations.

9. If a film is overexposed the information is still there. Often it can be recovered by use of the hot light, or a lighter copy can be made in the dark room. If, however, the film is underexposed, the information is lost.

10. Use a system to be sure you have gotten every bit of information necessary from the radiograph to make a reasonable diagnosis. A system is basically a memorized checklist, which I will give you as we proceed. I tell our students that I don't care what system they use or in what order as long as it covers the essentials. Later you will appreciate the value of using a system.

Now with these basics in mind, let us turn to the first topic, one which is the most common, and one in which the second part of the diagnostic triangle, i.e. the differential diagnosis, is almost endless without appropriate history... the chest.

CHAPTER TWO

CHEST

A system that is useful for interpretation of chest radiographs includes evaluation of the lungs, heart, mediastinum, diaphragm and bony thorax. S. K. Imes, MD, a solid teacher and a product of the University of Colorado originally taught this system to me. To that system I would add 1) the corners of the film and 2) a check of the labels. I also routinely check the medial ends of the clavicles when there are prior studies to compare. This is done not particularly to look for pathology, although occasionally abnormalities are seen, but because the clavicles are the "fingerprints" of the chest radiograph. I can't tell you how many times I've caught another person's chest film in the wrong envelope by comparing the clavicles. Keep in mind my additions to the checklist, but memorize in some order the basic system, which is:

1. LUNGS
2. HEART
3. MEDIASTINUM
4. DIAPHRAGM
5. BONY THORAX

Now let's talk for a minute about abnormal patterns in the lungs. You will often get radiology reports describing different types of infiltrates in the lungs. The commonest are interstitial and alveolar. The difference can best be appreciated by looking at a photomicrograph of normal vs. diseased lung. Presented below is a section of normal lung as seen under the microscope. (Figure #4).

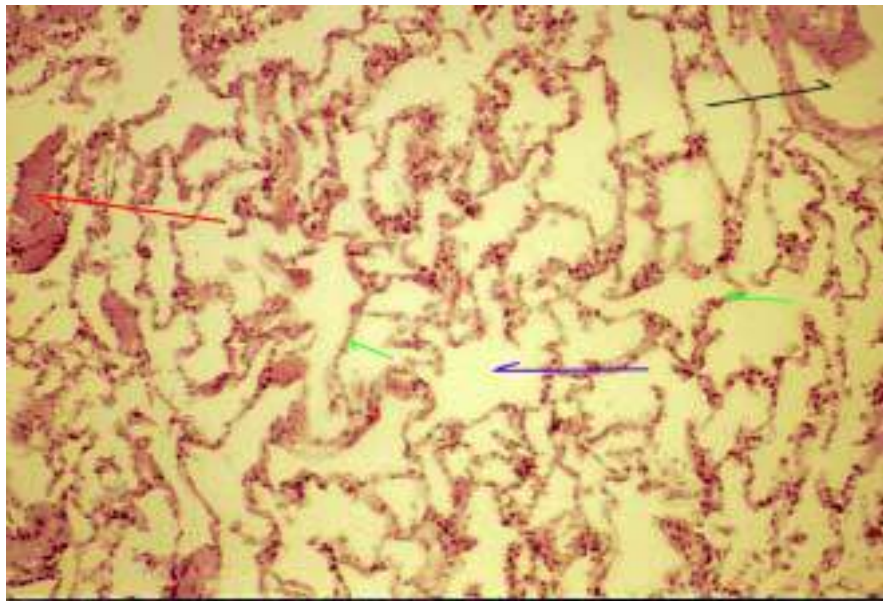


Figure #4. Photomicrograph of a section of normal lung. Red arrow points to a small area of fibrosis in this "normal lung" section. Green arrows show the alveolar walls and the blue arrow points to an alveolus. The black arrow indicates an artery. A bronchiole is not seen in this particular section, but the alveolar walls, the vascular walls and the walls of bronchi and bronchioles constitute the interstices of the lungs which when invaded by inflammatory cells results in (you guessed it!) interstitial infiltrate. Courtesy of MedCenter One, Bismarck, N.Dak., Dept. of Pathology.

For radiologic-pathologic correlation a PA (posterior-anterior) view of a normal chest is presented in Figure # 4a below.

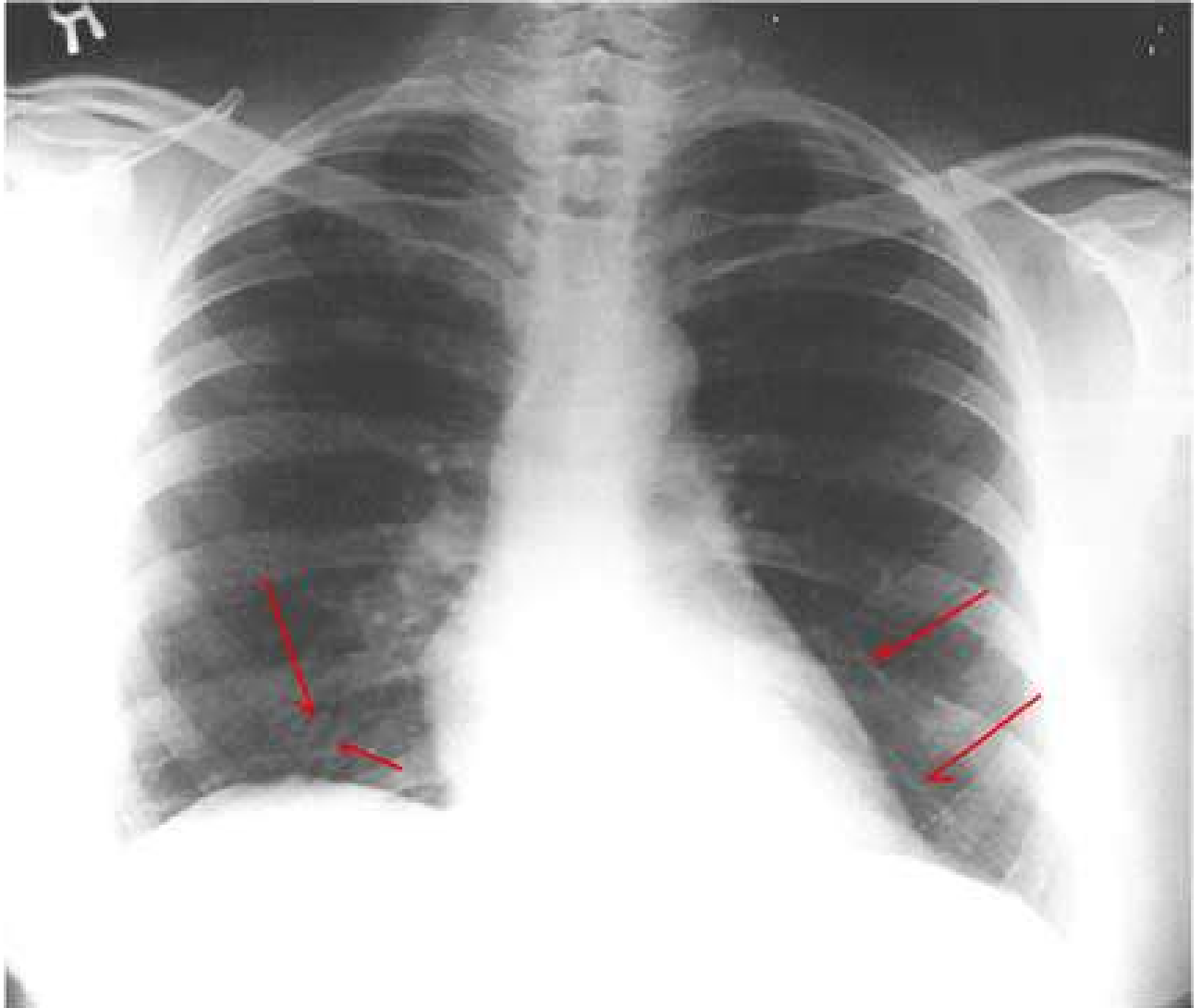


Figure # 4a. Normal chest. Note the appearance of the bronchovascular markings (red arrows) just above (cephalad) of the hemidiaphragms. Compare to other abnormal cases presented later in the text. The markings are called bronchovascular because small pulmonary arteries, veins and bronchioles travel together throughout the lungs and cannot be separated grossly in the radiograph unless there is disease present. See text for explanation of silhouetting.

In the photomicrograph above (figure # 4, page6) you will note the normal relationship of the small bronchioles to the tissue that separates them from the alveolar cells, adjacent vessels etc. This tissue is the interstices of the lungs, and if inflammatory cells such as neutrophils and phagocytes invade it, we see the gross result as interstitial infiltrate, as demonstrated in the photomicrograph below (figure #5).

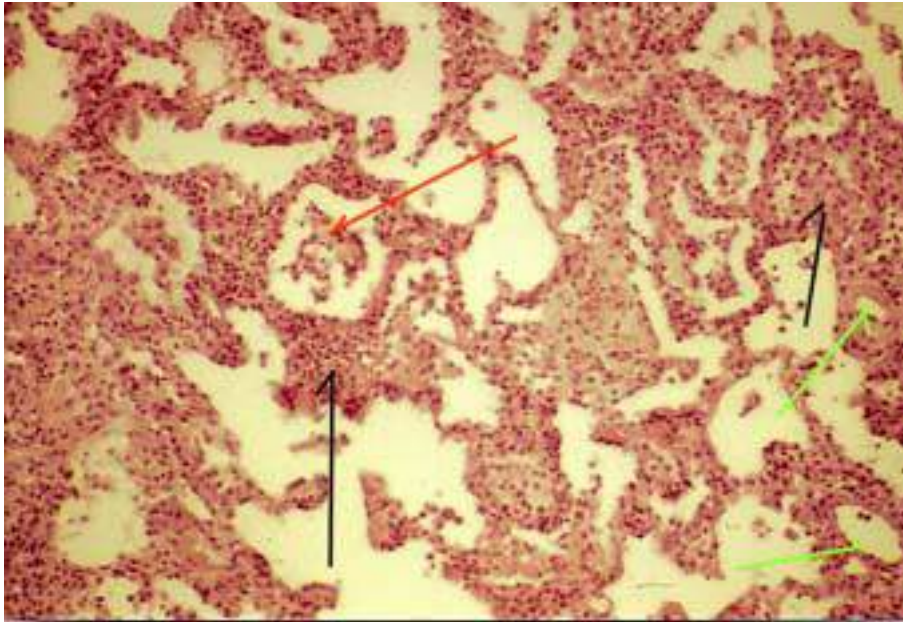


Figure # 5. Photomicrograph of a section of lung in a patient with acute interstitial pneumonia. Red arrow shows beginning alveolar filling as well, which is what happens as the inflammation progresses. The black arrows show the invasion of the interstices by inflammatory cells. The green arrows point to small arteries. Courtesy of MedCenter One, Bismarck, N.Dak., Dept. of Pathology

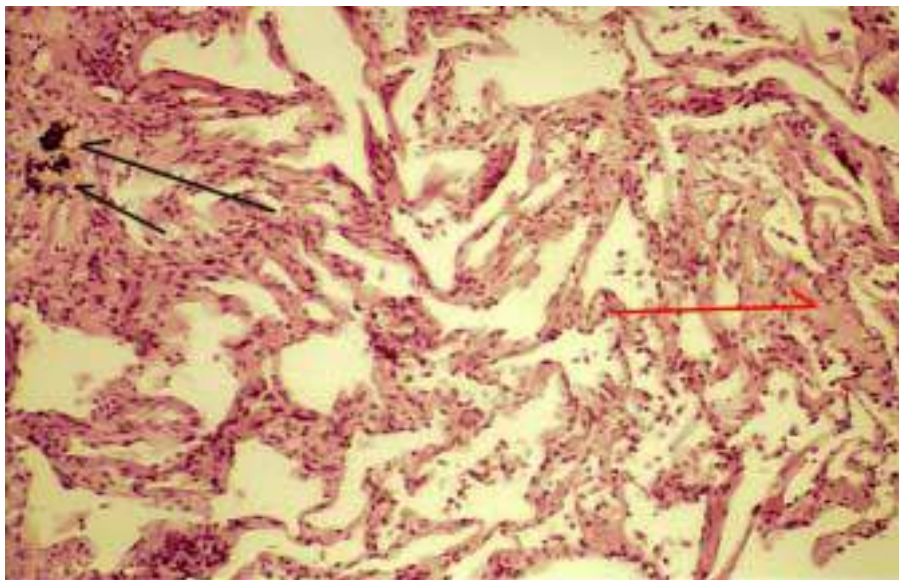


Figure # 5a

Photomicrograph of a patient with chronic or usual interstitial pneumonia. Note the increased amount of fibrosis (red arrow). The black arrows point to deposits of anthracosis. One would not be able to tell the difference from the acute phase on a chest radiograph until comparison films showed the process to have not changed significantly over a period of time. *Courtesy of MedCenter One, Bismarck, N.Dak., Dept. of Pathology.*

Interstitial infiltrate can be recognized in the chest radiograph by the phenomenon of silhouetting, which is basically a rule that states:

Any two water density structures that touch each other will obliterate the border between them.

This rule gives the diagnostic radiologist a tremendous advantage in several areas as we will see later, but in the case of interstitial infiltrate it allows us to recognize it for what it is by the following observations:

1 -The bronchovascular markings lose their borders and become fuzzy.

2-The air in a bronchus stands out as an "air bronchogram" because the water density inflammatory cells in the interstices of the lung silhouette out the wall of the bronchus.

Note the result in the chest radiographs of patients with typical interstitial pneumonia. In both cases below there are also some alveolar filling. The bright dots over the left side of the chest represent Bb's or buckshot in the soft tissues. The second case (Fig. 6a) shows An air bronchogram that is typical for pediatric (in this case- adolescent) pneumonia and the student should look for the phenomenon in all sick children.

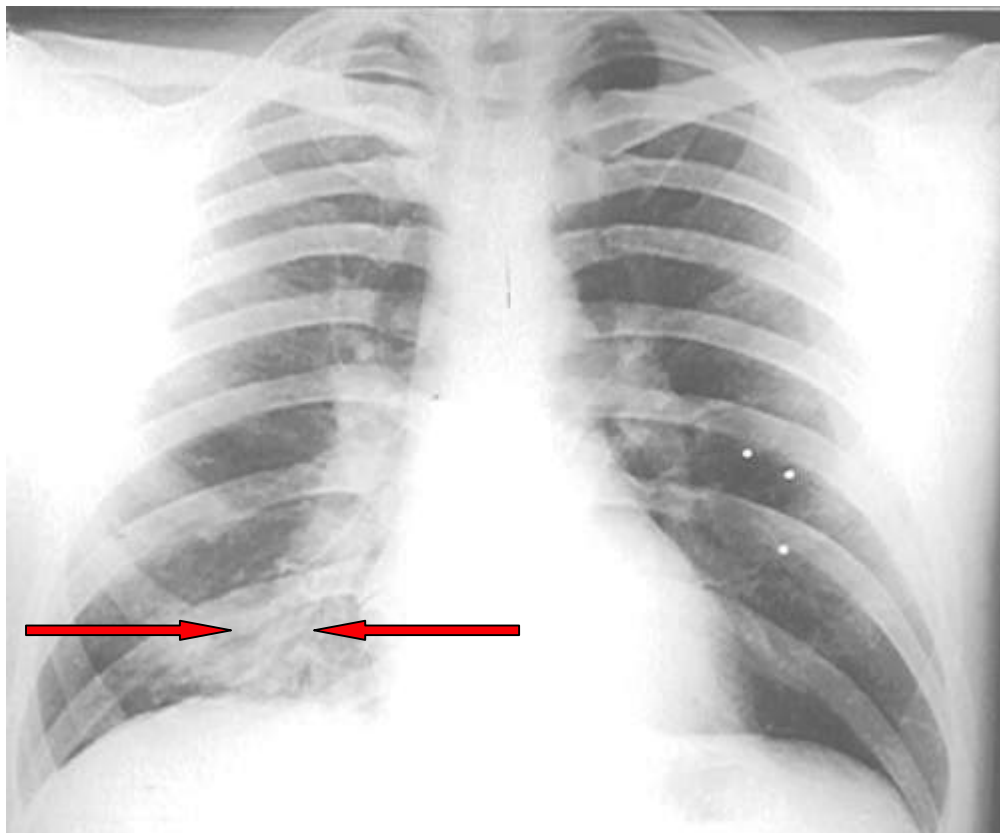


Figure # 6. The red arrows point to typical air bronchograms in a patient with a segmental pneumonia. Note there is no silhouetting of the right heart border, indicating the infiltrate is in one of the posterior segments of the right lung base.

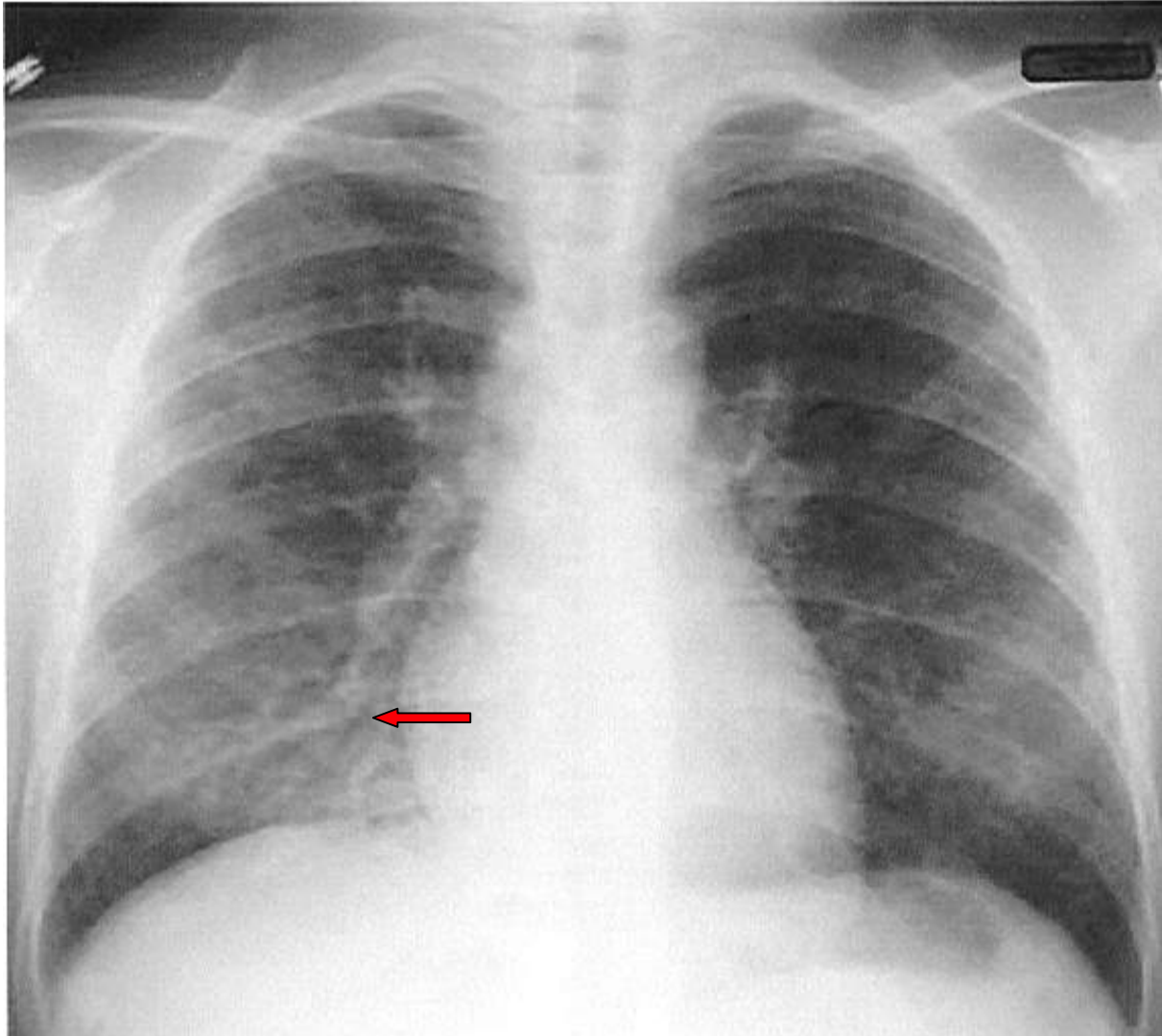


Figure # 6a. Another patient, this time an adolescent with pneumonia. Note the obvious combined interstitial and alveolar filling infiltrates, as well as an air bronchogram (red arrow).

A note of caution: If a shallow inspiration radiograph is presented for interpretation the bronchovascular markings might not be separated enough to distinguish a real interstitial infiltrate from silhouetting due to failure to get enough air between them. Also an underpenetrated film may cause you problems. Sometimes it takes a magnifying glass to be sure of the findings, especially in kids, obese patients or women with large breasts. I tell our students that if they can follow a bronchovascular marking out to its termination, then there is no silhouetting and thus no interstitial infiltrate.

Now, if the inflammatory infiltrates in the interstices progress and begin to fill in or “spill over” into the alveolar spaces, the result is an alveolar-filling infiltrate. This reaction results in a whiteout of the alveolar air spaces and is called by radiologists "alveolar filling infiltrate" or "air-space disease". In the example in figure # 7 below is a patient with this phenomenon.

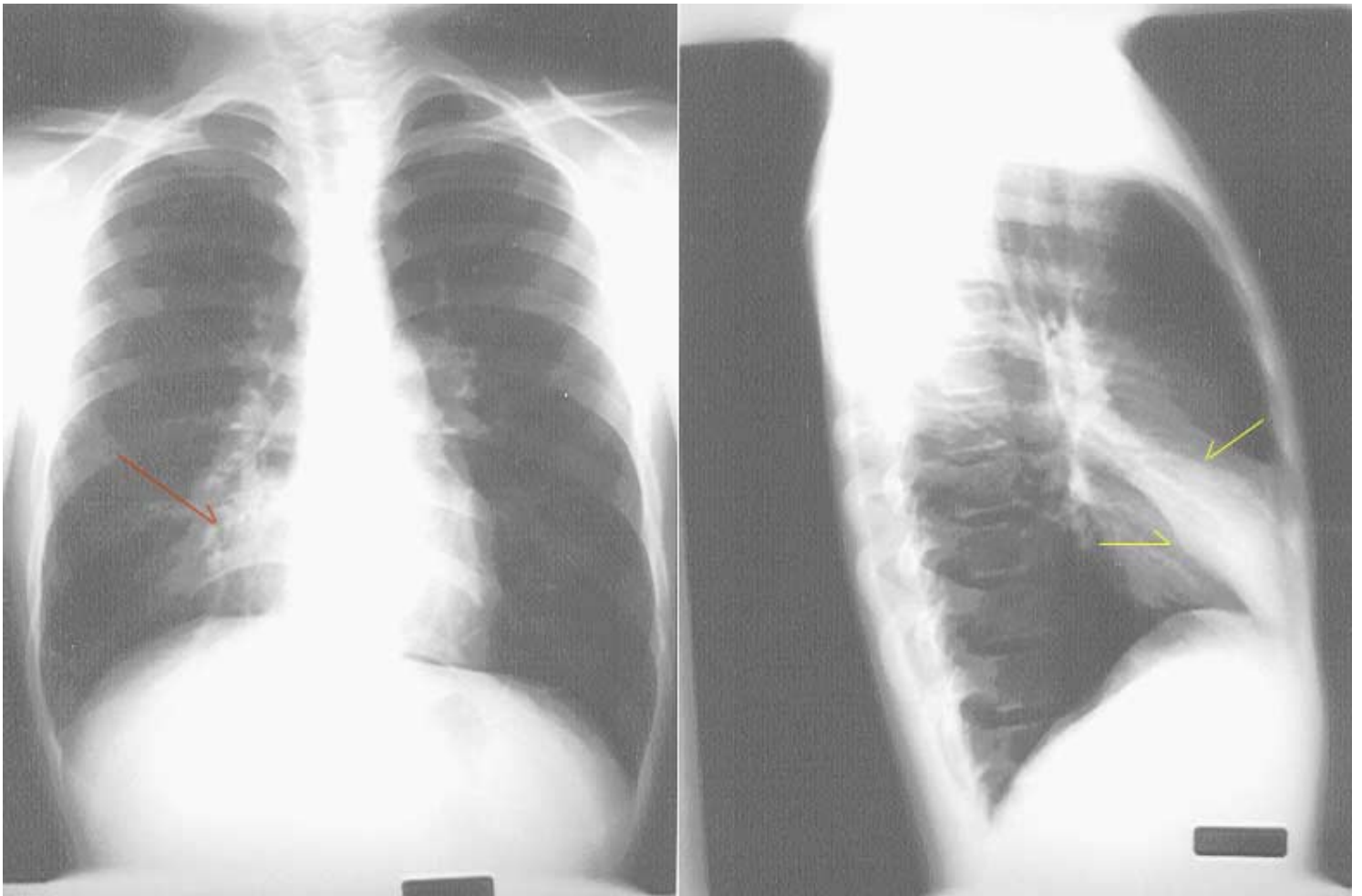
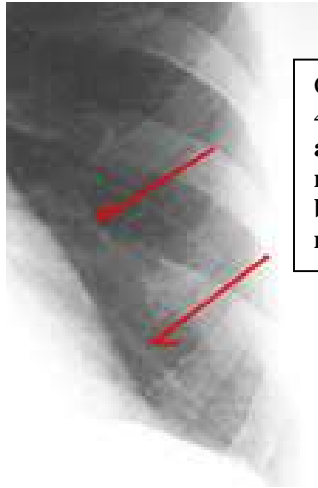


Figure # 7. A patient with alveolar filling infiltrate in the right middle lobe. Note the positive silhouette sign obliterating the right heart border in the PA (posterior-anterior) projection (red arrow). The yellow arrows indicate the whiteout of alveolar air spaces resulting in a solid band of consolidation in this patient who likely has some associated atelectasis of the right middle lobe as well.

There are other patterns seen in the lungs in a chest radiograph that effect the air spaces or the interstices or both, but the recognition of these still requires your evaluation of the bronchovascular markings and air spaces. Some of these patterns include disseminated small irregular shadows and are termed reticular, reticulonodular, linear, or ill defined. There are also patterns such as the honeycomb lung (interstitial fibrosis), miliary nodules, nodules (single or multiple), cavitations, interstitial edema, Kerley's lines, masses, hyper lucencies, atelectasis, pneumothorax, etc., which will all fall into place as you gain experience.

The important thing, though, is to be consistent in looking for and recognizing abnormalities, and that requires evaluations of the markings and air spaces. In figure #8 on the next page is an example of a

patient with a reticulonodular pattern. This one happens to have silicosis (occupation: sandblaster), but it could just as easily represent any other pneumoconiosis, sarcoidosis, idiopathic interstitial pulmonary fibrosis (Hamman-Rich), bronchiectasis, or even histiocytosis x. Note what happens to the bronchovascular markings.



Close up of *figure 4a (left)* **Red arrows show normal bronchovascular markings.**

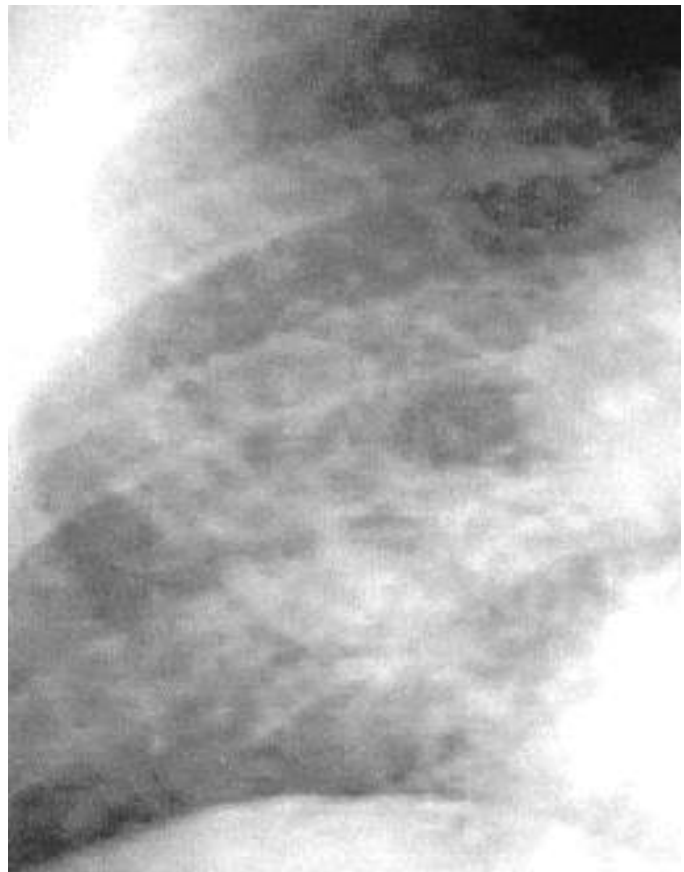


Figure # 8 (right). **Reticulonodular pattern in a patient with silicosis. Compare to the normal chest bronchovascular markings in Figure 4a (above and page 7).**



Figure # 9 (left) **Diffuse miliary pattern in a patient with Boeck's sarcoid.**

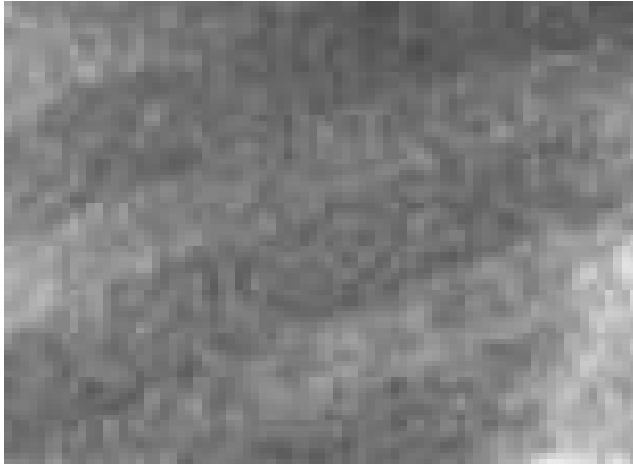


Figure # 9a (left. Magnified view of a miliary pattern in the lung of a patient with miliary tuberculosis. Posterior ribs are seen in the background and a portion of the right heart border is seen in the right lower part of the section. Image courtesy of Radiology Central Resource (Brigham. Harvard Radiology. Edu) via the Internet.

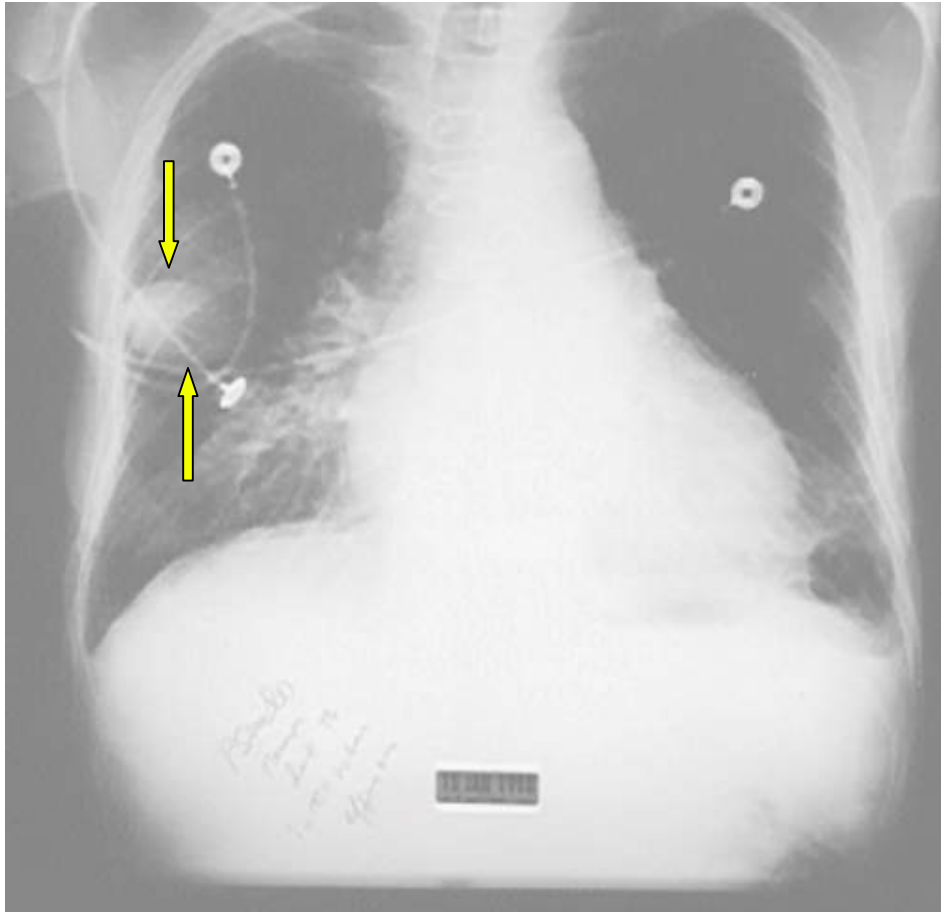
In the case of pulmonary nodules the important things to establish are whether or not the lesion(s) are old or new, and whether or not it (they) contain calcium. The first question is usually easily answered if old studies are available for comparison. The density of the lesion(s) on the radiograph can often answer the second question. If there is still a question after careful analysis, the steps to take include chest fluoroscopy (the simplest and least expensive), plain film tomography, or CT (most expensive).

Sometimes one has to use common sense and a few weeks or month's follow-up may be the procedure of choice vs. interventional biopsy, especially in the case of the elderly. One should also make sure the nodule in question is indeed within the pulmonary parenchyma and not an artifact, skin lesion, nipple shadow or some other red herring.

These kinds of problems are easily solved by the radiologist using fluoroscopy, repeat films with skin or nipple markers or additional views or imaging. The student also needs to have a basic knowledge of chest anatomy such as the bronchopulmonary segments and location of the fissures. For instance the right middle lobe touches the right heart border and the lingular segment of the left upper lobe is in a similar position with the left heart border. Thus silhouetting phenomena such as occurs with pneumonia will obscure these borders, making the location of the pathology easily identified.

Likewise fluid in the major or minor fissures follows a typical pathway. Illustrated below in figures 10, 11, and 11a and 11B are patients with inter lobar effusions.

Figure # 10 (below). **Yellow arrow points to a rounded density in the minor fissure that resembles a mass. Actually it represents an intralobar effusion, and therefore could be called a pseudotumor.**



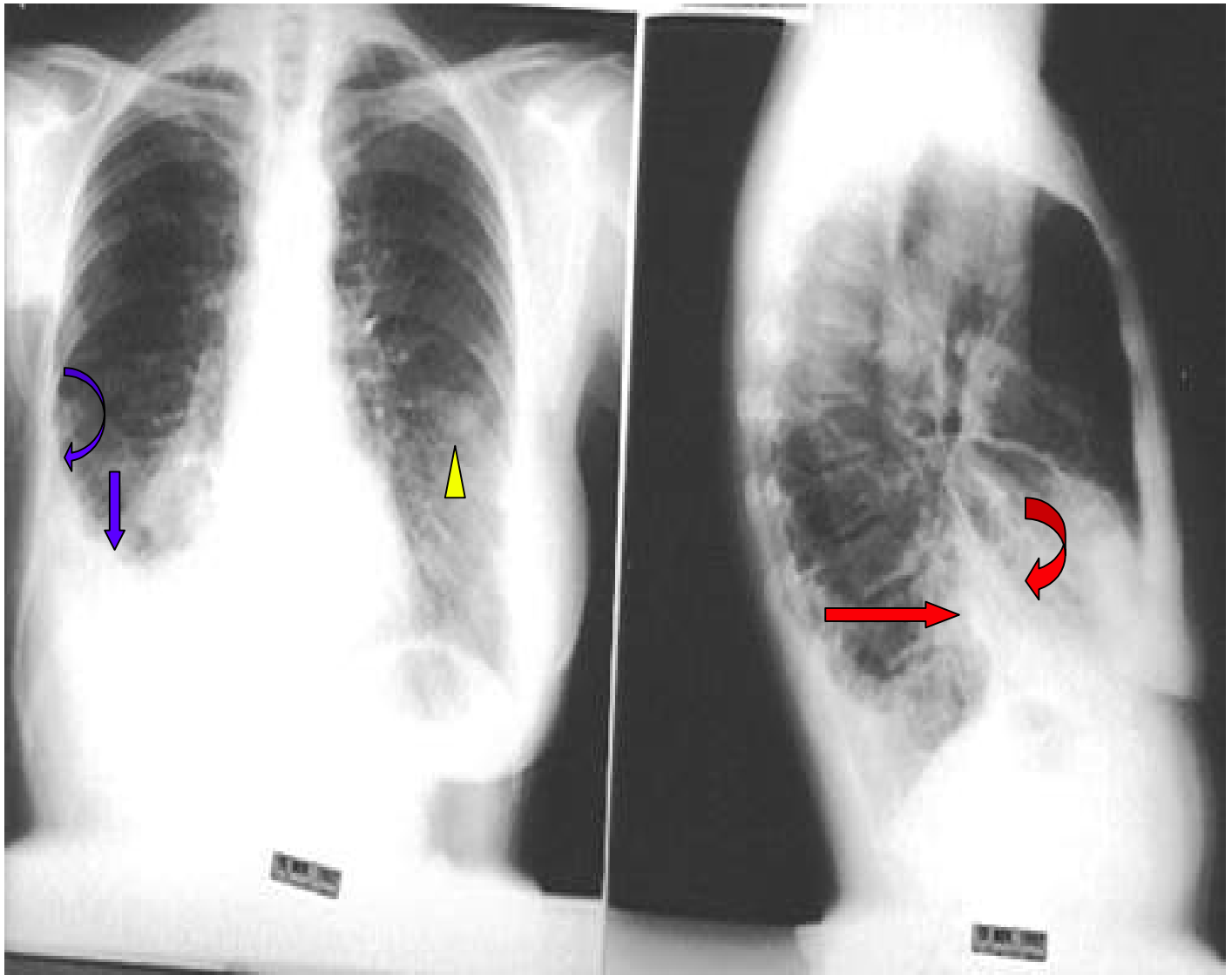
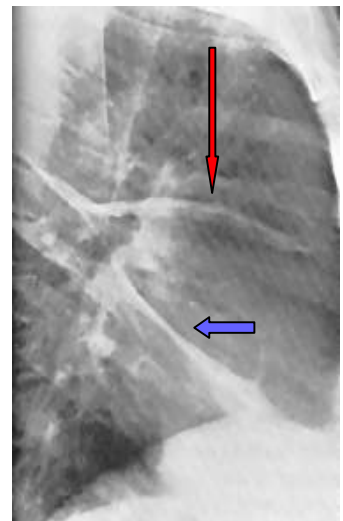


Figure # 11 (above). Blue arrows show a typical meniscus of a right pleural effusion. Note the loss of the normal right hemidiaphragm due to the silhouette sign phenomenon. The red arrows show a band of fluid in the major fissure (interlobar effusion). Note also the absence of the right breast shadow and the metastatic mass in the left mid lung field. (yellow arrowhead).



Figure # 11A (left & right). Red arrows point to fluid in the minor fissure and blue arrow shows fluid in a major fissure.



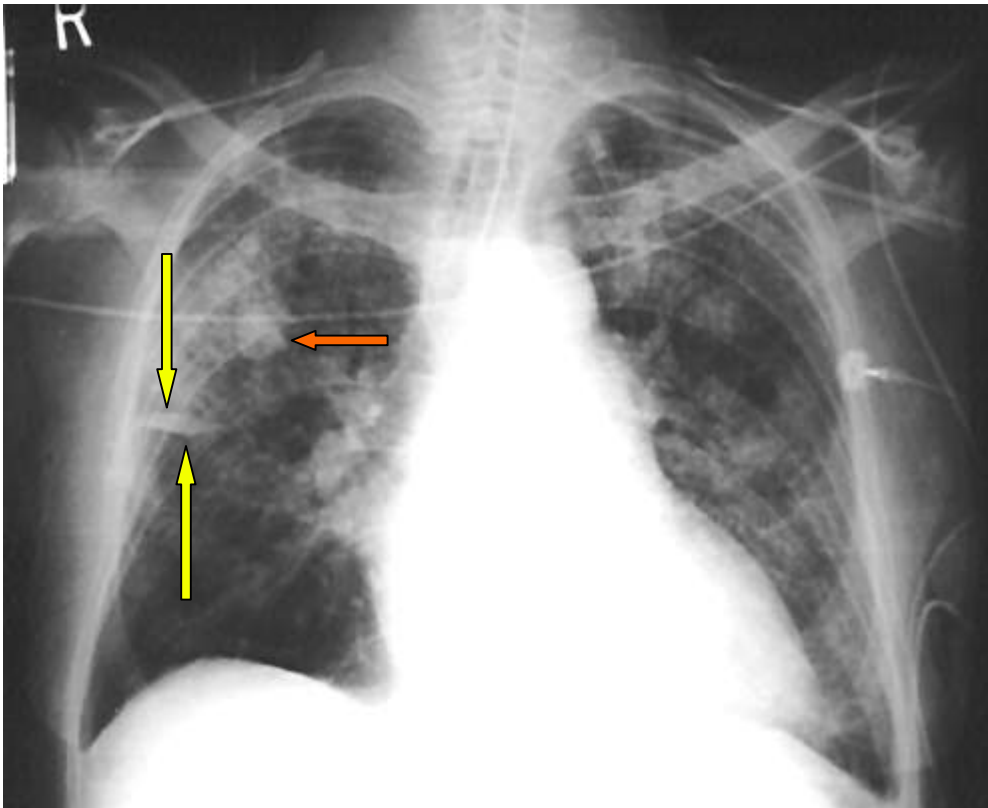


Figure # 11B. Although the patient in figure 11B has metastatic disease (orange arrow) and pneumonia, he also demonstrates a band of fluid in the minor fissure (yellow arrows). The band-like density is more commonly seen in interlobar effusions than the pseudotumor presented in figure 10.

One of the exceptions to the diagnostic triangle of objective findings, differential diagnosis and history is the "Aunt Minnie". I'm not sure who coined the term but it is commonly used by radiologists to refer to a radiograph that conjures up an instant diagnosis. That is, the picture or pattern is instantly recognized for what it is. "It looks like Aunt Minnie therefore it must be Aunt Minnie."

One of the normal "Aunt Minnies" is the aszygous lobe fissure that occurs in a small percentage of the population. Once you see one you will always recognize it for what it is. A patient with an aszygous lobe fissure is presented in figure 12.

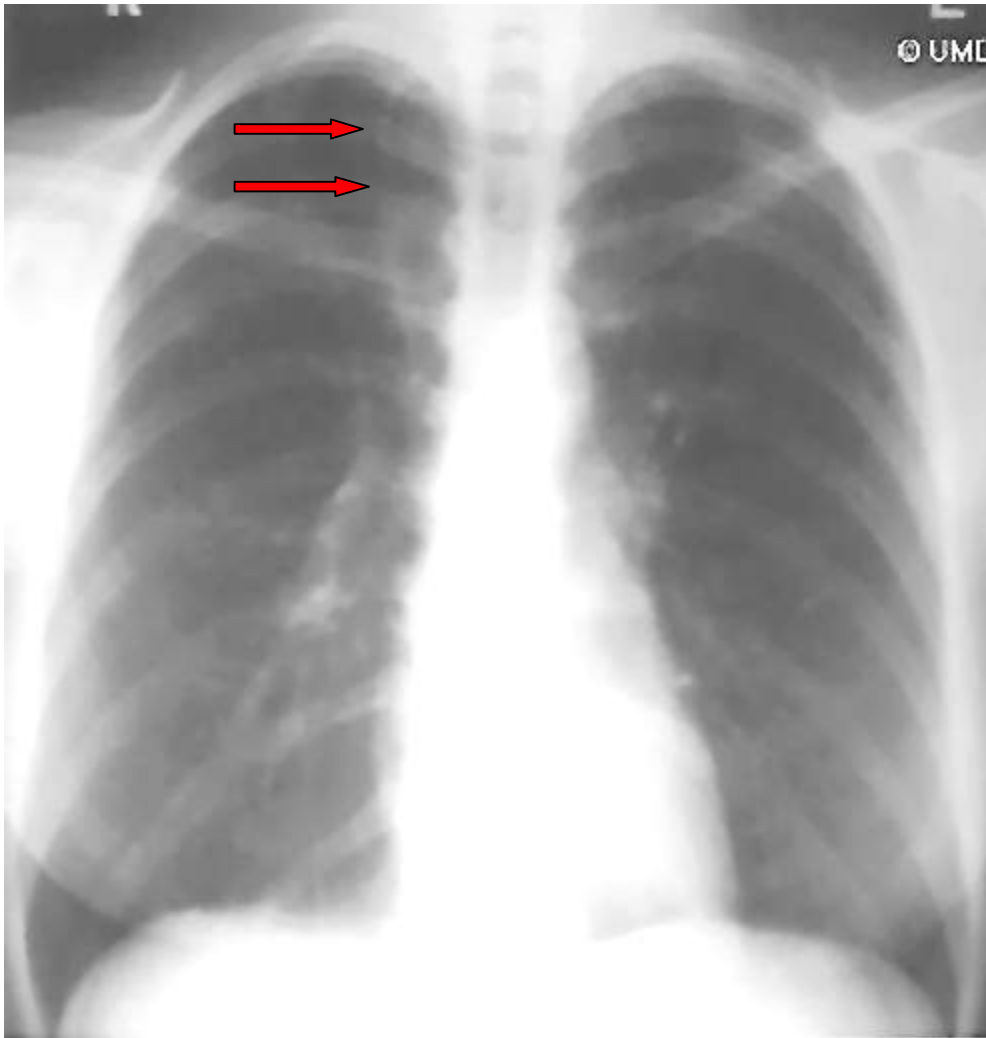


Figure 12. Red arrows point to an azygous lobe fissure in an asymptomatic patient.
*This case courtesy of The Xray Files: Teaching radiology on the Internet. Thanks to Dr. Andrew Downie.
<http://www.radiology.co.uk>. Credit to Scottish Radiological Society. Reprinted with permission.*

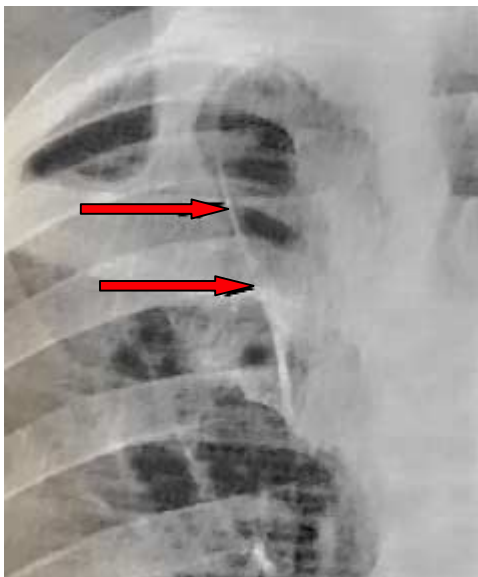


Figure 12A (left). Right apex close-up of another azygous lobe fissure). Red arrows point to an azygous lobe fissure, a classic “Aunt Minnie”.

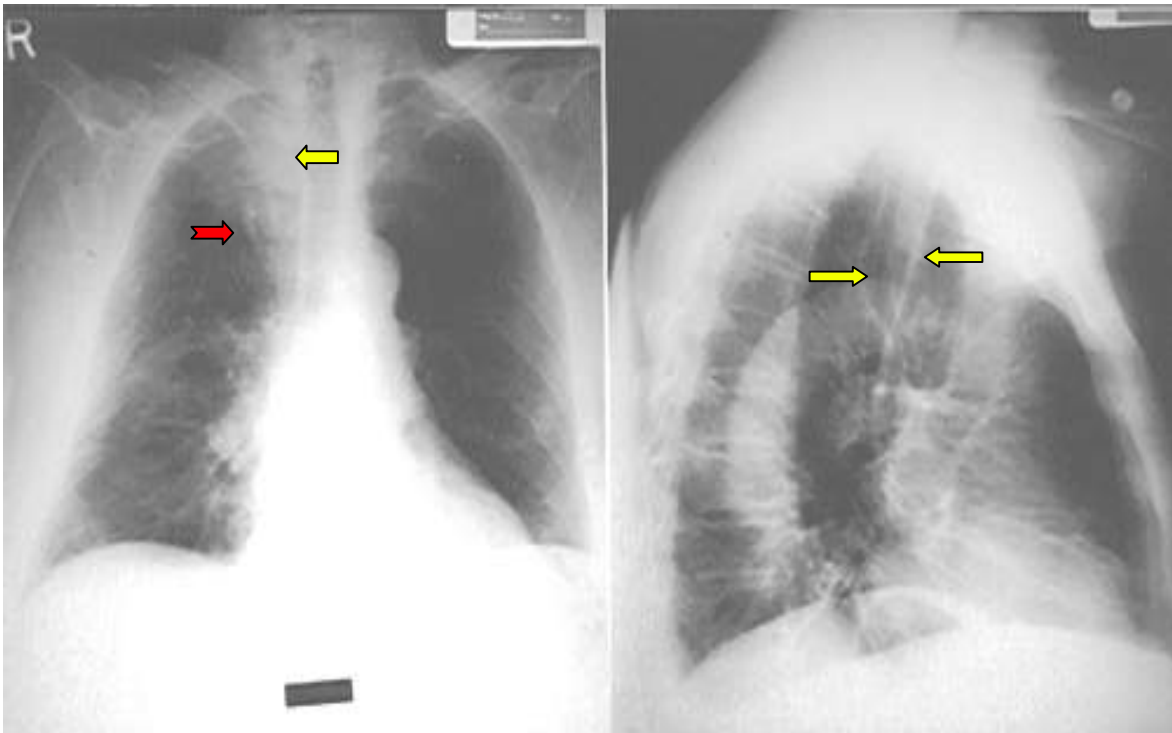


Figure # 12a. Another patient with an azygos lobe fissure (red arrow) who also has pneumonia with consolidation in the azygos lobe (yellow arrows). This is an unusual occurrence and the only case I've seen in over 30 years of practice. *Courtesy of Dr. Norb O'Keefe.*

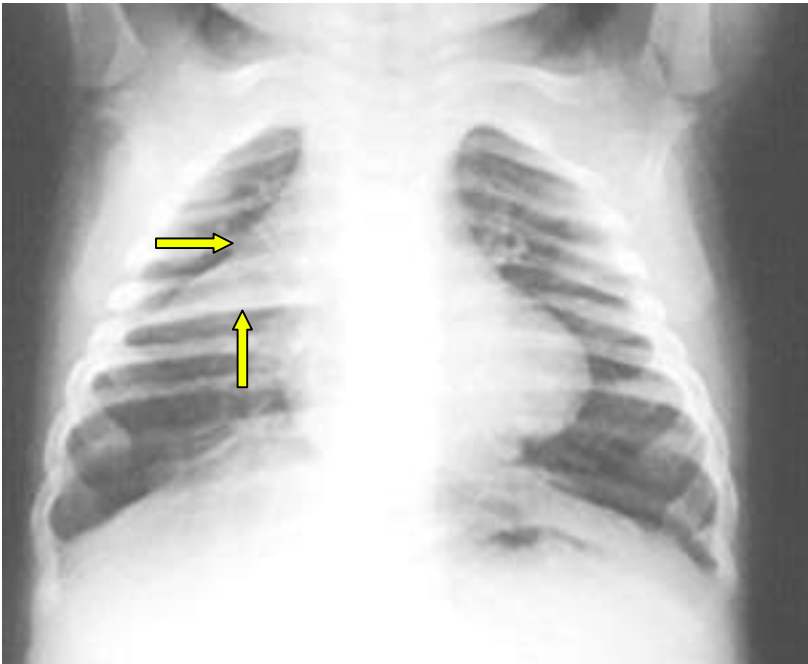


Figure 12b Classic sail sign of a normal thymus is outlined by the yellow arrows. The sail sign is another normal "Aunt Minnie".

“Aunt Minnies” also includes some abnormal. One such case is a chest film showing multiple nodular double densities that at first glance may seem to represent metastatic disease, as in figure 13 below.



Figure # 13. Here's a case with multiple nodular densities and it's also an "Aunt Minnie". Can you spot the abnormalities before referring to the next figure?

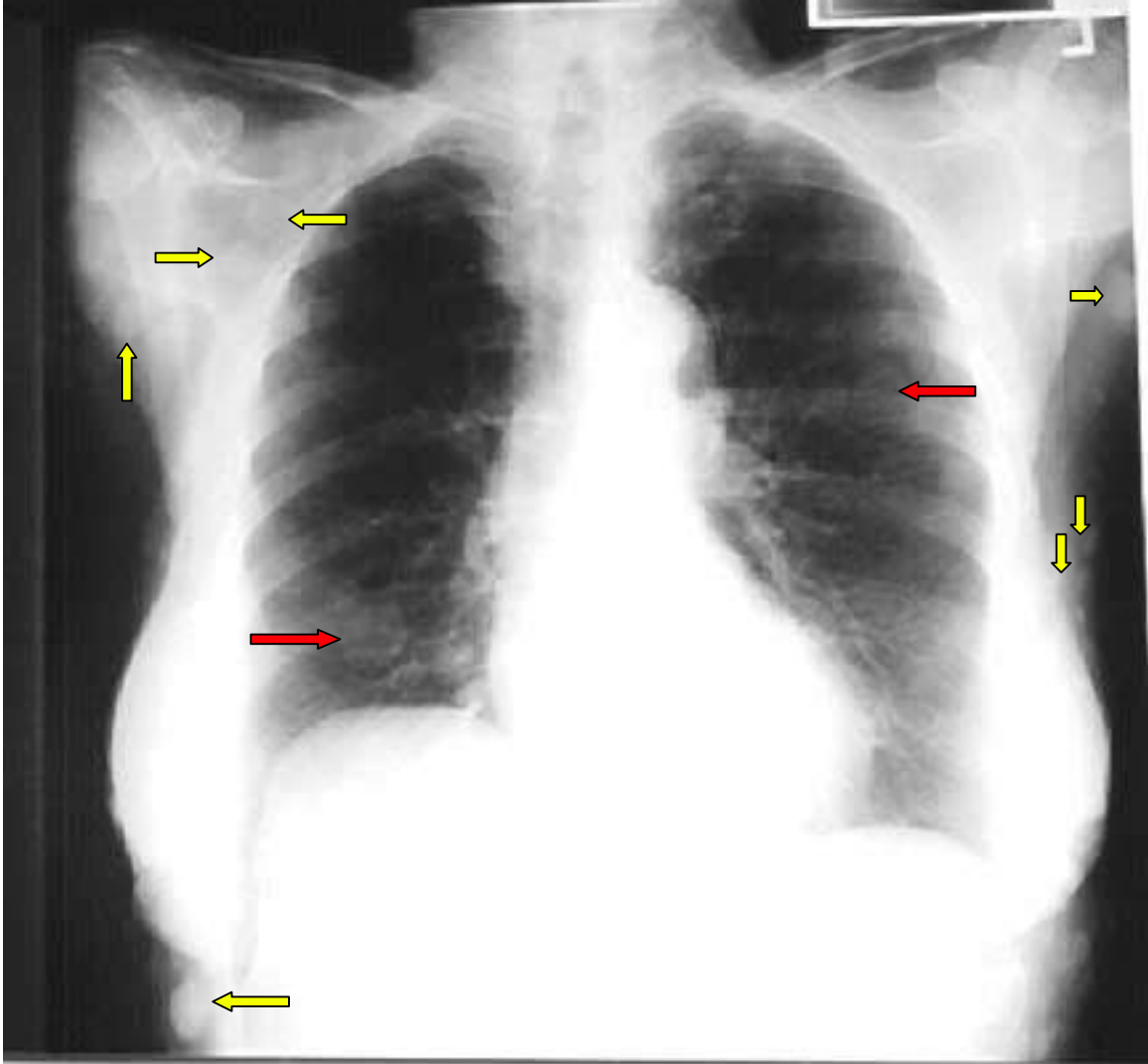


Figure # 13a. Note the multiple nodules as indicated by the arrows. The yellow arrows show the nodules best against the fat density background of subcutaneous fat in the axillae and flank, and the red arrows show them against the background of gas in the lungs. These are multiple neurofibromas in a patient with neurofibromatosis (von Recklinghausen's disease). Not all of the nodules are marked by arrows. The case is a classic "Aunt Minnie".

Chronic obstructive pulmonary disease or COPD is usually recognized on a radiograph by hyperlucency of the lungs, increased A-P diameter of the chest, bullae which contain no bronchovascular markings and flattened diaphragm, the latter being the only consistent finding. Sometimes the clinical diagnostic findings are much worse than can be imagined by studying the films, since the radiographic changes are typically late in the course of the disease. Shown on the following pages are typical patients with moderately severe COPD.

Case courtesy of J. Kevin Smith, MD, Ph.D. U. of Alabama Dept. of Radiology via the Internet. UAB Teaching files.
Reprinted with permission.



Figure #14. Emphysema secondary to serum Alpha 1 antitripsium deficiency. This type of COPD is of the Panacinar type, is relatively rare and classically is more pronounced in the lower lobes or zones of the lungs. Note the hyperinflation of the lower lung fields, and attenuation (loss of or diminished) bronchovascular markings in the lower lung fields.

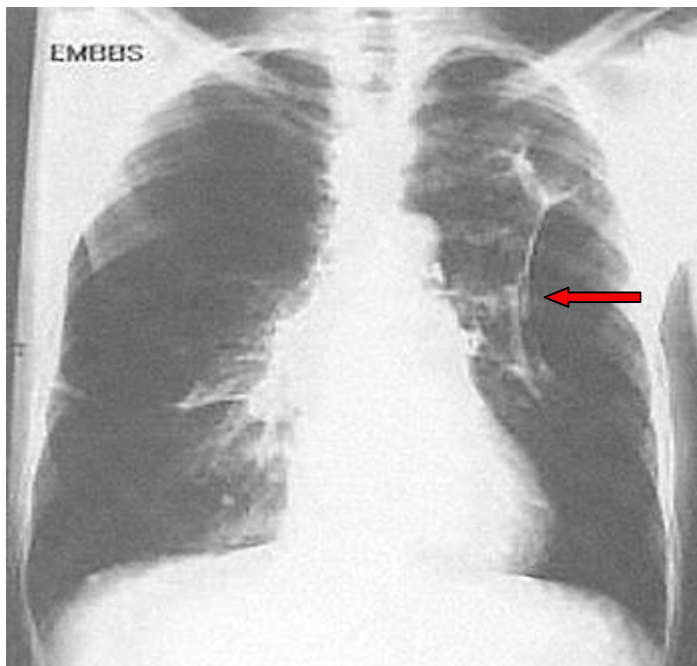


Figure #14a. Red arrow points to the curvilinear medial margin of an emphysematous bleb in this patient with bullous emphysema. If multiple blebs coalesce they represent so-called “vanishing lung”. As they enlarge they also represent a danger of tension pneumothorax should one of them rupture. One of my instructors had that happen while crossing a mountain pass at high altitude, as the trapped air in the bleb expanded. *Figure 14a* courtesy of embbs.com library via the Internet.

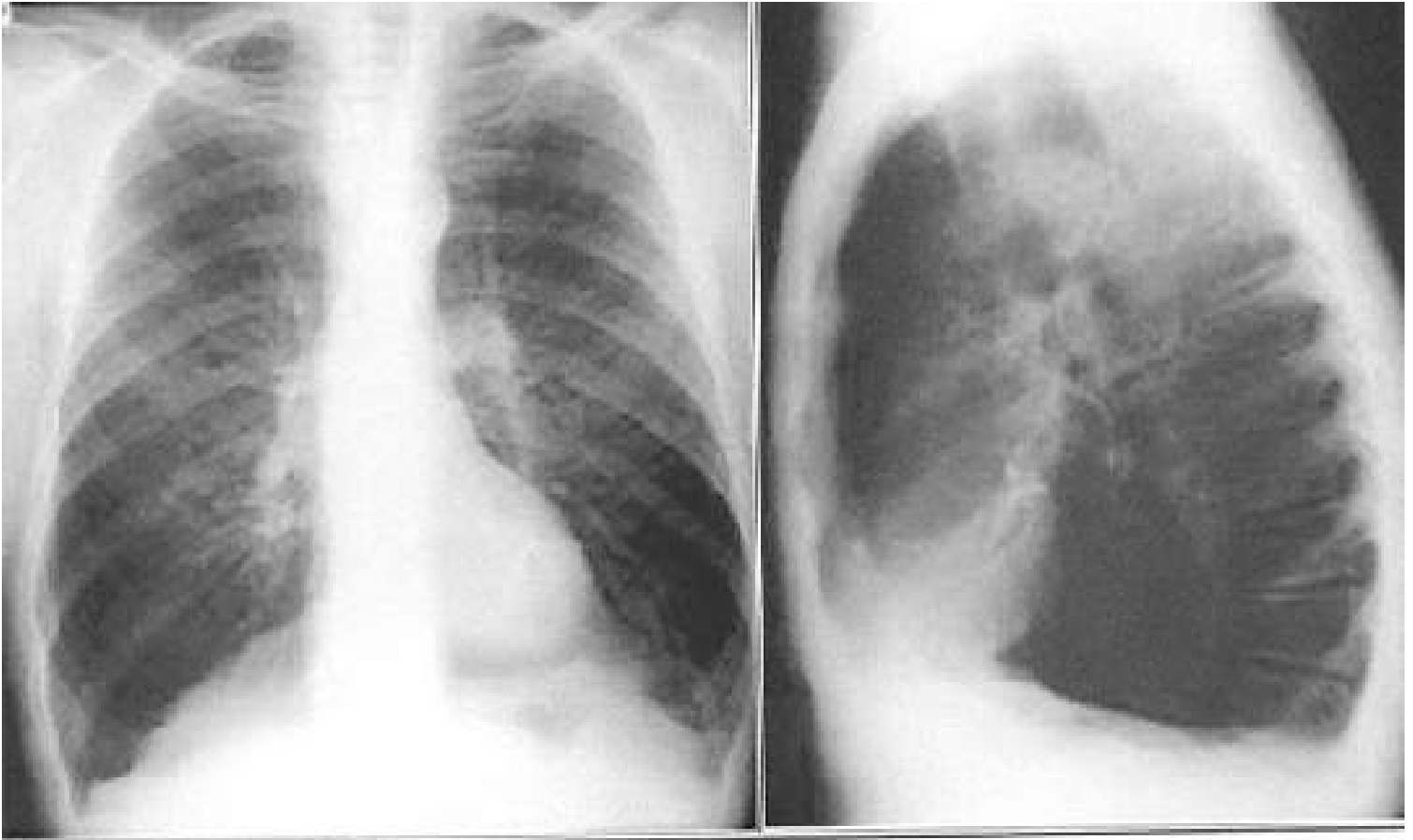


Figure # 14b. Emphysema. Note low, flat hemidiaphragms, upper zone vascular attenuation and over-inflated lungs. Pulmonary arteries are also enlarged, particularly on the left, suggesting pulmonary hypertension. There is also increased A-P diameter of the chest as seen in the lateral view. Images courtesy of Brigham. Harvard Radiology Depts. via the Internet. <http://brighamrad.harvard.edu>.

Obviously there are many more findings we could discuss with regards to the lungs, but the scope of this text is not intended to be comprehensive. Three of the things we should probably mention are common occurrences in emergency rooms and should be recognized by the practitioner. They include obstructive emphysema, pneumothorax and pleural based densities.

If you run into a youngster in the ER who is wheezing and short of breath, it may not represent pneumonia, asthma, or bronchitis. With any of the above there may be a normal chest radiograph or minimally hyperinflated lungs at the most. Recognizable radiographic findings are often delayed by several hours in these cases and we need to keep that in mind. One of the things to look for and be suspicious of is obstructive emphysema, a not uncommon occurrence. Evaluate the chest radiograph on the next page before checking the results in the illustration to follow.



Figure # 15. What do you see? Note that the left hemithorax looks darker than the right, which should be your first observation. The rib spaces are further apart on the left and there may be a mediastinal shift to the right. If there is a mediastinal shift there has to be either 1) atelectasis on one side or 2) excess gas (over inflated lung or possibly tension pneumothorax) on the other. Which is it and how do you prove it?



Figure #15a. The same patient as in figure 15, with the film exposed in expiration. This method exaggerates the findings confirming the mediastinal shift. Note the right hemidiaphragm moves cephalad as you would expect with expiration, but that the left hemidiaphragm is relatively immobile. This confirms the diagnosis of obstructive emphysema. The culprit was a foreign body (peanut) in the left main stem bronchus.

Pneumothorax can be recognized by the absence of lung markings peripherally, recognition of a pleural reflection or edge of a partially collapsed lung, mediastinal shift, and frequently, air-fluid levels or subcutaneous emphysema, i.e. air in the soft tissues.

One of the tricks of the trade to confirm your clinical or radiological suspicion of pneumothorax is to take a film in expiration, which exaggerates the findings. Demonstrated on the following pages in figures 16 & 17 are examples of pneumothorax.

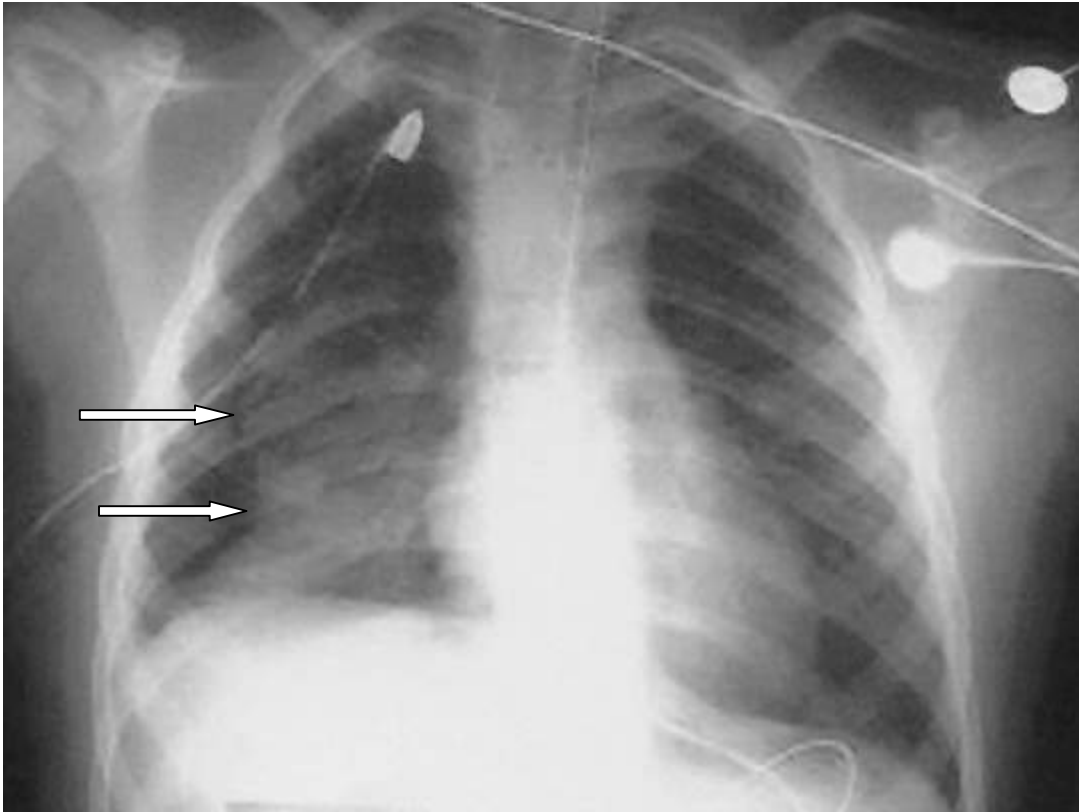


Figure # 16. Pneumothorax is not always easily identified in poorly exposed films. Although bright lighting the film may demonstrate a suspected pneumothorax, taking a properly exposed film in expiration is the method of choice. No need for a film in expiration in the case demonstrated above. The edge of the partially collapsed right lung is easily seen (white arrows).



Figure # 17 (left). Using your system what do you see on the portable study to the left? See next page for labeled answers.
Ps. We realize the film is overexposed to adequately evaluate the bronchovascular markings. This is one of those you would have to bright light or ask for a light copy.

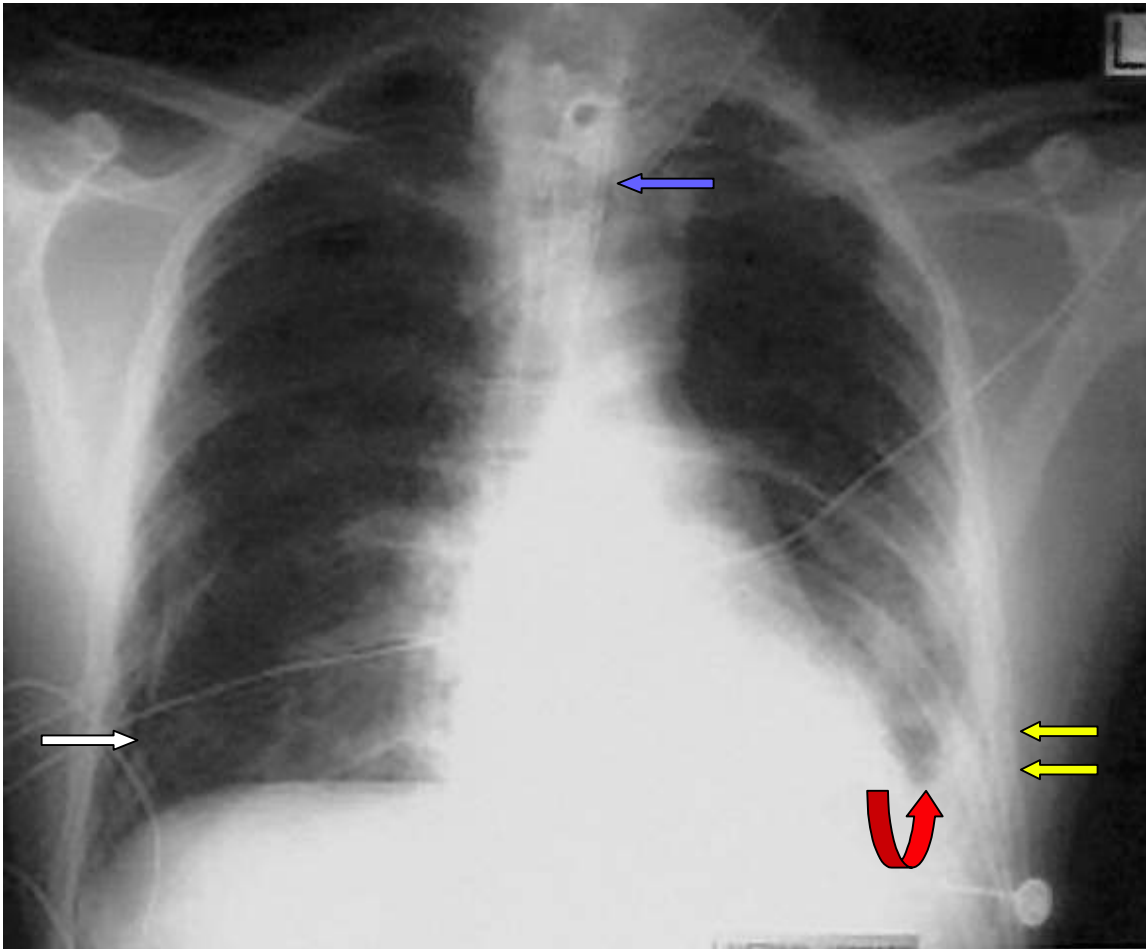


Figure # 17a. White arrow shows pleural reflection from partially collapsed lung in this patient with a small pneumothorax. There is also a small left pleural effusion (red arrow) in this trauma victim, and I suspect at least one fractured rib (yellow arrows). Additional films would be necessary to confirm the latter. Did you note the metallic density of the tracheotomy tube (blue arrow)?

Pleural based densities are recognized by their peripheral position and include pleural fluid, pleural calcifications, extrapleural lesions and soft tissue masses frequently associated with trauma or rib destruction. Commonly pleural fluid is associated with other radiographic evidence of chest disease such as malignancy, CHF (congestive heart failure), pulmonary infarction, abscesses or trauma.

Another trick of the trade is to obtain films with the patient in a decubitus position, which allows free fluid to layer out and helps differentiate effusion from pleural thickening or solid pleural based density. In figures 18 through 22 are examples of pleural based densities.

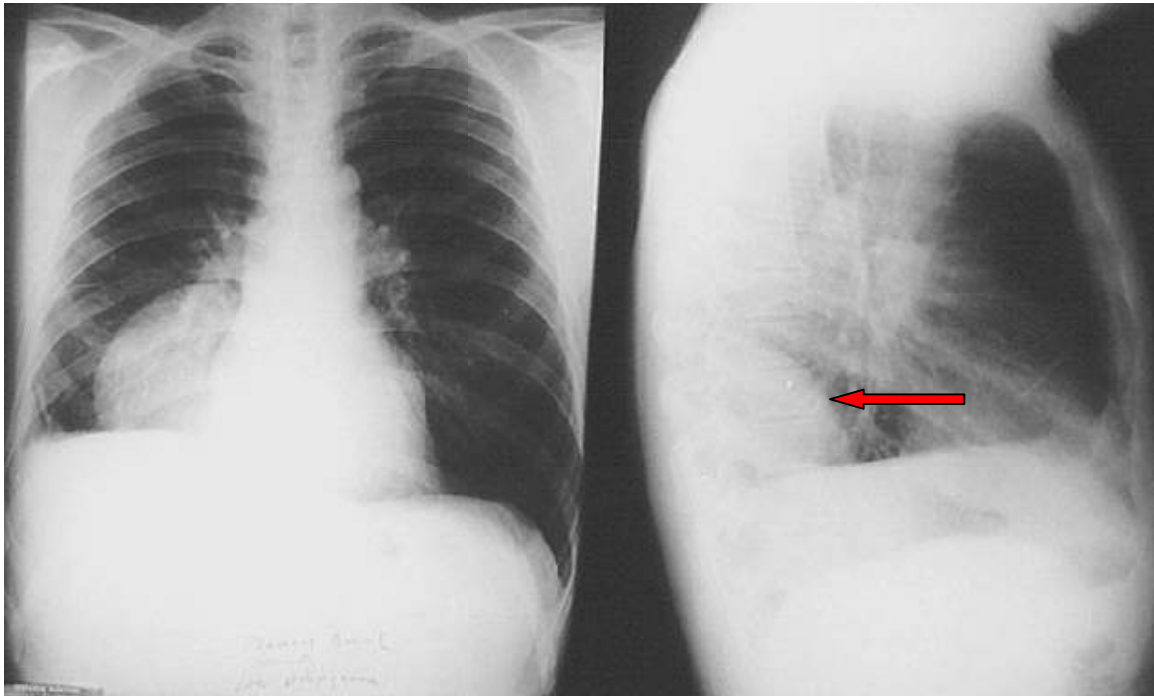


Figure # 18. Pleural based density adjacent to the right heart border. Note there is no silhouetting of the right heart border, which indicates the density, is posterior as confirmed in the lateral view (red arrow). This particular density proved to be a loculated pleural effusion.

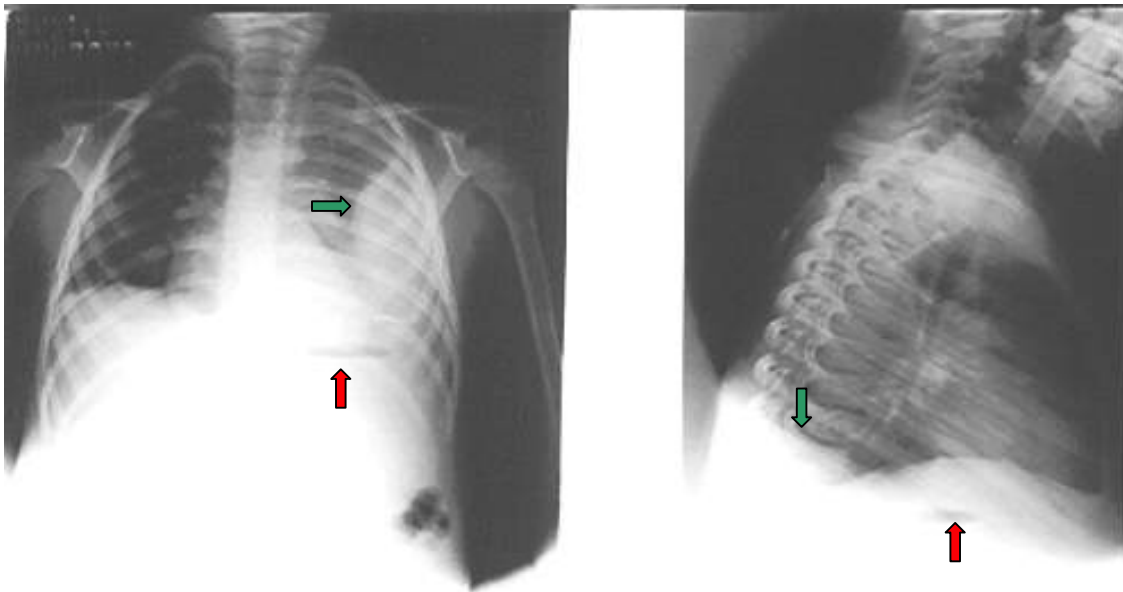


Figure # 19. Another pleural-based density represents a loculated or encapsulated empyema (green arrows). The red arrows point to the gastric air bubble, which gives you some clue as to where the left hemidiaphragm should be. The pleural fluid silhouettes the left hemidiaphragm out. Note that you can still identify the left heart border, so the fluid must be posterior as confirmed in the lateral projection, although it extends more cephalad than the lateral view alone would suggest.

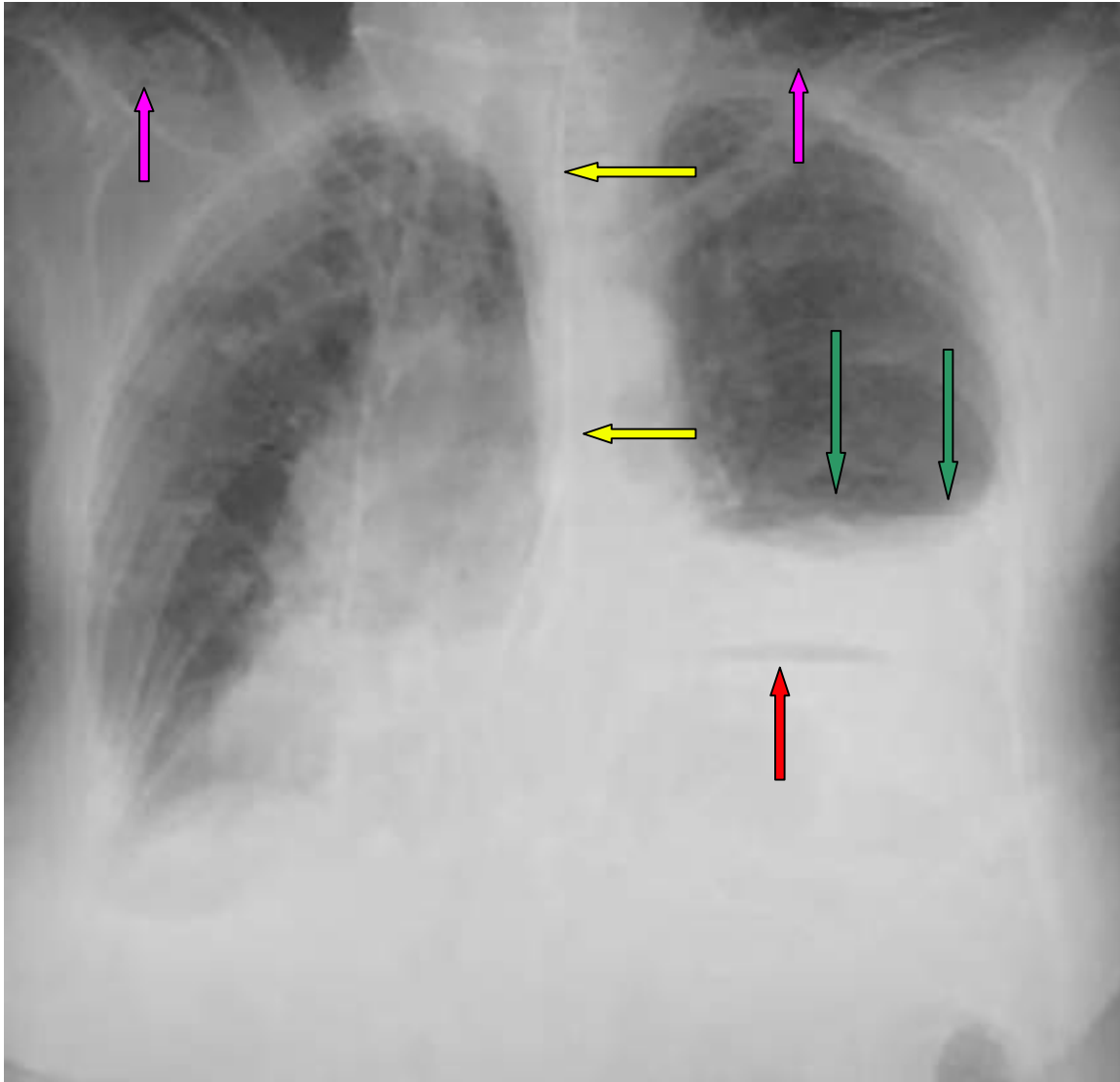


Figure # 20. Fluid in the left pleural cavity (green arrows). The sharply outlined fluid level under the lateral green arrow suggests there is *hydropneumothorax* as well. Pneumothorax is also suggested by subcutaneous emphysema as indicated by the pink arrows. A film taken in expiration (not available) would likely confirm the suspected *hydropneumothorax*. Red arrow points to the gastric air bubble. Note the metallic density of the nasogastric tube (yellow arrows). The right heart border is silhouetted out by atelectatic lung and there is also some fluid in the right chest cavity. See correlating gross pathologic specimen photograph in figure # 21. In this case the pleural-based density is chylous fluid secondary to lymphomatous involvement of chest lymphatics.

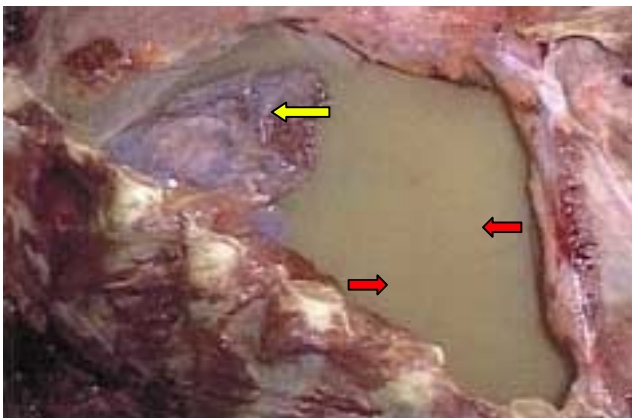


Figure # 21. Pleural cavity is filled with yellowish-tan fluid typical for *chylothorax* (red arrows). Atelectatic lung is noted in the upper left portion of the specimen photograph (yellow arrow).
 Figures 20 and 21 are the Courtesy of Edward Klatt MD, U. of Utah Dept. of Pathology, via the Internet.

Since major texts have been written about diseases of the lungs it is obvious that our discussion is cursory at best, but then again we are not attempting to make experts out of you, but only to give you a few tips until you are able to consult with a diagnostic radiologist on any given case. With that in mind, let us turn to the next step in our system of chest evaluation, which is the heart.

This overview should include size and shape of the cardiac silhouette, the outline of the various chambers, a look for calcifications in the valves and pericardium, the cardiac fat pads and the effect of the thoracic cage on the size and shape, variations of which you will see with conditions such as pectus deformities, surgery, COPD, and others.

One of the few measurements still valid in diagnostic radiology is the c-t (cardiac-thoracic) ratio. Most of the abnormal conditions involve cardiac enlargement. In fact you can count on your fingers the conditions that result in a small heart, which include normal variant, wasting diseases, emphysema, adrenal insufficiency, constrictive pericarditis and dehydration. Cardiomegally, on the other hand, has numerous etiologies and include all of the pathologic categories of congenital anomalies, degenerations, inflammations, physical disturbances and tumors.

The cardiac-thoracic ratio or c-t ratio, is a simple rule that says the transverse cardiac diameter should not measure more than 50% of the diameter of the rib cage. The measurement should be taken across the widest part of the heart on a PA view, and the thorax should be measured from the inside of the ribs.

Be sure you are dealing with a standard 72 " target to film distance radiograph to avoid any magnification of the heart which will occur on some portable studies or on films taken with the patient supine or in a sitting position. (The "target" is the point of origin of x-rays in the x-ray tube). Also be sure to give yourself a cm. of leeway when comparing old films to new to account for whether the film was taken with the heart in systole or diastole.

The shape of the cardiac silhouette will become familiar after seeing several normal chest films. Anything out of the ordinary, then, should be evaluated based on the suspected abnormality observed. In order to pin down the etiology of the suspected bulge or deviant outline, one must be familiar with the proportion of the various chambers visible in the PA and lateral projections. Below are photographs of a heart model as viewed from the front (really the back in a posterior-anterior or PA projection), and the side or lateral projections.

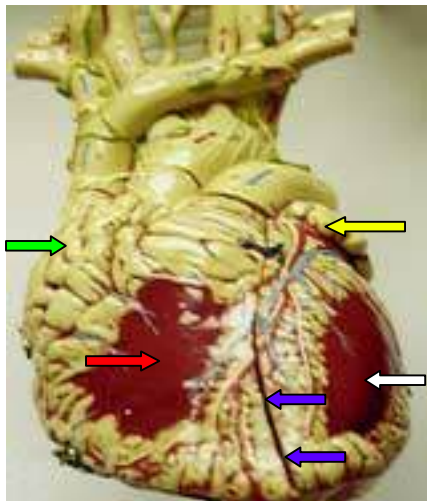


Figure # 23. AP view of heart.

White arrows indicate the left ventricle, only the posterior margin of which is seen in the lateral projection. Red arrows point to the right ventricle, which accounts for the major portion of the heart silhouette on a two-view radiographic study. Green arrows show the right atrium, and the yellow arrow points to the left atrial appendage. Blue arrows show position of the intraventricular septum.

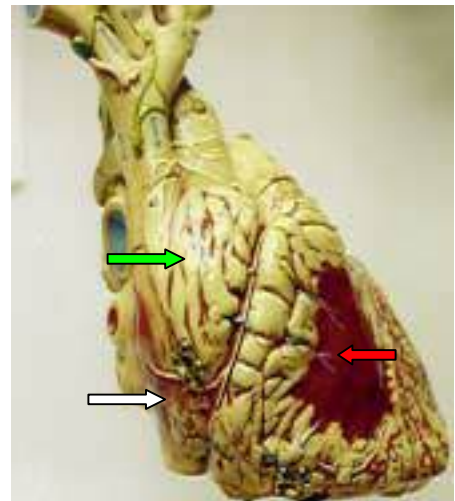


Figure # 24. Right lateral view

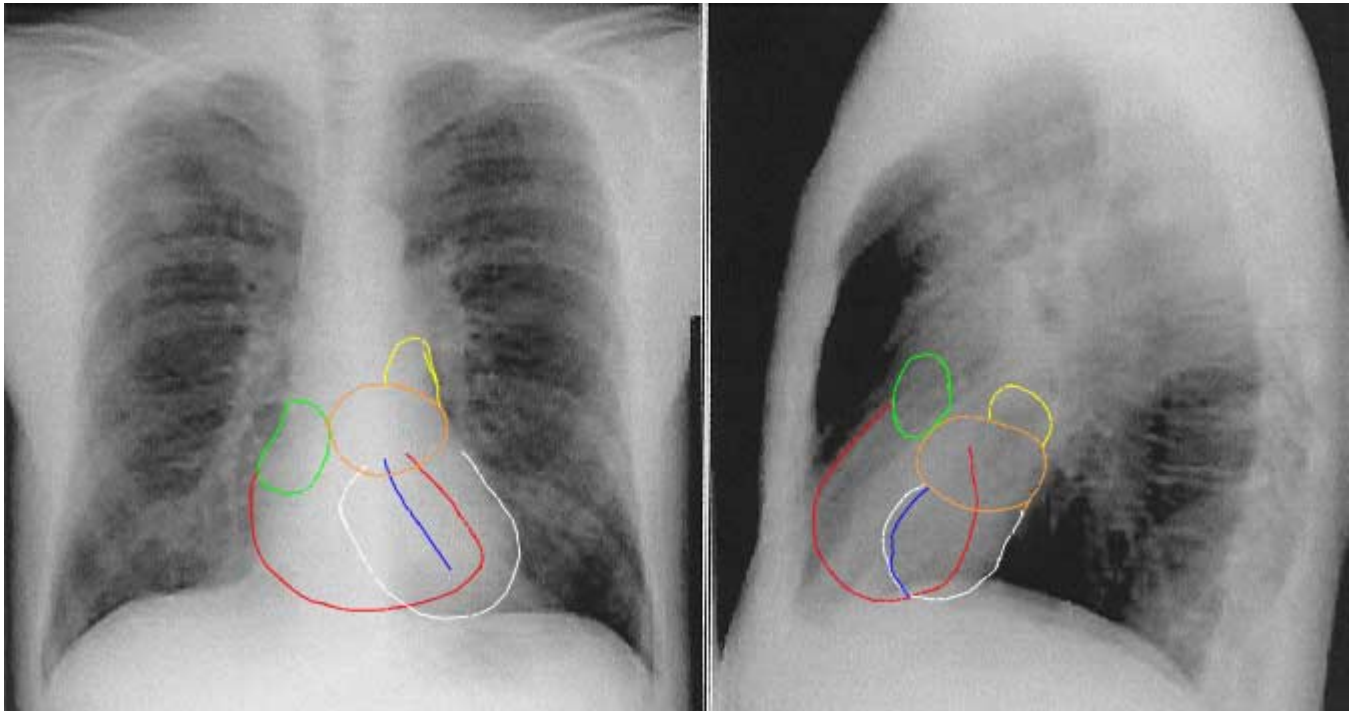


Figure # 25. Approximate positions of the various chambers as seen on PA and lateral views of the chest. Red outlines the right ventricle, green-the right atrium, white- the left ventricle, orange-the left atrium, and yellow- the left atrial appendage. Blue suggests the position of the interventricular septum. (PS. Did you see the pulmonary nodule in the right upper lobe? It overlies one of the vertebral bodies' anterior margin in the lateral view. See white arrows in figure 25a below.)

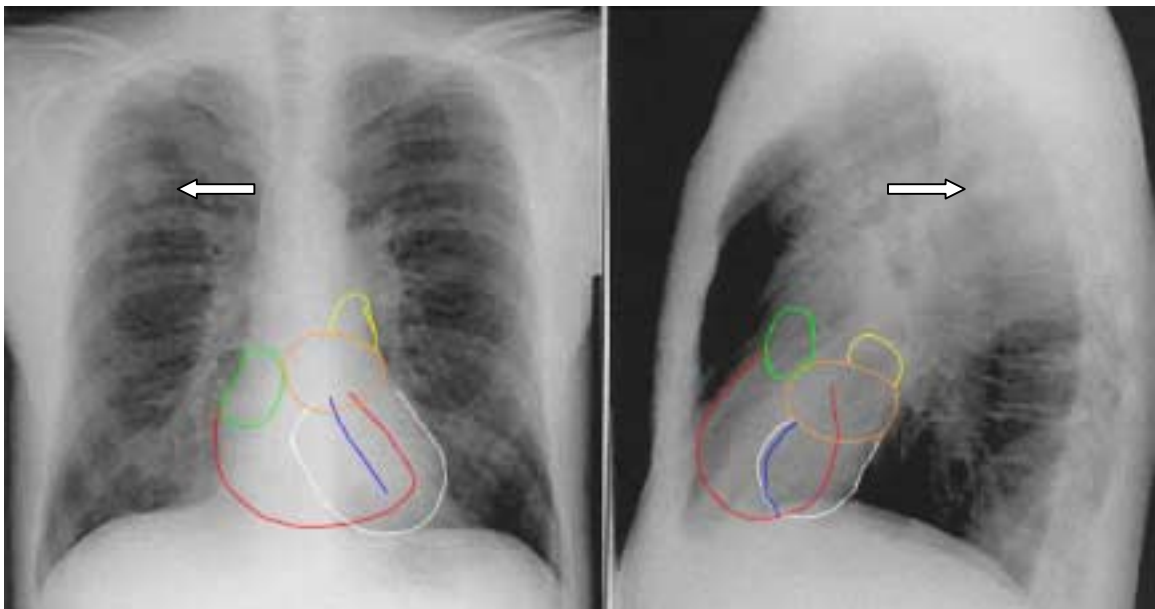


Figure # 25a White arrows show pulmonary nodule.

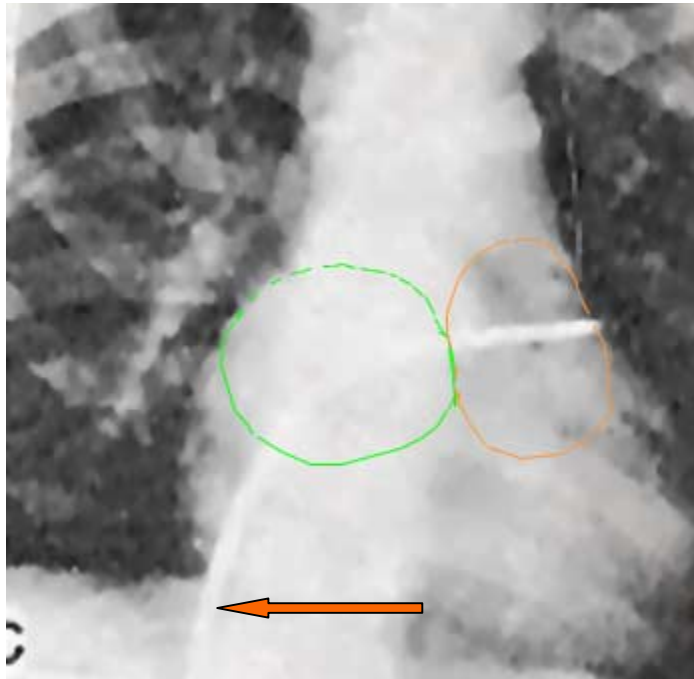


Figure # 26. Catheter in the Inferior vena cava (orange arrow) has passed through an atrial septal defect with the tip of the catheter now encroaching on the lateral wall of the left atrium. Right atrium position outlined in green and left atrium in orange.

Figures 27 through 30 to follow show the effects of various chamber enlargements on the cardiac silhouette.

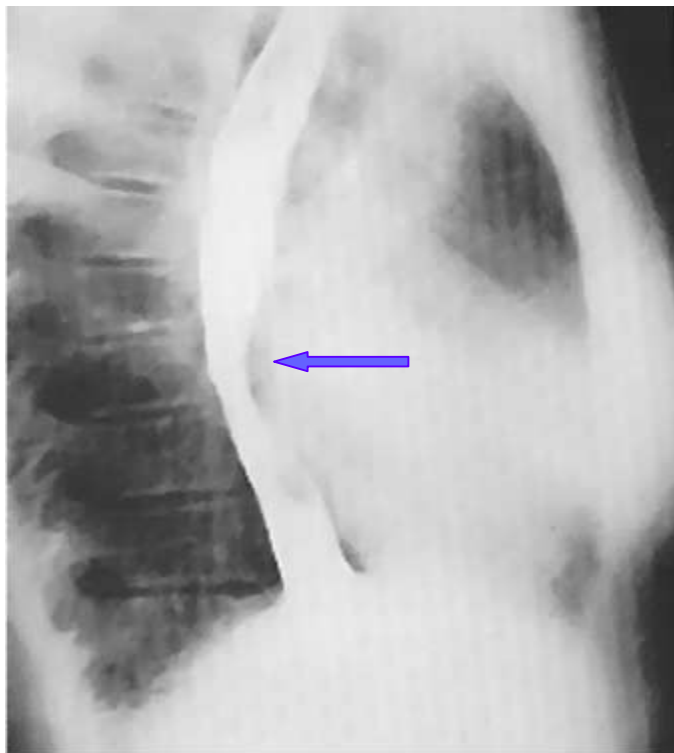


Figure # 27. With barium in the esophagus, left atrial enlargement is easily demonstrated as indicated by the blue arrow.

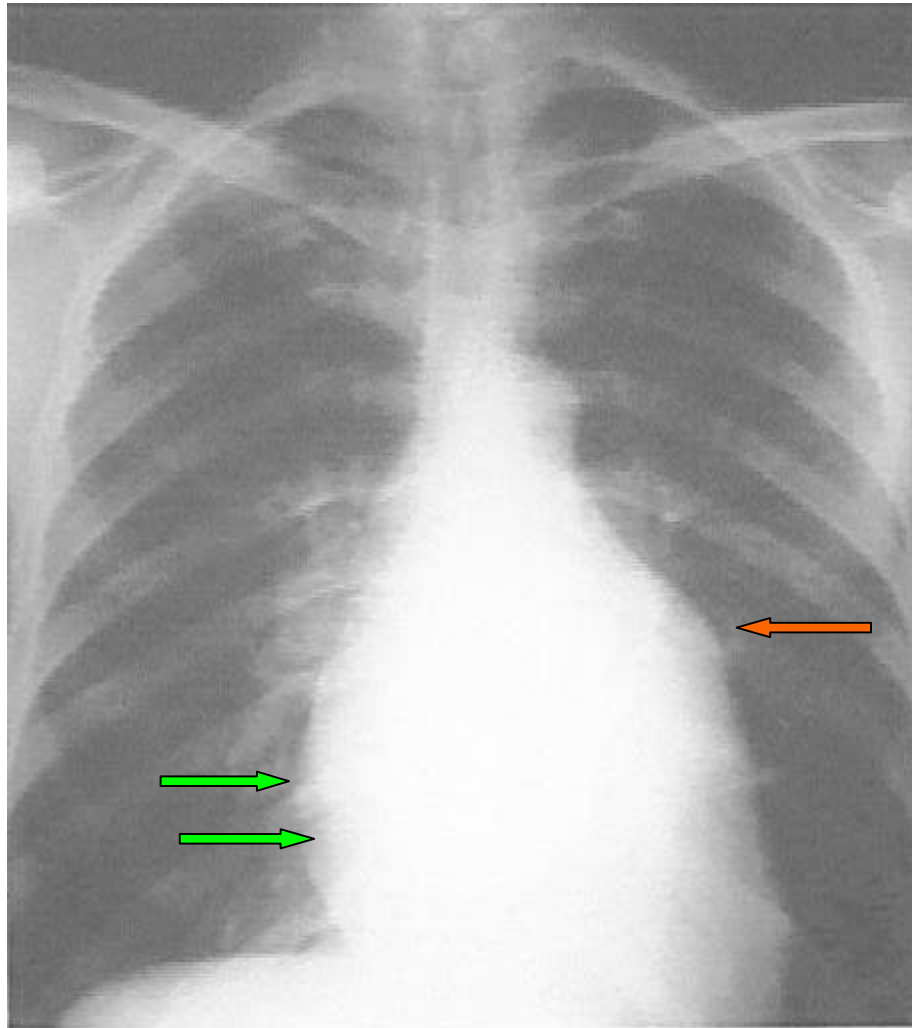


Figure # 28. Patient with mitral regurgitation. Left atrium enlargement is indicated by orange arrow and can be seen also as a double density in the PA view (green arrows). The transverse cardiac diameter is not particularly enlarged in this gentleman.

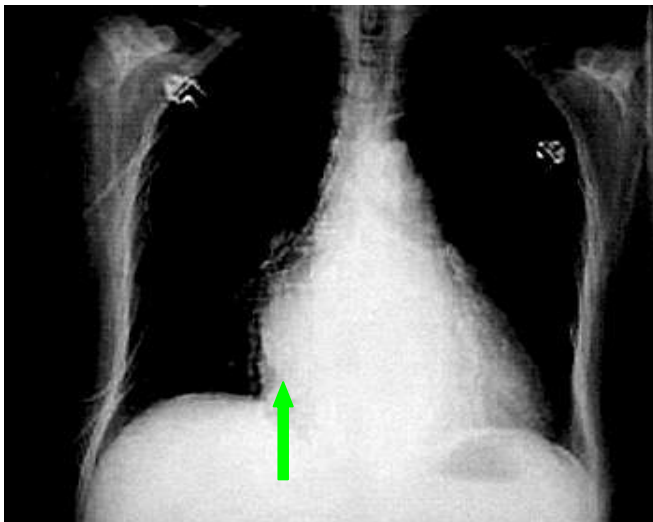


Figure 28a (left). Same film as figure 28 above with the contrast manipulated to demonstrate the double density of the enlarged left atrium (green arrow).

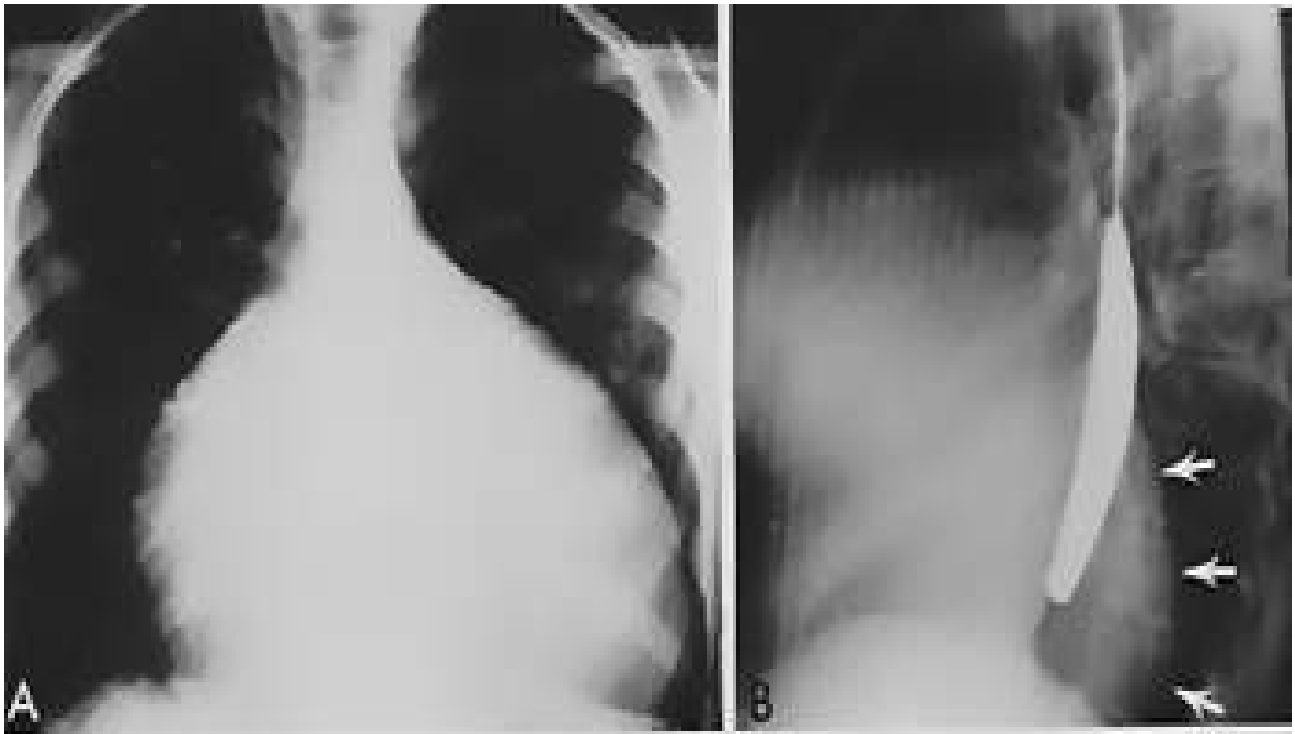


Figure # 29 above. Ebstein's anomaly of the tricuspid valve results in an enlarged right heart. The enlarged right atrium (arrowheads) extends posterior to the barium filled esophagus. Kelley, Jaffe, Shoum, Kleinman. *Radiologic Clinics of North America*. Vol 18, No.3, Dec.1980

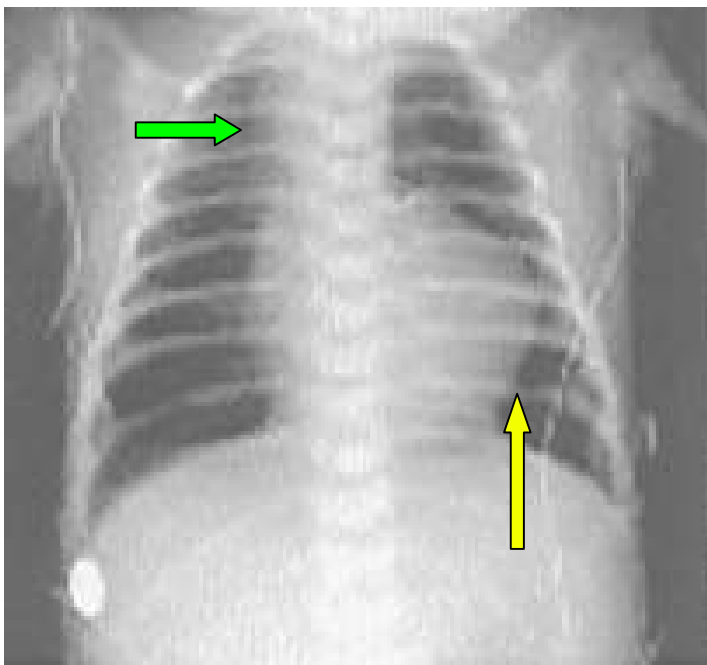


Figure # 30 (left). Pulmonary stenosis results in right ventricular hypertrophy and decreased pulmonary vascularity as shown above in this infant with tetralogy of Fallot. The tetralogy consists of 1) pulmonary stenosis; 2) ventricular septal defect; 3) dextroposition of the aorta (green arrow); and 4) right ventricular hypertrophy (yellow arrow). Note the absence of distinct bronchovascular markings, the result of diminished pulmonary blood flow. The condition accounts for about 75% of cyanotic congenital heart disease.

Figures 31 and 32 show pericardial and mitral valvular calcification respectively.

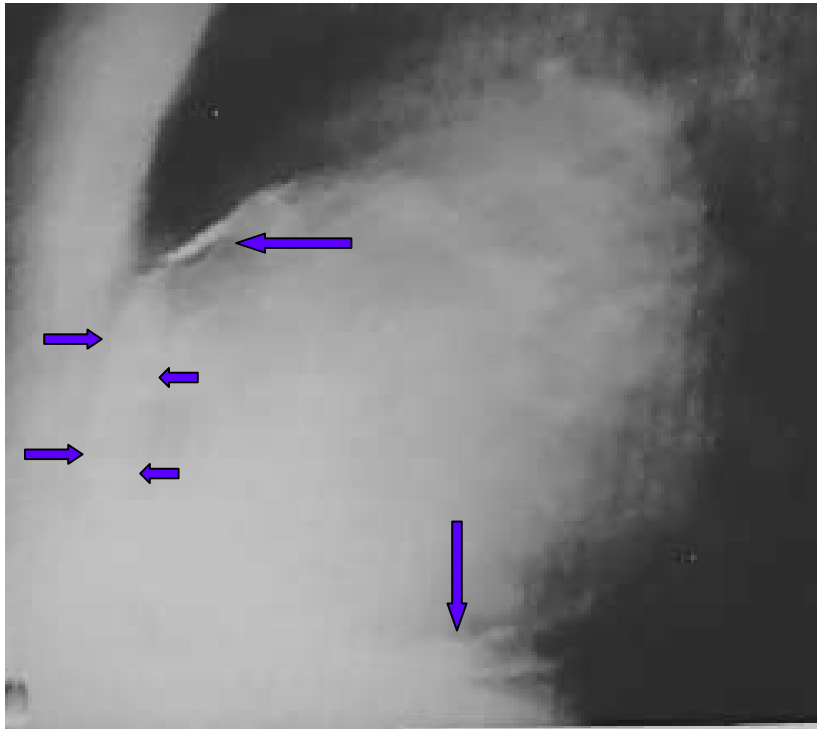


Figure # 31. Blue arrows point to pericardial calcification in a patient with a history of pericarditis.

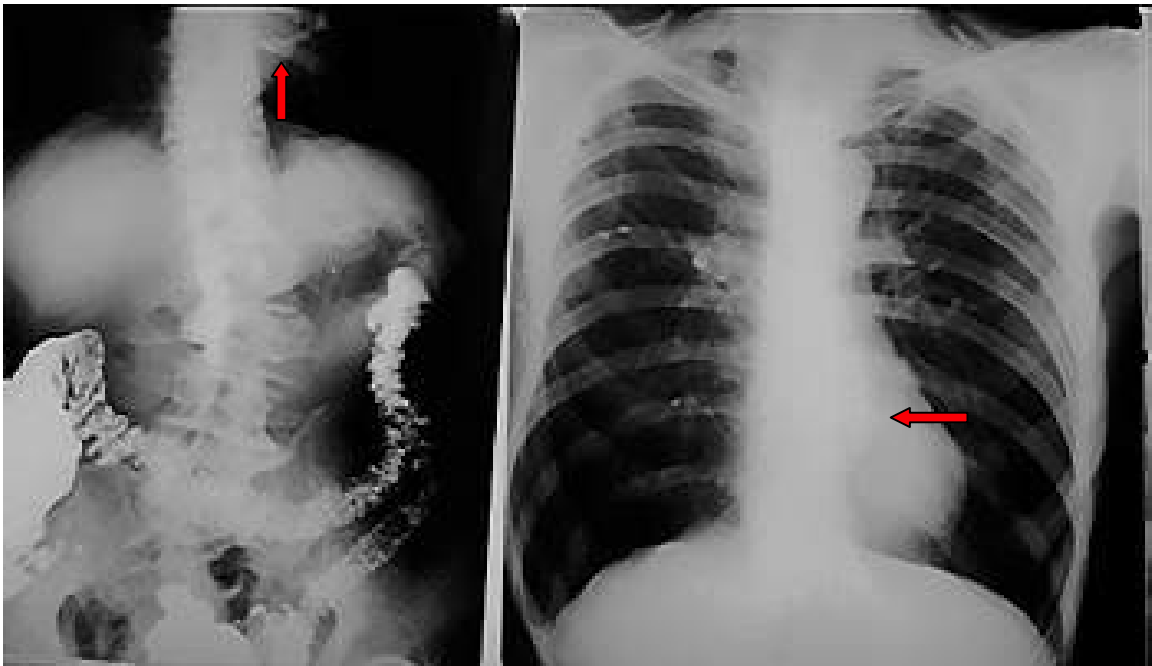


Figure # 32. Red arrows point to mitral valve calcification, better demonstrated on the KUB than on the chest film.

Note the location and orientation of the mitral and aortic valves best demonstrated by the prosthetic valves in figures 33 and 34.

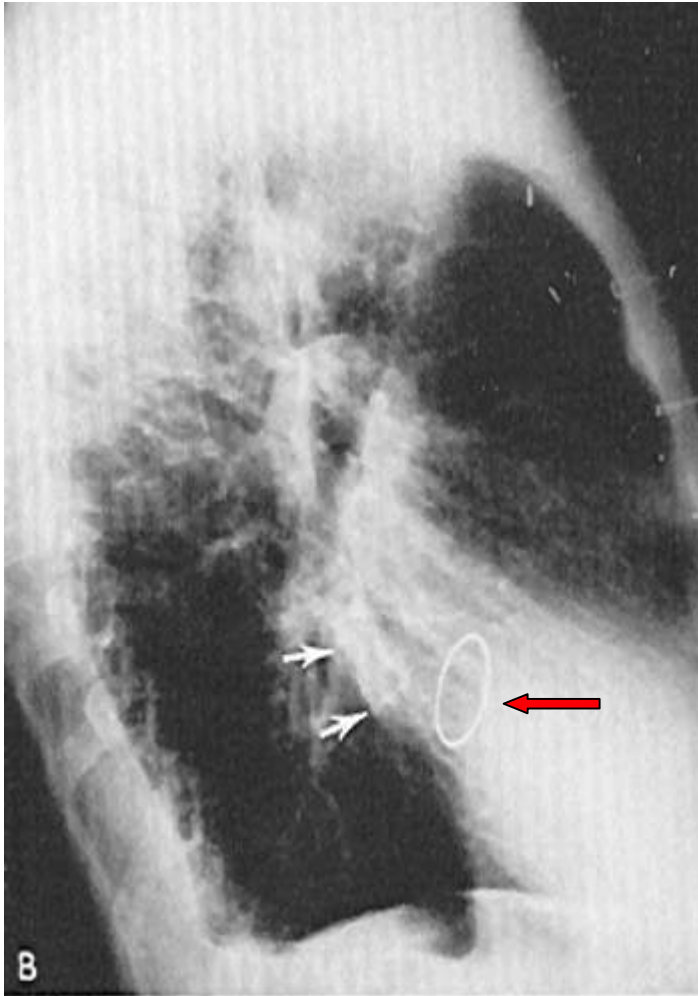


Figure # 33 (left). The red arrow indicates the position of the mitral valve prosthesis. The smaller white arrows point to the slightly enlarged left atrium, the result of the diseased mitral valve prior to replacement.

Figure # 33 Green and Kelley, *Radiologic Clinics of North America* Vol. 18, No. 3, Dec. 1980

Figure # 34 (right). Note the proximity and orientation of the mitral and aortic valves as seen in a slightly oblique lateral view in a patient who has prostheses of both valves.



Figure # 34. *Ibid.*

Cardiac fat pads seem at first glance to widen the transverse diameter of the cardiac silhouette. Careful scrutiny, however, can usually separate the true outline of the heart border due to the darker density of fat in relation to the water density of heart muscle. Sometimes cardiac coelomic cysts can mimic a cardiac fat pad, especially in an under penetrated film. In that case one must accept both possibilities in the differential diagnosis, but since neither is of great clinical significance the finding is academic and only important in order to exclude pathology such as cardiomegally or tumors of the heart or mediastinum. Note the effect of a prominent fat pad on the cardiac silhouette in figures 35 and 35a.

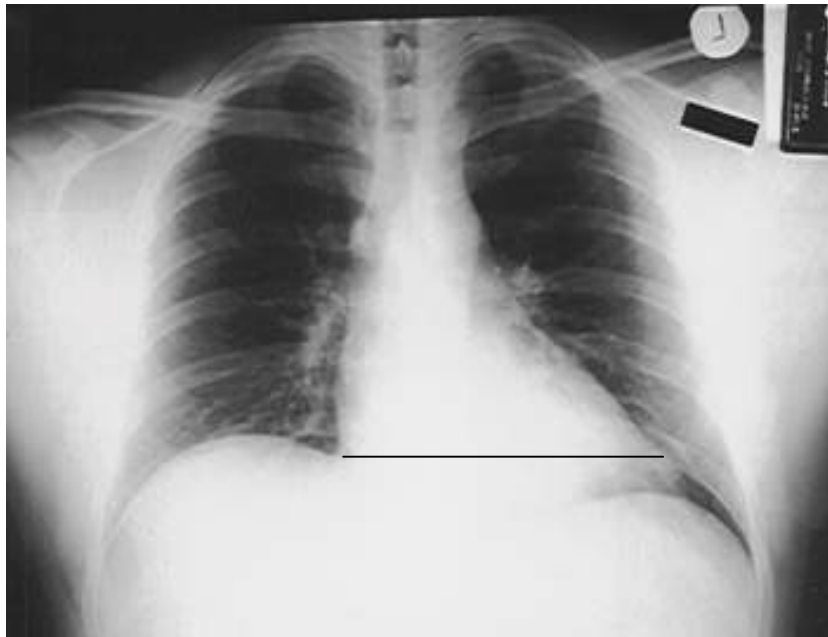


Figure # 35. Transverse cardiac diameter shown above by the black line is in error because it includes the cardiac fat pad.

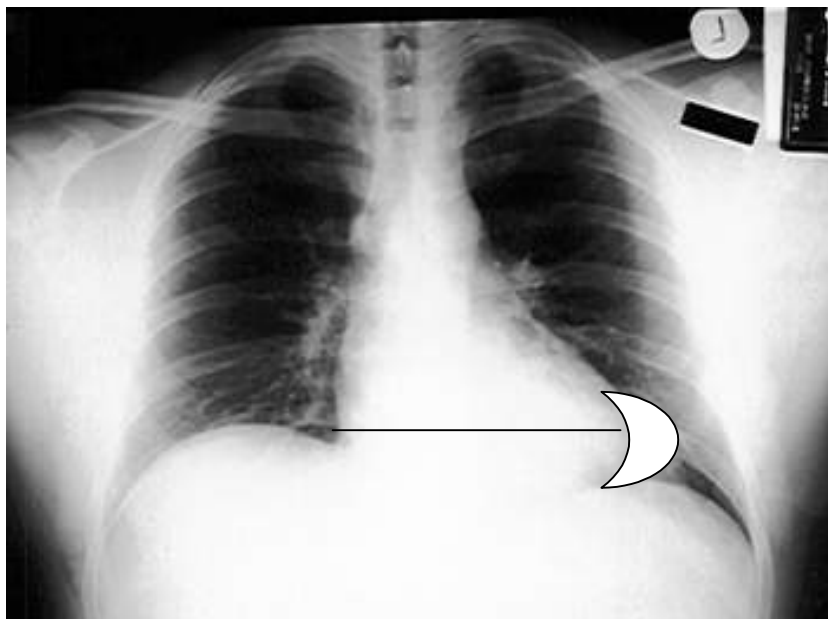


Figure 35a. True transverse cardiac diameter does not include the fat pad indicated by the quarter moon. Same radiograph as figure 35 above.

Pectus excavatum can cause a visual loss of the right heart border or an apparent mediastinal shift in the PA projection. If you have only the PA view you have to learn to be suspicious of the cause of the abnormality. You can always get a lateral view to confirm. Note the effect of a pectus deformity on the appearance of the mediastinum and right heart border in the PA view in figure 36 and the confirmation of the cause in the lateral view.



Figure # 36. The cause of the partial loss of the right heart border in the PA view of the chest above is not due to silhouetting. Experienced radiologists recognize this as an almost “Aunt Minnie”. The cause is a pectus excavatum of the sternum (red arrow) which displaces the heart to the left.

The third step in the system to evaluate the chest is the mediastinum, which can be divided into anterior, mid and posterior compartments and for our purposes, subdivided into superior and inferior portions as well.

The anterior compartment can be described as " anterior to a curved vertical line extending along the posterior border of the heart and anterior margin of the trachea" -3. It includes the heart and pericardium, the ascending aorta, thymus, the retrosternal space, various vessels, lymphoid tissue, some bronchial origins, anterior leaf of the diaphragm and on occasion, the thyroid.

The mid mediastinum is simply that area between the anterior and posterior compartments. It contains the arch of the aorta, azygos vein, other bronchial origins, esophagus, thyroid, parathyroids, trachea, vagus and phrenic nerves, vessels etc. The posterior mediastinum lies anterior to the spine but includes the thoracic gutters, and extends to the esophagus. It includes the descending thoracic aorta, posterior leaf of the diaphragm, vessels, nerves etc. It will take scrutiny of numerable films before the student becomes familiar with the normal bulges of the mediastinum. The next few figures illustrate some of the common normal and abnormal bulges we encounter in daily practice.

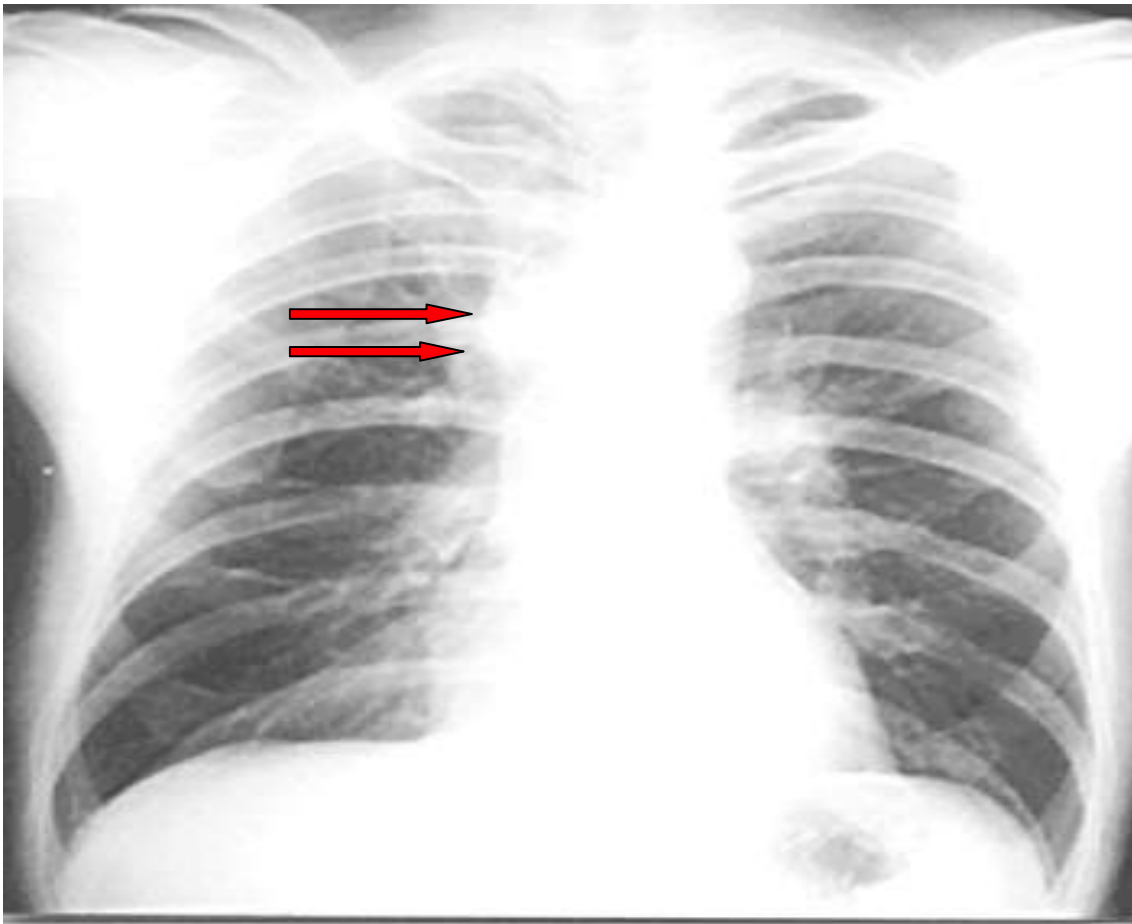


Figure # 38. Red arrows point to a bulge in the right superior mediastinum, which proved to be a bronchogenic carcinoma after an angiogram eliminated the possibility of a vascular shadow. (Before the days of CT access).

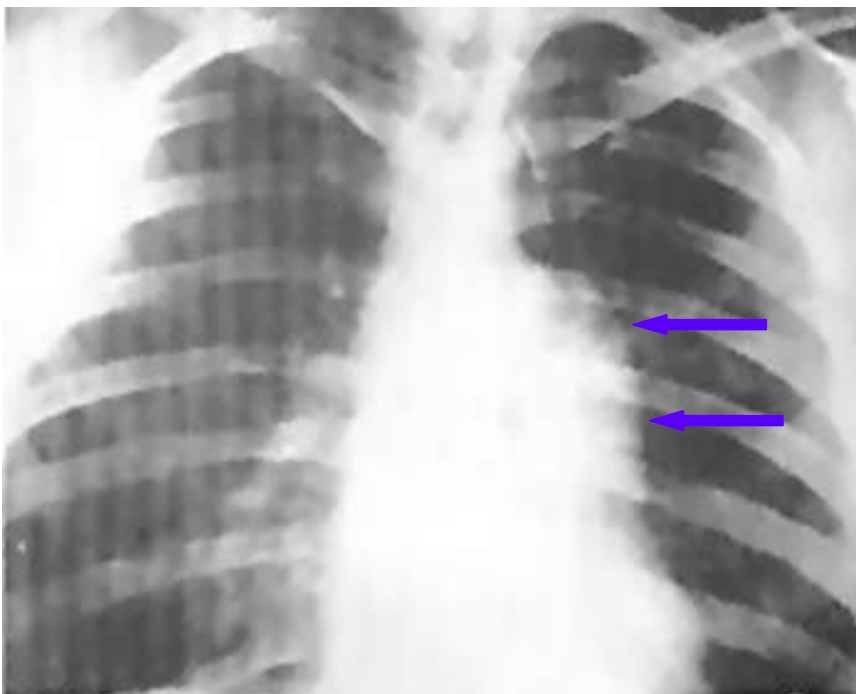


Figure # 39. Mass distorting the normal contour of the left side of the mediastinum (blue arrows) proved to be a non-Hodgkin's lymphoma in a 26-year-old male. The vertical stripes over the right side of the chest are computer or scanner artifacts.

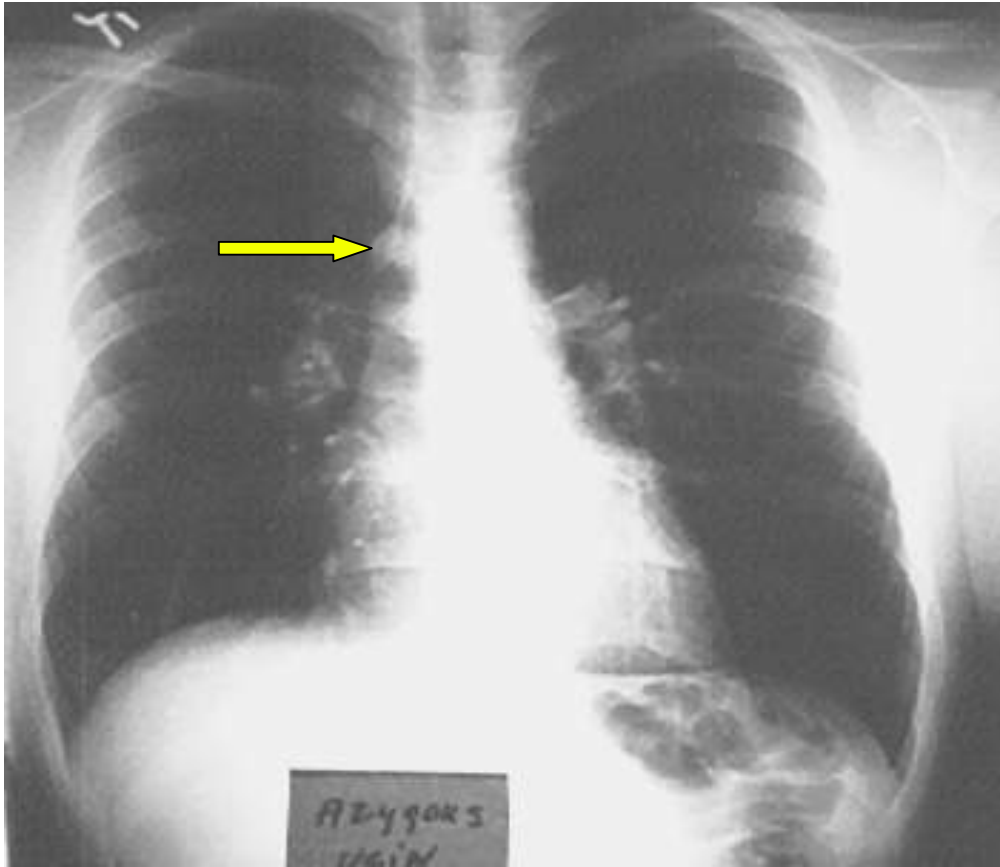


Figure # 40. Yellow arrow points to another bulge along the right superior mediastinum, but this time representing a normal finding, a prominent azygous vein. The demonstration represents another “Aunt Minnie”, although the index of confidence may not always be high in inexperienced interpreters and additional studies may be necessary to confirm a normal finding.

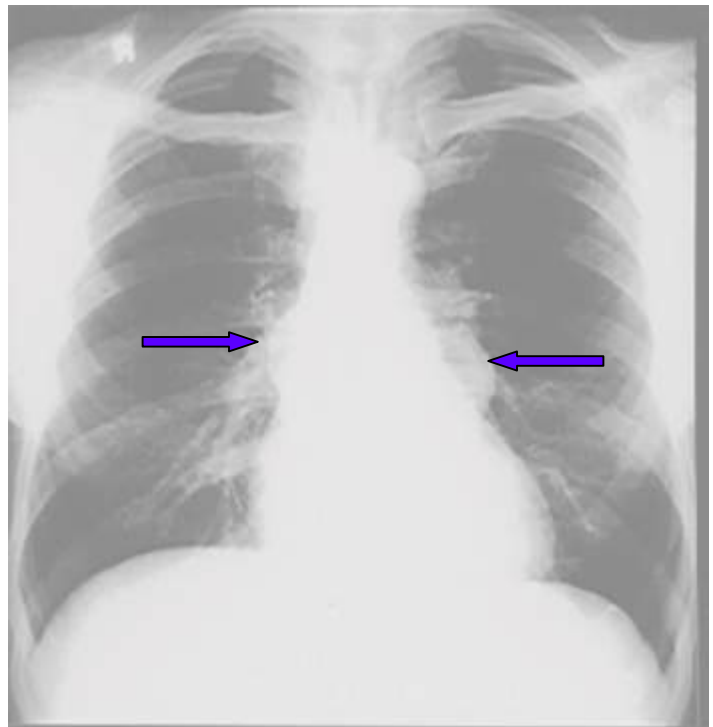


Figure # 41. Blue arrows point to abnormal bulges of the mediastinum, which proved to be benign teratomas.

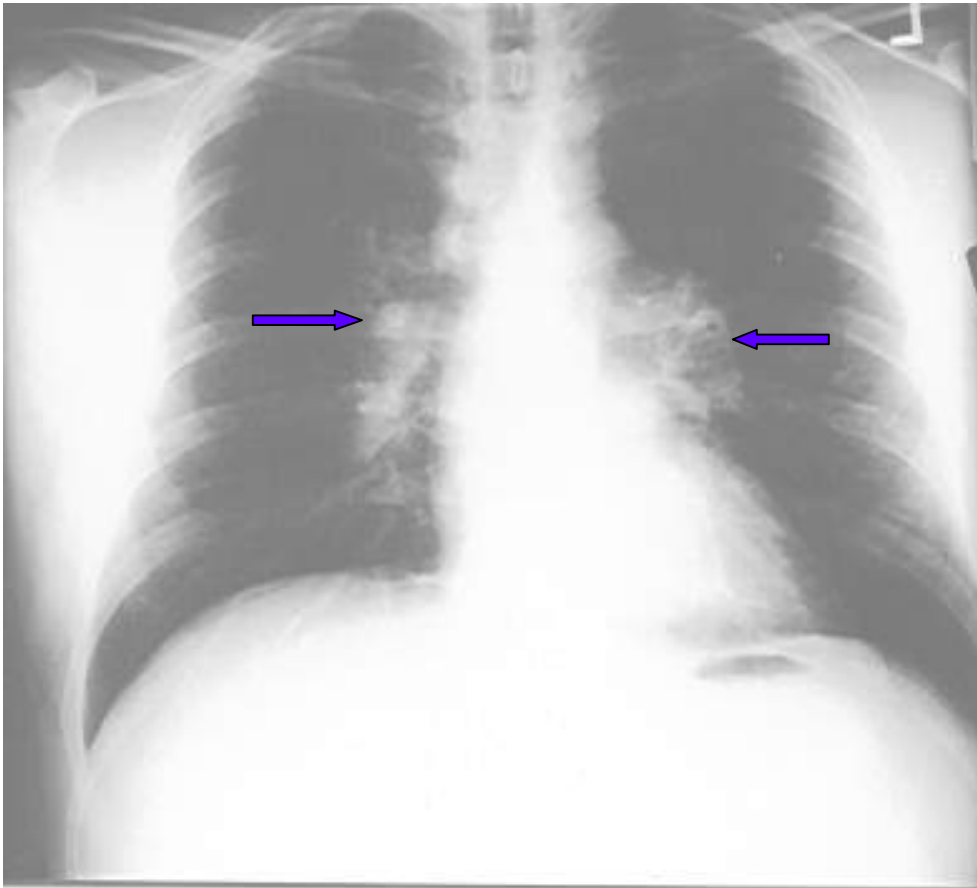


Figure # 41. Blue arrows point to full, abnormal hilar shadows, which proved to be hilar adenopathy in a patient with lymphoma. If there is any question as to normal vs. abnormal, the problem is easily solved by a CT study.

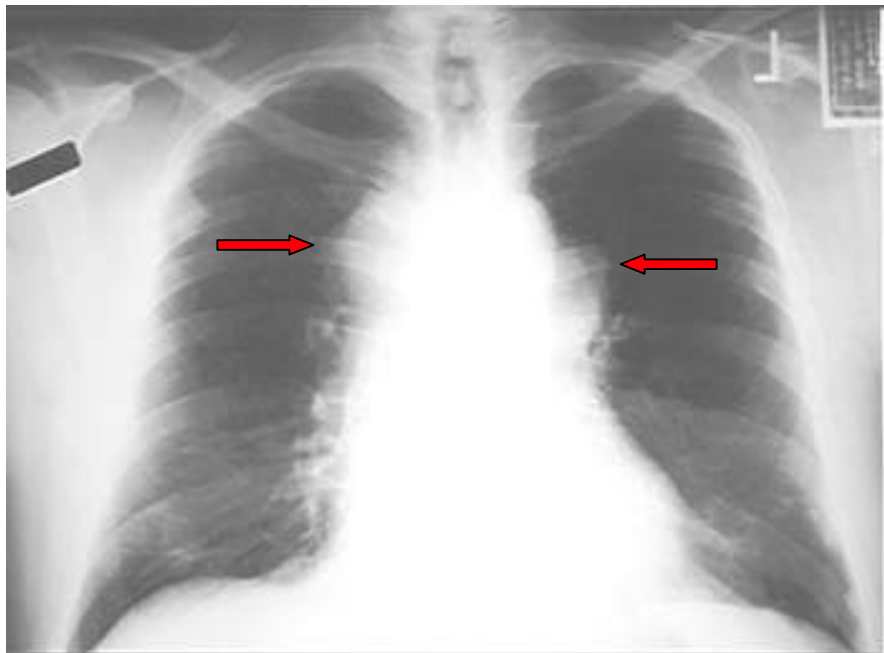
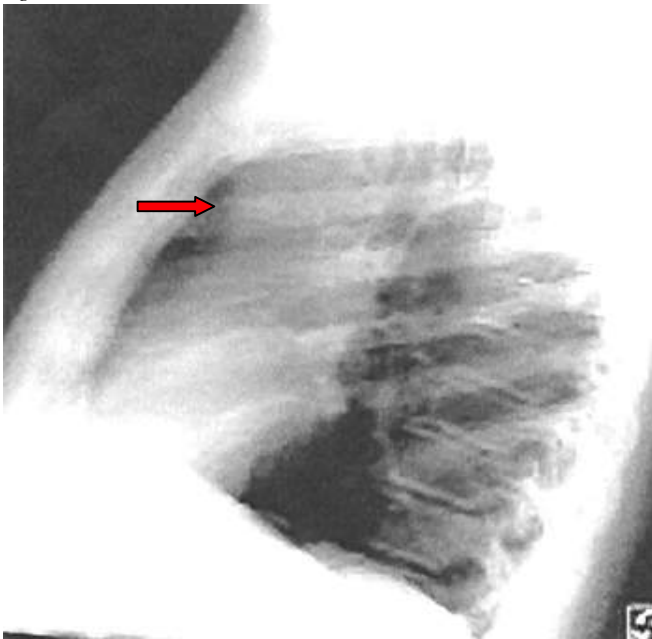


Figure # 42. Red arrows point to abnormal mediastinal contour, which proved to be another lymphomatous mass.

Figure # 43.



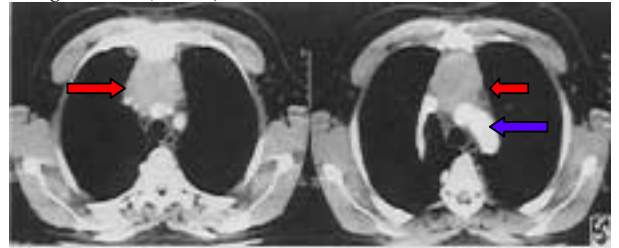
Figure # 44.



Figures # 43 and 44 (left).

Red arrows point to a more subtle abnormality in the anterior mediastinum. Note partial silhouetting of the arch of the aorta. The CT images below confirm the presence of a thymic mass, which proved to be malignant carcinoma.

Figure # 45 (below).



In figure 45 above the blue arrow indicates the arch of the aorta in this CT study. The aorta is filled with iodinated contrast, which accounts for its bright white appearance. Remember that when you look at a CT (Computerized Tomogram) study, you are observing a cross section of anatomy as if you were standing at the patient's feet with the patient supine. Thus the patient's right side will be to your left.

The red arrows point to the thymic mass. Note the encroachment on the arch of the aorta, which accounts for the positive silhouette sign.

Images 43-45 courtesy of Brigham, Harvard Radiology Depts. via the Internet. <http://brighamrad.harvard.edu>.

Double densities are another thing to explain. For example the figures below show mediastinal densities not seen on a normal radiograph of the chest.

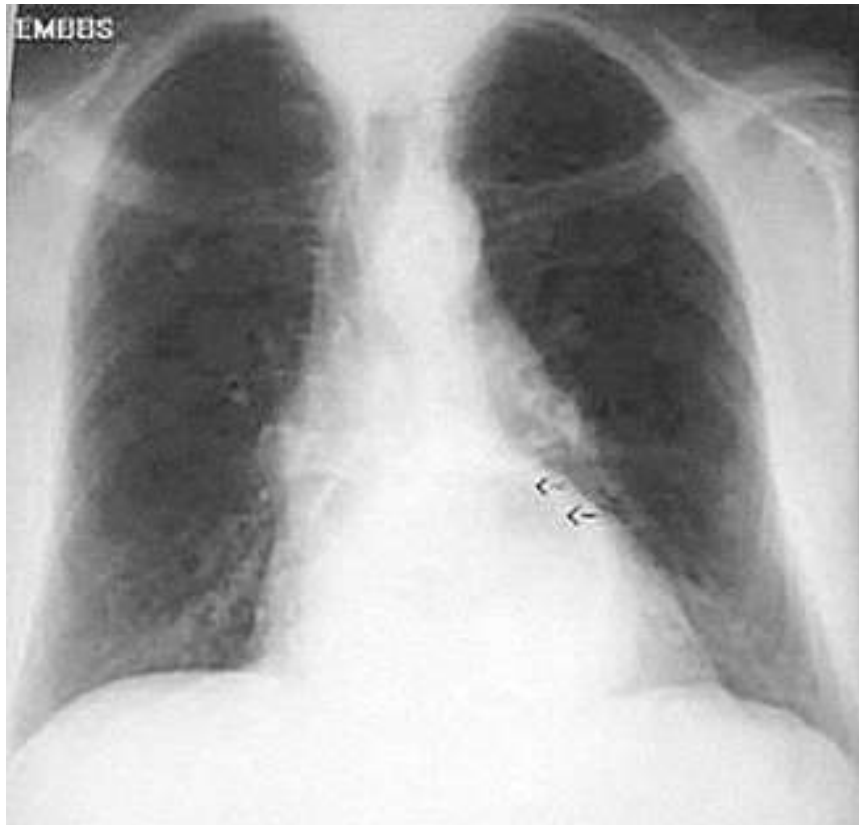


Figure # 46. Small black arrows point to gas density overlying the cardiac silhouette. The gas in this case represents gas in the fundus of the stomach and is thus diagnostic of a hiatus hernia. If it had an air fluid level it would be considered an “Aunt Minnie”.



Figure # 47 (left). The lateral view of the patient in figure #46 shows the gas bubble in the herniated stomach above the diaphragm (small arrows). The lateral view also shows an air fluid level in the stomach (red arrow) confirming the diagnosis of hiatal hernia. Images courtesy of embbs.com library via the Internet.

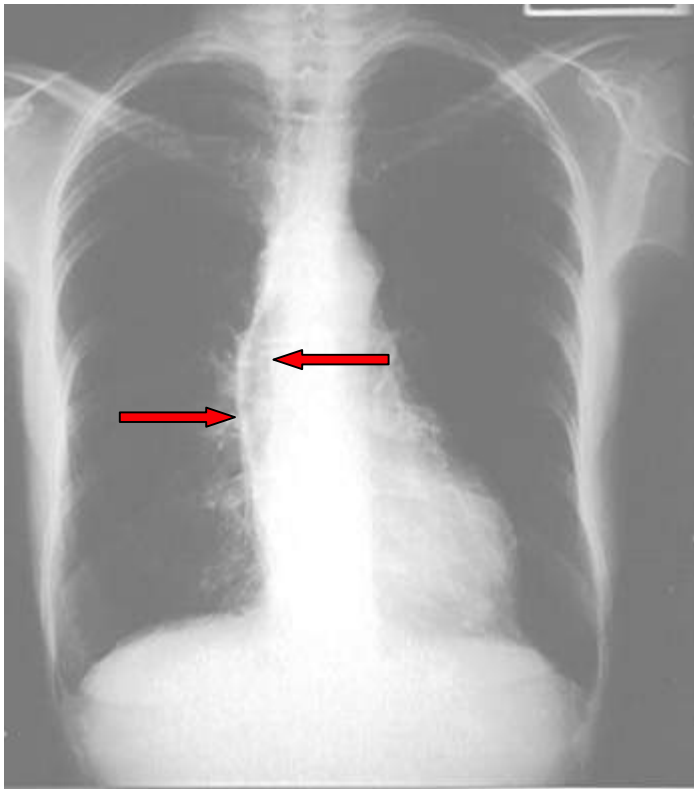


Figure # 48. Red arrows point to a “tube” of gas density in the right side of the mediastinum. Can you offer an opinion as to what it might represent?

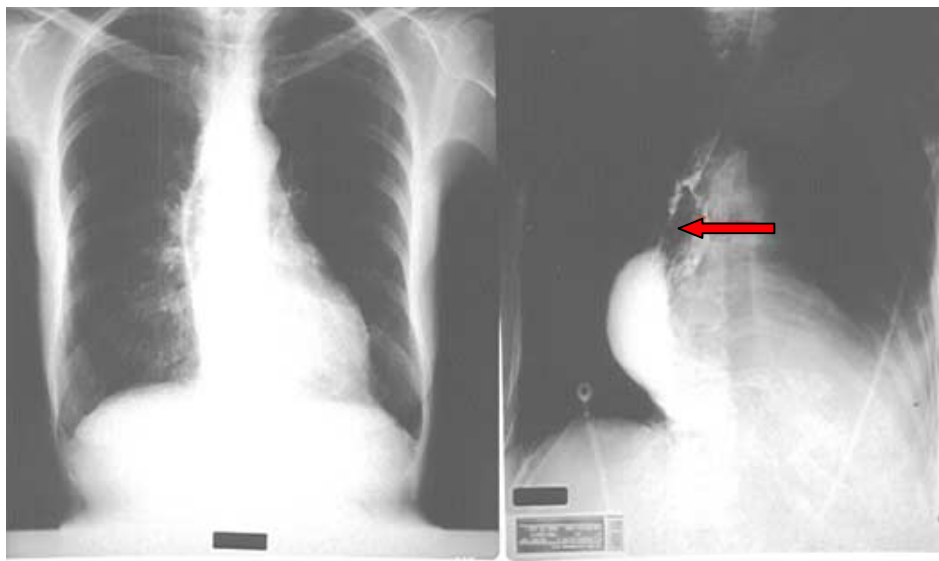


Figure # 49. Actually after you have seen a few of these, they become “Aunt Minnies”. With barium in the upper GI tract, it is obvious this patient has had a sub-total esophagectomy with a gastric pull-through for carcinoma of the esophagus. The red arrow points to gas in the fundus of the stomach, which you saw on the chest radiograph. One does not ordinarily see gas in the esophagus unless there is an obstruction distally (not uncommon), a severe infection with gas forming organisms (very rare), or in the case of some newborns, a TE fistula.

Figure # 50 (right). **Yellow arrow points to a double density along the right border. Can you offer an opinion as to the cause? Do you see any other clues? For answer refer to figure 51 below.**

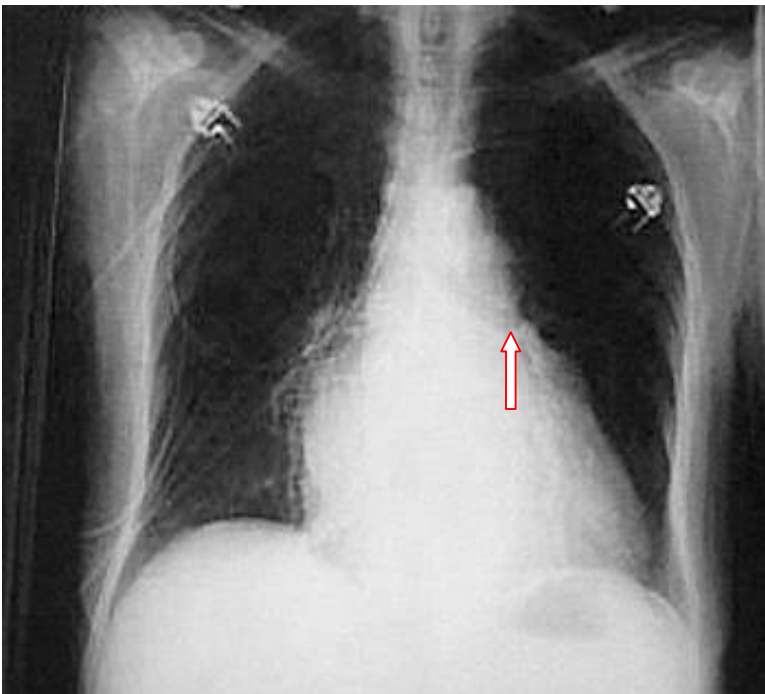
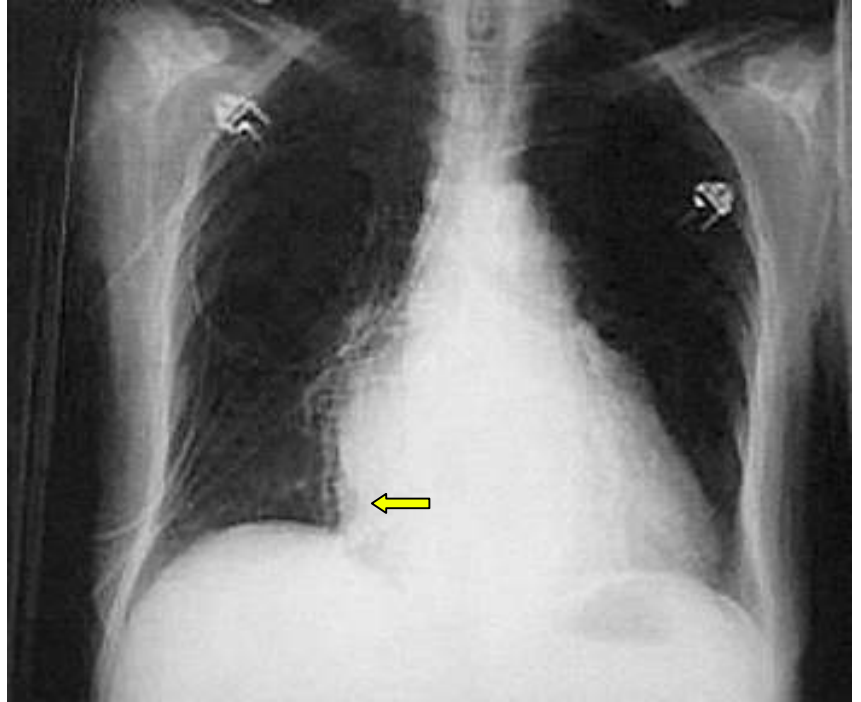


Figure # 51 (left). **Red outlined arrow points to a relatively horizontal left mainstem bronchus, which is elevated by an enlarged left atrium, secondary to mitral valvular stenosis. Compare to figure 28.**

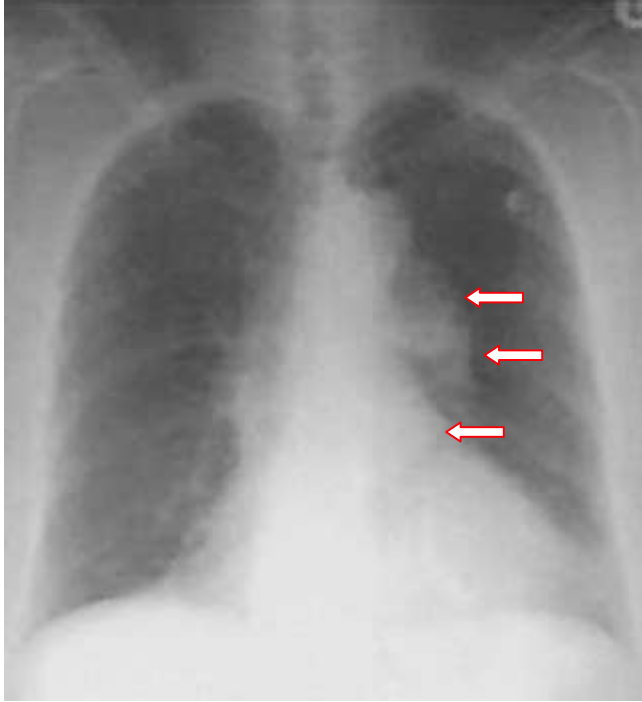
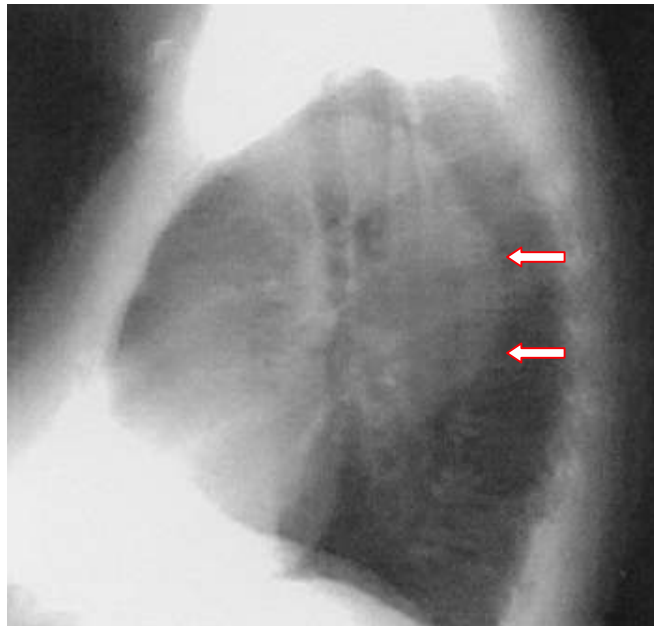


Figure # 52. Red outlined arrows point to a double mediastinal density. Note that it does not silhouette out the left heart border or left pulmonary artery. What do you need to make the diagnosis?

*Images
courtesy of
Challenger
Corporation
via the
Internet.*



Challenger Corporation
Medical Images
Demonstration

Figure # 53. The answer to the above question is a lateral view. The red outlined arrows point to the posterior margin of a descending thoracic aortic aneurysm.

Figure # 54 (right). Red arrow points to another double density in the mediastinum, this time representing gas density, but not in a location for hiatus hernia. Can you offer an opinion as to what it might be? See figure 55 below. For green arrow see text in figure 55 below.

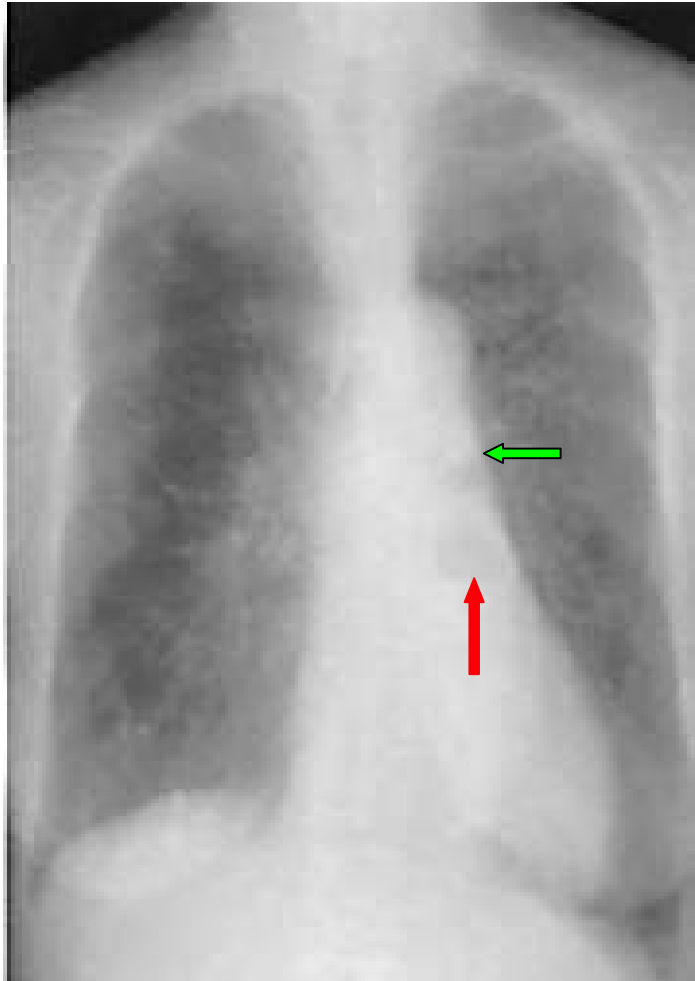


Figure # 55 (left). Barium in the esophagus demonstrates a large diverticulum (red arrows) containing a bezoar (yellow arrow) and air (blue arrow) which accounts for the double density seen on the plain film radiograph. Also note a calcified granuloma (green arrows) which was present in figure 54 but not well demonstrated in the underpenetrated film.

The next item in your system for evaluating the chest is the diaphragm.

Evaluation of the diaphragm is relatively easy compared to the rest of the chest. Remember that you are only seeing the anterior leaf of the diaphragm in the PA projection except for the costophrenic angles and that there is a lot more of the lungs below the anterior leaves. This is where the value of the lateral projection comes in handy to explain any double densities or shadows you are worried about.

The silhouette sign is extremely important in assessing for fluid or pleural thickening, and in order to tell the difference a lateral decubitus view will answer the question of free fluid, especially if no prior films are available for comparison.

There is also a variant of the diaphragm with which you should become familiar which is an eventration, simply a weakness of the muscle fibers of the diaphragm usually congenital in origin, and which can affect either leaf. Eventrations cause the hemidiaphragm to appear elevated, but usually are of no clinical significance or importance in asymptomatic adults. Eventrations in the newborn may cause respiratory distress in some cases and are subject to surgical intervention. In utero they may be a precursor to diaphragmatic hernia.

Abnormal defects in the diaphragm include Bochdalek's hernia (remember B for back) in the posterior portion, Morgagni's hernia (which is more anterior), ruptures of the diaphragm and other hernias.

Calcification in the diaphragm is almost pathognomonic for asbestos exposure. Illustrated below are some of these "aunt Minnies".

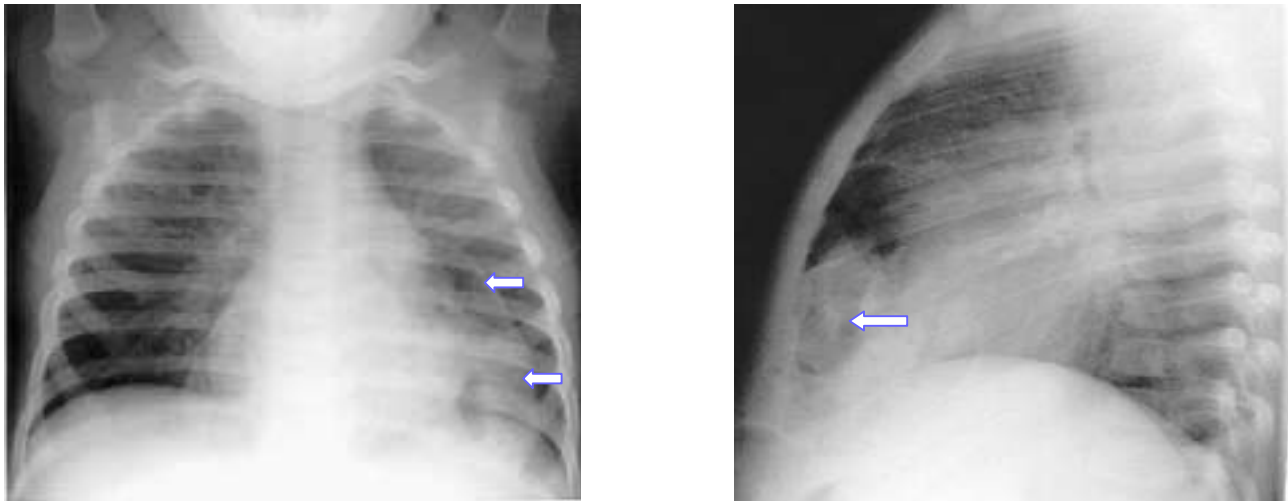


Figure # 56. Blue outlined arrows point to a gas filled structure superimposing the left heart border in the PA projection and seen to be anterior in the lateral projection. This is a classical presentation of a foramen of Morgagni hernia as confirmed in barium GI series in figure 57.

Images in figures 56 and 57 courtesy of Madigan Army Medical Center via the Internet.



Figure #57. Barium in the upper GI tract confirms a loop of bowel has herniated through the foramen of Morgagni.

A Bochdalek hernia, demonstrated below, is the most common of the diaphragmatic hernias and the most common surgical emergency of the neonate when it compromises lung capacity.

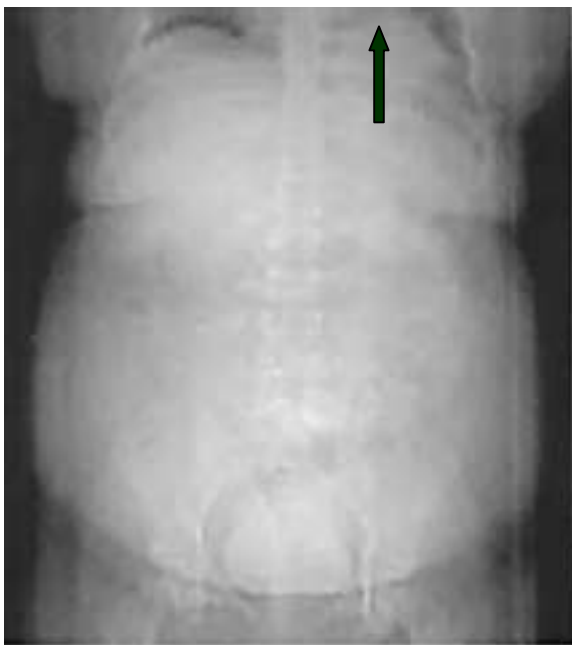
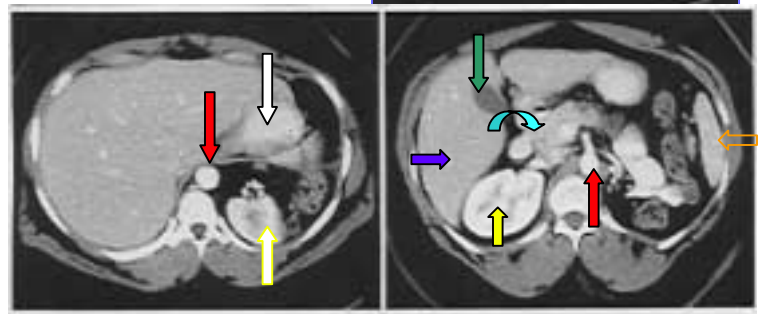
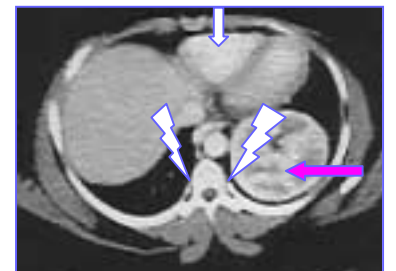


Figure #58. Dark green arrow shows location of Bochdalek hernia.

Case courtesy of J. Kevin Smith, MD, PhD. U. of Alabama Dept. of Radiology via the Internet. UAB Teaching files. Reprinted with permission.

Figures # 59 and 60 (below).

- White -contrast in distal stomach
- Pink - herniated stomach
- Orange-spleen
- Red - aorta
- Yellow- kidneys
- Blue - rt. lobe of liver
- Green - gall bladder
- Turquoise- pancreas
- Lightning bolts- diaphragmatic crus



Figures # 60 & 61 (right and below right).
Red arrows point to diaphragmatic calcifications in this patient with documented asbestos exposure.

The last major system to evaluate in the chest radiograph aside from a couple of other tips is the bony thorax. It requires just one rule: Look at every bone! I tell my students that after looking at chest radiographs for 30 years I can usually see everything at once but that it took years of practice and looking at every bone before I felt comfortable with it. I still carefully examine every bone, (now using a magnifying glass) if looking for fractures or metastatic pathology. I further inform them that to reach a level of competence, the practice of scrutinizing each bone is an absolute necessity, and that to program that computer between their ears to easily spot abnormalities of the bony thorax can not be done in a short period of time. Just to illustrate the point, see if you can spot the bony abnormalities in the following figures before reading the answers under each picture.

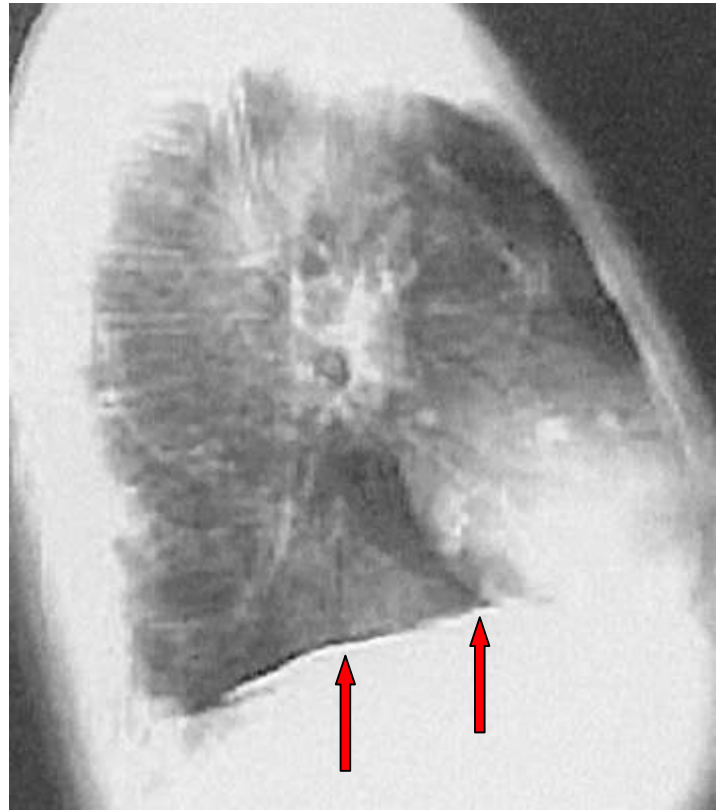
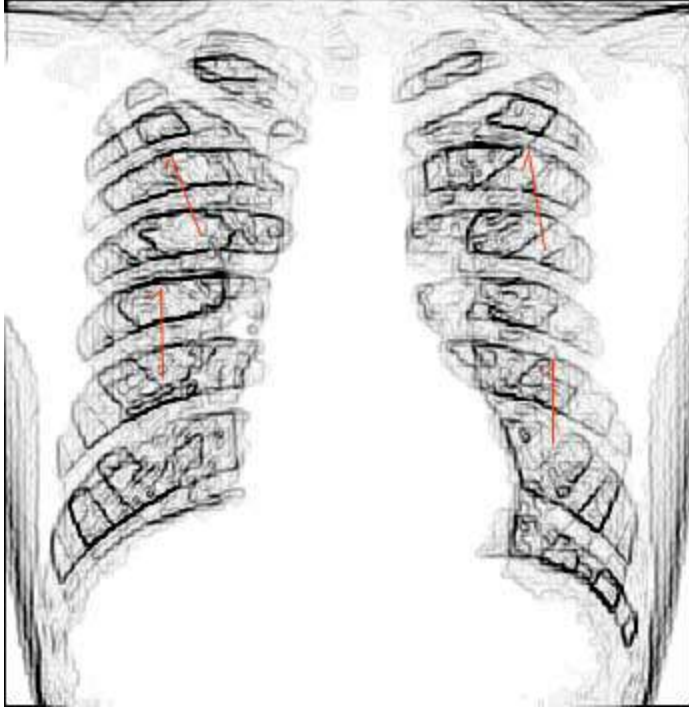




Figure #63. See if you can spot any bony abnormalities (subtle) before referring to the sketch below.

Computer sketch of figure 63 (left). Red arrows point to rib notching in this patient with coarctation of the aorta.



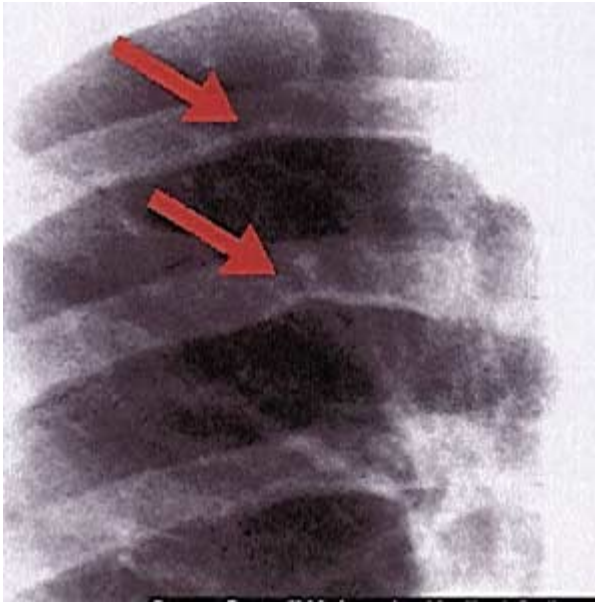
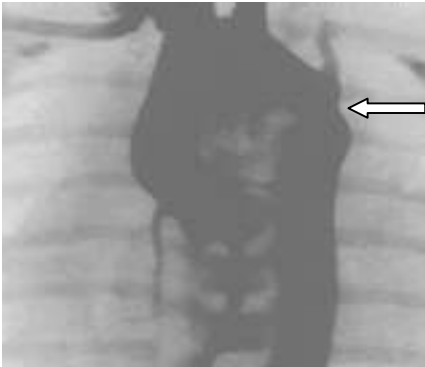


Figure # 63a (left). Here's another case of rib notching (red arrows) in a patient with coarctation of the aorta. The negative study of an aortic arch angiogram in this same patient shows the coarctation (white arrow) in Figure # 63b (below). Films courtesy of Cornell U. Medical College via the Internet.



The next case (below) demonstrates another bony abnormality that may be difficult to see for the inexperienced eye. See if you can spot it.



Figure # 64(above). Look carefully at the bony thorax. Can you spot an abnormality?

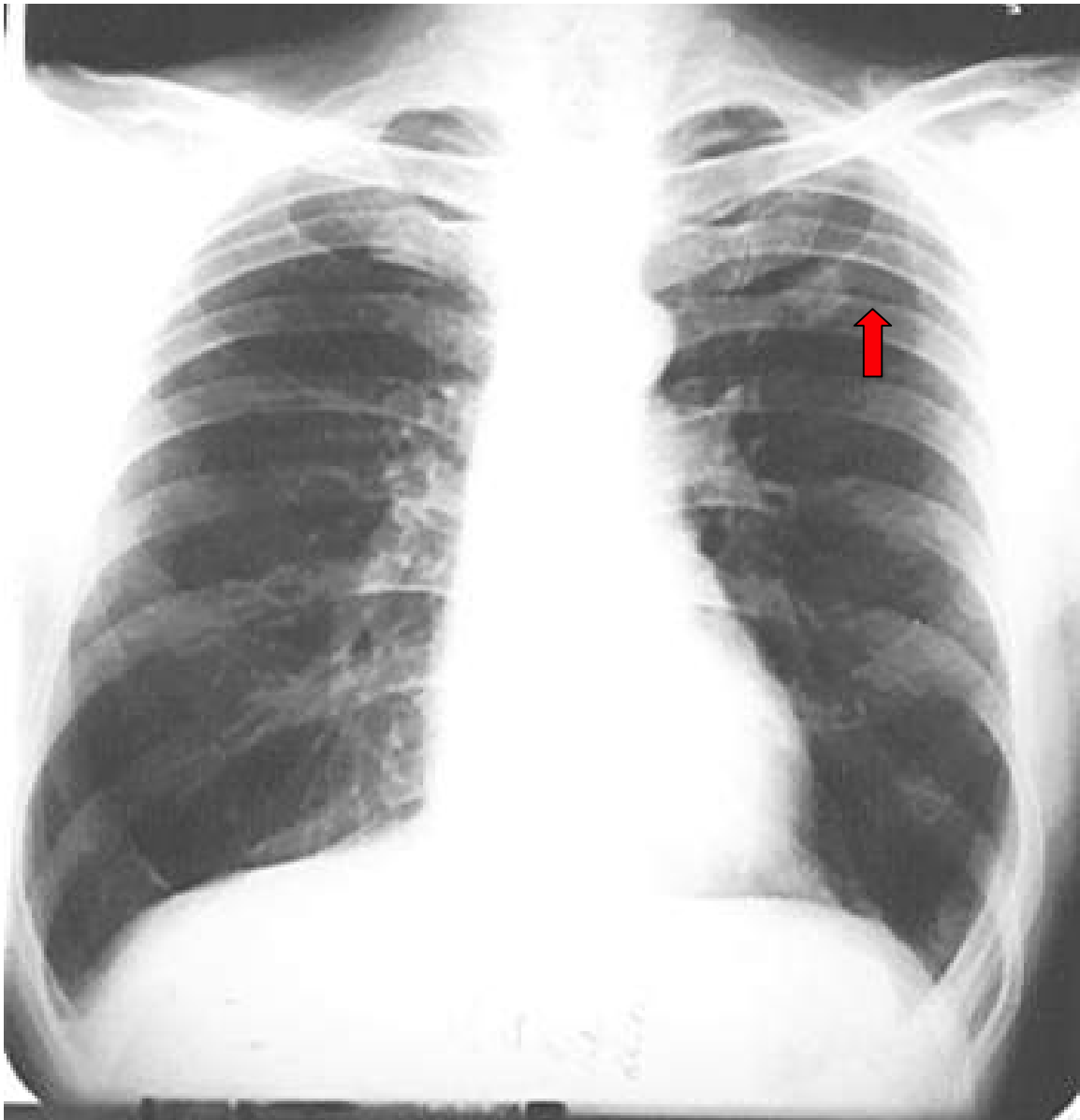


Figure #65. (above). Red arrow points to the inferior margin of the left second rib. There is no discernible inferior cortex. Tomograms of this area shown in figures 66 and 67 on the next page demonstrate the bone destruction caused by metastatic carcinoma. (A tomogram or laminogram is a technical study that blurs everything on either side of a designated focal point, which can be adjusted from the height of the x-ray table on which the patient lies. Thus by “stepping through” an area of interest fine line detail can be ascertained).



Figures # 66 and 67. Red markers and arrows show the rib destruction caused by metastatic carcinoma.

Aside from the systems evaluation of the chest radiograph, remember a couple of other important tips: 1) check the patient's ID, 2) compare the ends of the clavicles 3) check the left and right markers, 4) look at the corners of the film.

If you use a system, preferably the one we gave you here, it won't be long before you will begin to see things that you would have missed before. Remember for the chest it's:

LUNGS
HEART
MEDIASTINUM
DIAPHRAGM
BONY THORAX
CORNERS
ID-CLAVICLES
RIGHT & LEFT MARKERS

CHAPTER THREE

ABDOMEN

A system for evaluation of the abdomen includes a look at the abdominal gas pattern, the psoas and renal shadows, the edge of the liver and spleen, the preperitoneal fat lines, a search for abnormal calcifications, and a review of the skeletal structures. Again one should memorize this short checklist in some order:

ABDOMINAL GAS PATTERN
PSOAS AND RENAL SHADOWS
LIVER AND SPLEEN
PREPERITONEAL FAT LINES
ABNORMAL CALCIFICATIONS
BONY SKELETON

The gas pattern evaluation includes identifying large vs. small bowel gas, a look for dilated or obstructed appearing loops, localized collections, extraluminal gas, volume of gas, extent of fecal material present in the large bowel and air fluid levels.

This sounds like a lot to consider, but in actuality the student will quickly make a decision as to whether or not the pattern is normal. If it is not, one then has to decide why not, and also if the pattern is specific or non-specific. In our department we routinely include an upright chest PA view with any order for abdominal films unless a KUB (KUB is a scout film of the abdomen) is specifically requested. We also include either an upright or decubitus film depending on the patient's condition.

The chest film is included for two reasons:

- 1) Many chest conditions such as pneumonia or pleural effusions can present as abdominal pain and
- 2) It gives us a chance to look at the diaphragm and for free air.

The upright or decubitus view lets us look for localizing signs such as air fluid levels or isolated and dilated loops of bowel. It also gives us another crack at eliminating free air as a cause of the patient's symptoms. Sometimes we are only given a single view to interpret, especially when the film comes from an outside source (St. Elsewhere?), but regardless, the system to learn applies to all views of the abdomen and includes the above checklist.

If one observes gas filled, dilated loops of bowel, we must then decide whether or not we are dealing with an adynamic ileus, an obstructive ileus, a localizing phenomenon such as might occur with appendicitis, cholecystitis or pancreatitis (sentinel loop), or a natural finding as occurs with aerophagia in a crying child or air forced into the gut during general anesthesia.

It is also important to recognize whether or not the gas is in large or small bowel. That is not always possible, but one of the things that helps tell the difference is to see if the haustral markings extend all the way across the loop or only part way. Colon haustral markings typically traverse only part of the way across the loop, whereas small bowel haustra usually extend the full diameter of the loop. Figures 68 and 69 illustrate the difference.

Another diagnostic pearl is the direction of orientation of the dilated loops. Obstructive ileus is usually oriented in an up and down or vertical pattern, whereas paralytic ileus is usually oriented in a transverse plane.

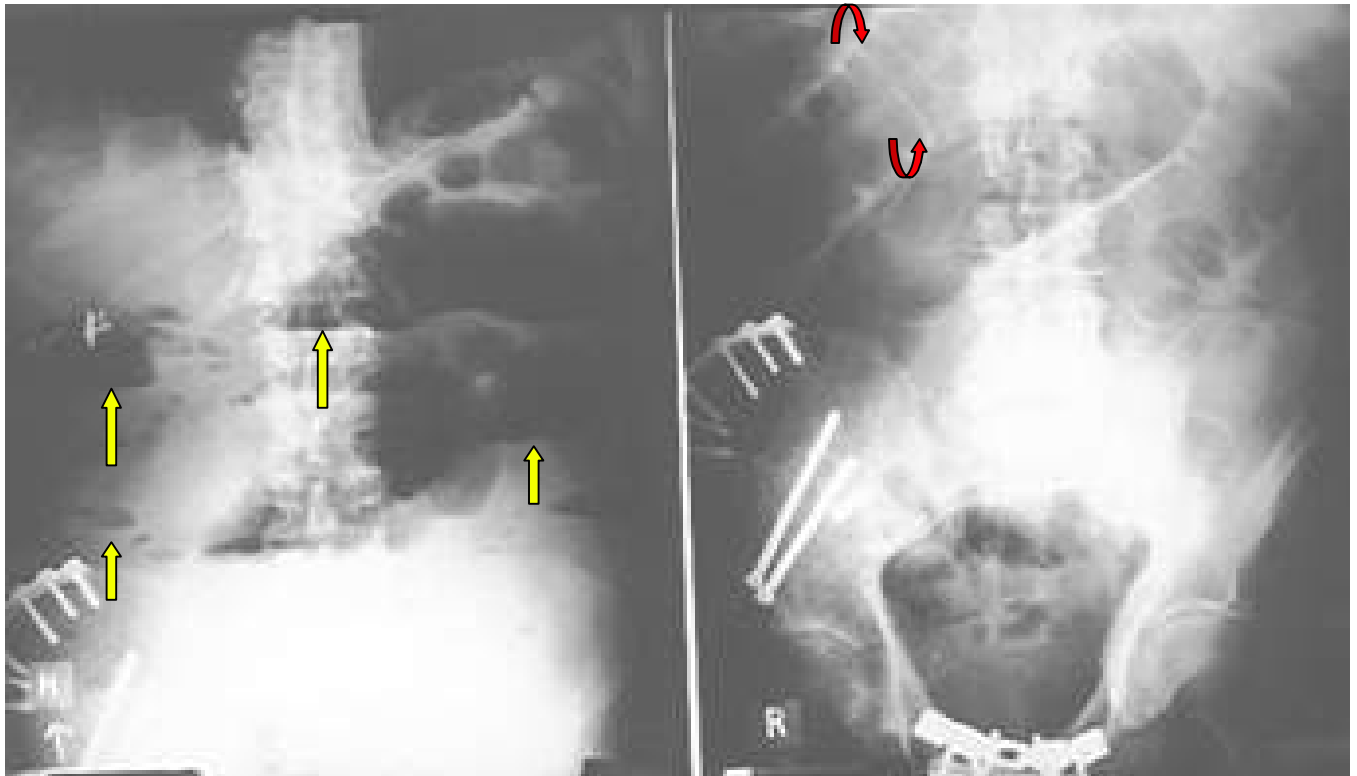


Figure # 68. Yellow arrows point to multiple air-fluid levels in this patient with obstructive ileus, The red curved arrows show the haustral markings extend the entire diameter of the bowel, thus identifying it as small intestine. Note there is very little gas in the colon, that the small bowel is markedly dilated and that these loops are vertically oriented.



Figure # 69. Red arrows point to haustra that do not traverse the diameter of the bowel indicating the dilated loops of this portion are likely colon. The blue arrows show haustra traversing the diameter of dilated small bowel. Note that both small and large bowel are dilated and that the loops have a relatively horizontal orientation. This patient has a paralytic or non-obstructive ileus, with gas extending all the way to the rectum.

Localization of gas in the intestine in a dilated segment or region occurs with a confined inflammatory process such as appendicitis (right lower quadrant), cholecystitis (right upper quadrant) or pancreatitis (sentinel loop). Gas may also appear in bile ducts or other extra-luminal locations under certain conditions. Figures 70 to 73 illustrate these phenomena.

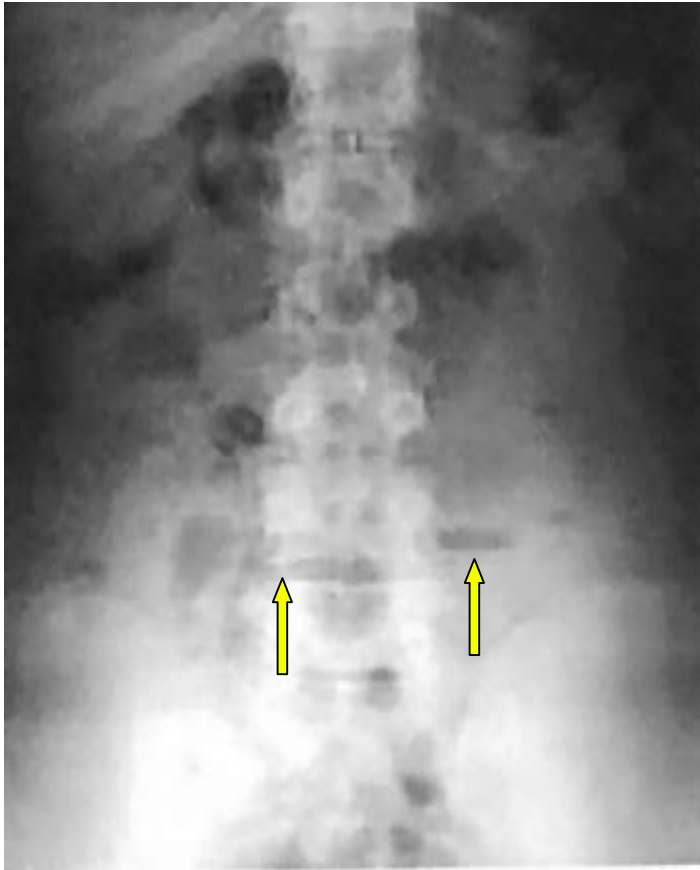


Figure # 70 (left). Upright film of a patient with acute appendicitis. This patient presented with epigastric pain which migrated to McBernie's point. Note air-fluid levels in the lower abdomen (yellow arrows). These radiographic findings are not specific, but do tend to localize an inflammatory process, and appendicitis should be included in the differential diagnosis. The next figure (#71) is a coned-down view of the right lower quadrant in this same patient.

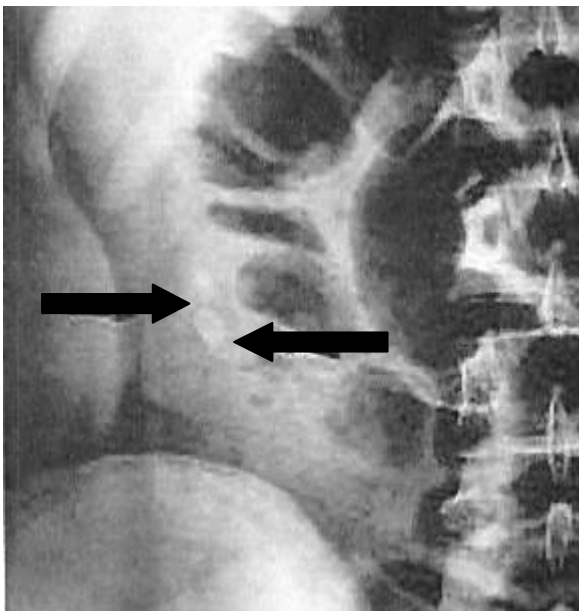


Figure # 71(left). Black arrows point to two oval-shaped calcifications in the right lower quadrant consistent with fecaliths of the appendix. These represent calcified bile contents associated with appendicitis. Remember that abnormal calcifications are the fifth item on your abdominal film checklist! By the way, I don't mean to imply that plain film radiographs are the imaging modality of choice for suspected appendicitis. Ultrasound studies are recommended for children, and US or CT may be helpful in adults. Nothing beats clinical suspicion, however, and persistent tenderness at McBernie's point is worth laparoscopy or laporotomy.

Figures 70 and 71 courtesy of U. of Iowa's Virtual Hospital via the Internet.

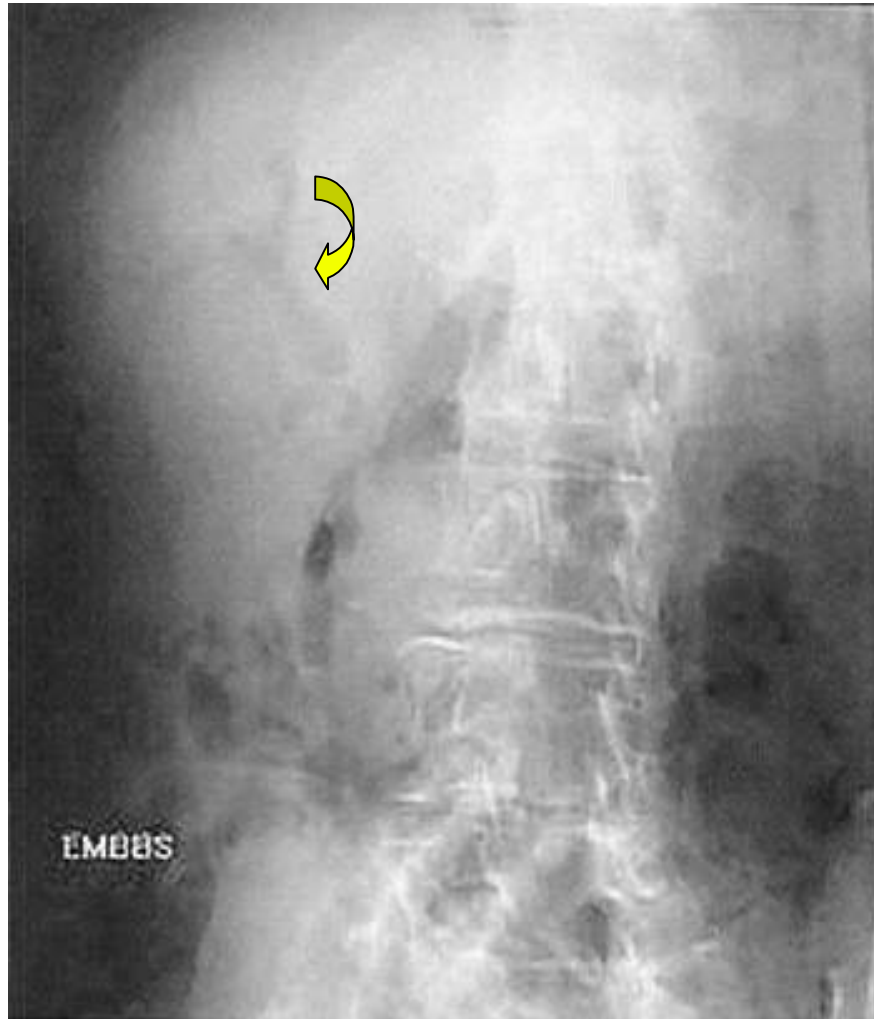


Figure # 72. Yellow arrow indicates gas in the biliary ducts system, which occurred after gallstone passage in this patient. Gas can also be seen in bile ducts after certain kinds of GI surgery, in emphysematous cholecystitis, or pyogenic infections with gas producing organisms. History is necessary to make an intelligent diagnosis. Image courtesy of EMBBS radiology library via the Internet.

Free air in the abdomen can be localized under the diaphragm or in the flank in viscus perforations as seen in upright chest films or decubitus views respectively. It is important to know the history when calling free air since it is to be expected after abdominal surgery or intraperitoneal endoscopy. Also occasionally air can be discovered superimposed between the liver and diaphragm that is not extraluminal but instead within an inter- positioned loop of bowel. When that occurs it may be necessary to obtain additional imaging to exclude a perforated hollow viscus. See figure 73 on the next page.

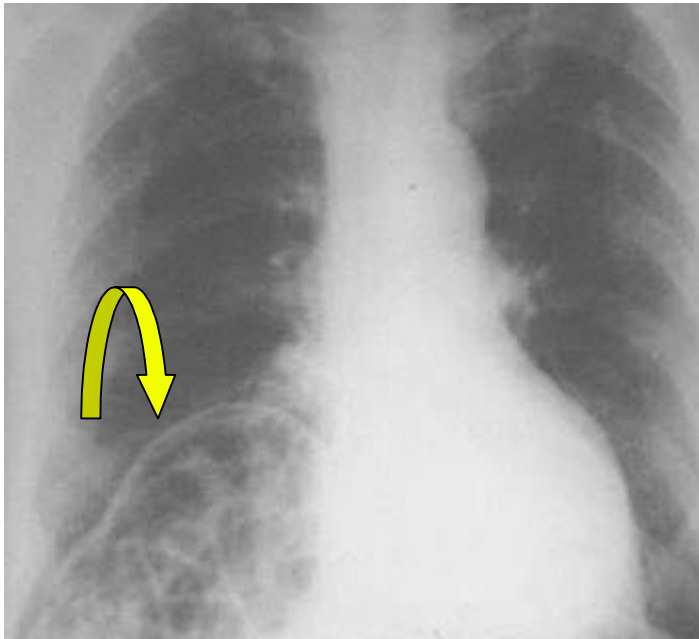


Figure # 73 (left). Yellow arrow points to the anterior leaf of the right hemidiaphragm, which has an eventration. Inferior to the diaphragm is gas filled bowel with haustral markings. Free air would layer out and since haustral markings are evident, the diagnosis of superimposed bowel between diaphragm and the dome of the liver can be made with confidence, at least in this case. Figure # 74 courtesy of Middlesex Hospital Trust via the Internet

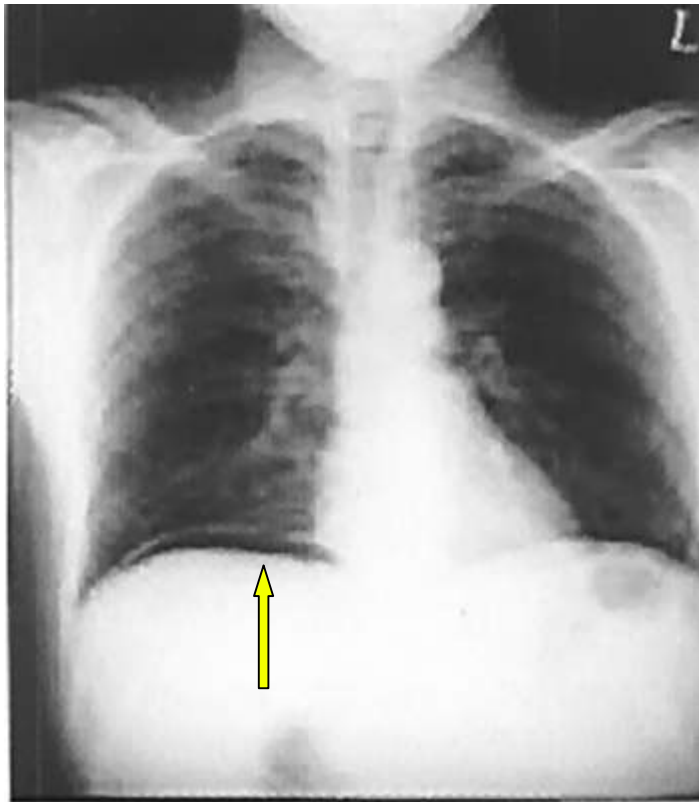


Figure # 74 (left). Yellow arrow points to an abnormal accumulation of gas representing free air under the diaphragm in this patient with a perforated duodenal ulcer. Image courtesy of Netmedicine Medical Photographic Library via the Internet

Diffuse free air in the peritoneal cavity outlines the peritoneal reflections if the film is a flat plate only and is often said to give the appearance of a football effect if the pneumoperitoneum is not under tension. In that case the falciform ligament may be outlined as the “laces” of the “football” (air) which outlines the entire abdominal cavity. Although the football sign of free air is not entirely rare, it is not common either since most cases of pneumoperitoneum are diagnosed by an upright film of the chest or a lateral decubitus film of the abdomen. I don’t think I’ve seen more than a dozen football signs in over 30 years. Figure 75 shows a pneumoperitoneum under tension in an infant with a perforated hollow viscus.

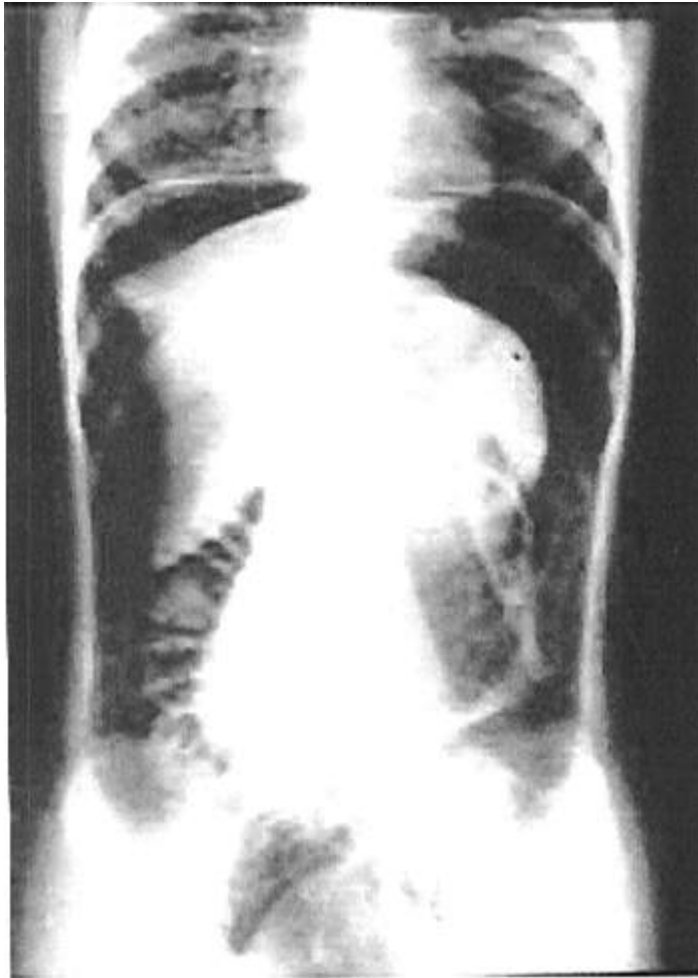


Figure # 75 (left). Abdominal organs are compressed by free air under tension in this infant with a perforated gut. Image courtesy of the U. of Kentucky via the Internet.

Gas patterns in the abdomen may offer specific signs to the astute clinician/radiologist too. One of these is the crescent sign associated with intussusception. It occurs when the leading edge of the intussusceptum projects into a pocket of gas as seen in figure 76. Another sign associated with intussusception is not really part of the gas pattern, but can be recognized if you are clinically suspicious and look for it. It is called a target sign and is the result of layers of peritoneal fat surrounding and within the intussusepted bowel, which is water density. Figure 77 shows a classic target sign, which is very subtle.

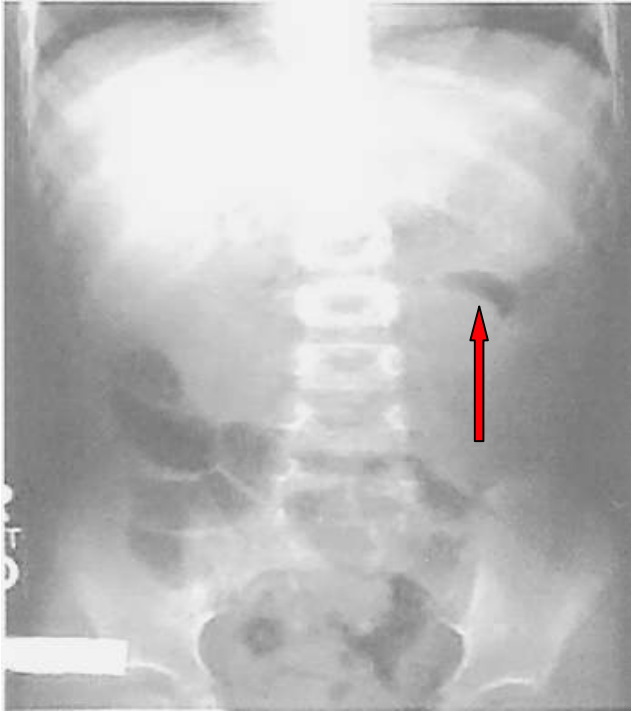


Figure # 76 (left). Red arrow points to a classic crescent sign in a child with ileocolic intussusception. Figures 76 & 77 courtesy U. of Hawaii via the Internet.

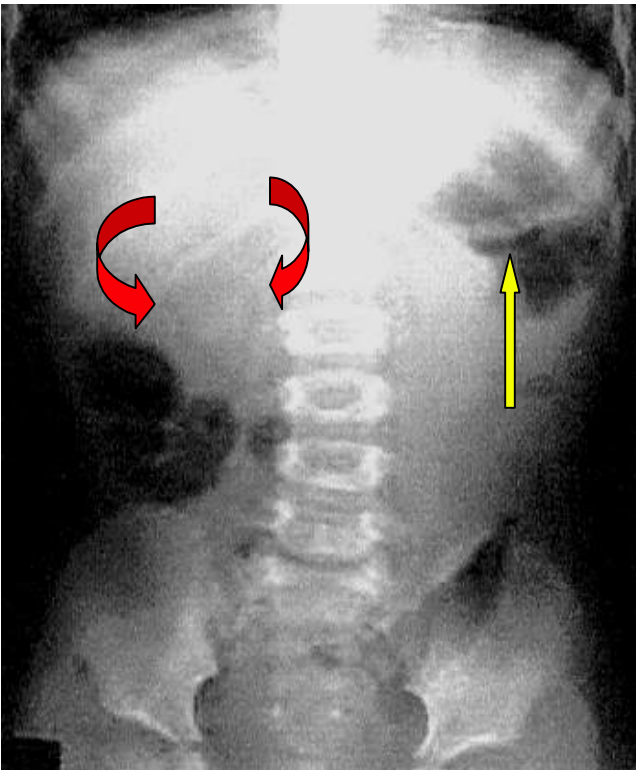


Figure # 77 (left). Red arrows point to a subtle target sign of intussusception. This patient also has a crescent sign that is obscured by adjacent bowel gas (yellow arrow).

Evaluating the psoas shadows is important because it gives us insight into not only the status of the retroperitoneum but also whether or not the patient is guarding the belly. If, for example, the patient is guarding the right side of the abdomen as occurs with acute appendicitis or cholecystitis, the right psoas muscle will be contracted and thus not as sharply outlined as the left. In cases of retroperitoneal hemorrhage or retroperitoneal fibrosis, the psoas shadows may disappear altogether.

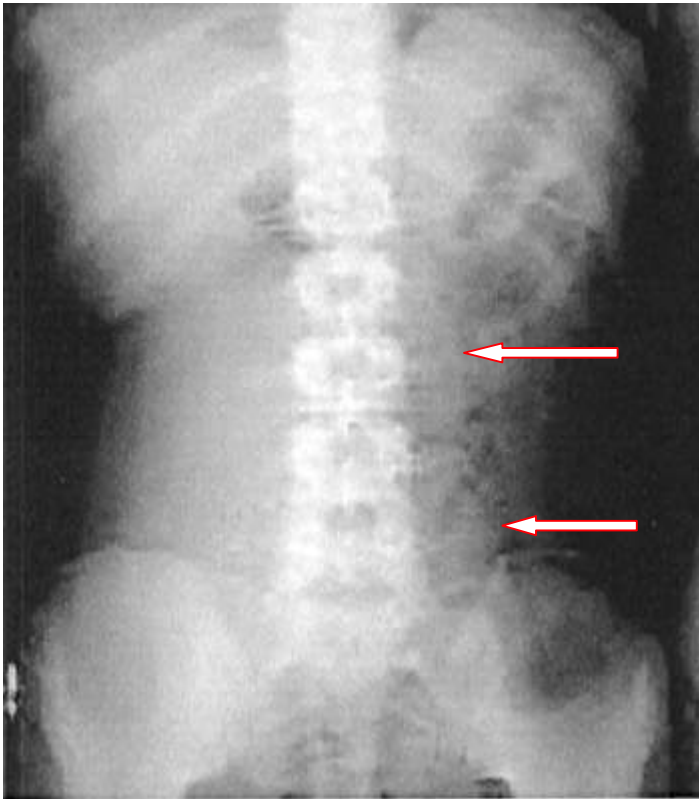


Figure # 78. Red outlined arrows point to a normal left psoas shadow in this gunshot victim. Note there is no discernible Right psoas shadow. The psoas muscles are usually seen Because of adjacent retroperitoneal fat. In this case retroperitoneal hemorrhage (water density blood) silhouettes out The right psoas margin.

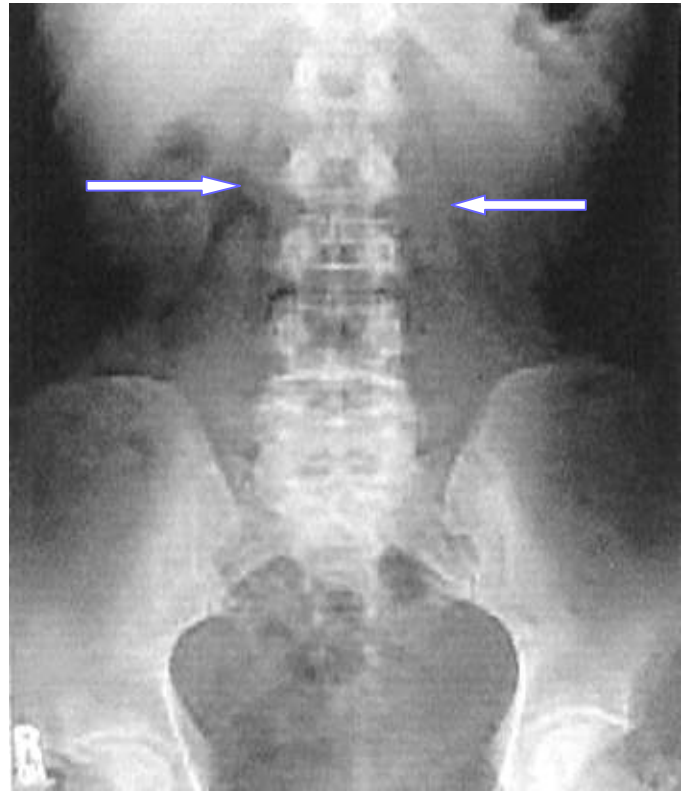


Figure # 79. Blue outlined arrows point to normal psoas muscle margins. Compare to figure 78 at the left.

The renal shadows are usually easily seen because of the contrast of the darker fat in Gerota's fascia outlining the kidneys. Note the normal renal outlines in figure 80 as opposed to the patient with horseshoe kidneys in figure 81.

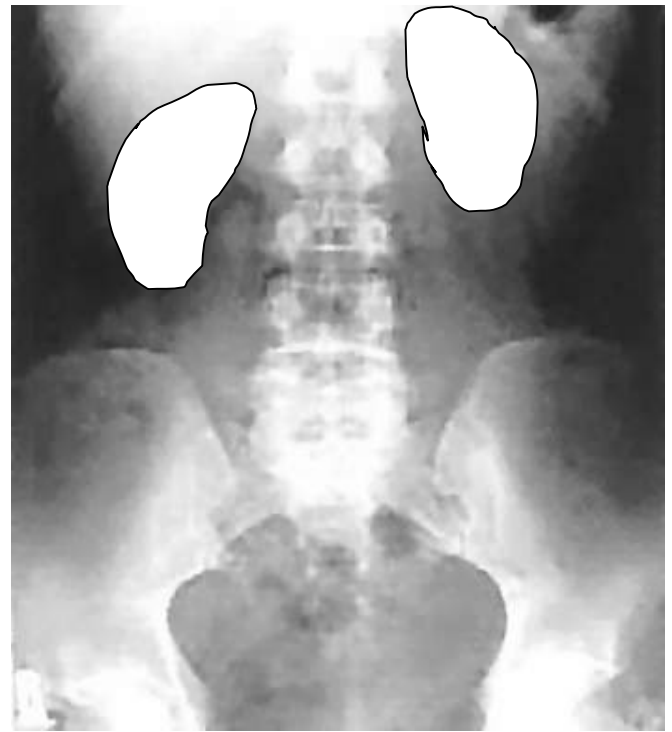


Figure # 80. Normal KUB film of the abdomen. It takes some scrutiny, but you can usually see the renal outlines because of Gerota's fascia (fat density) surrounding the kidneys. It is much easier when the patient's bowel is prepared as is usual before an IVP (Intravenous Pyelogram – kidneys studied by injecting dye visible on radiographs). exam. In the above example, we have outlined the kidneys in the second part of the figure, so that you can test your observation in this patient with unprepared bowel.

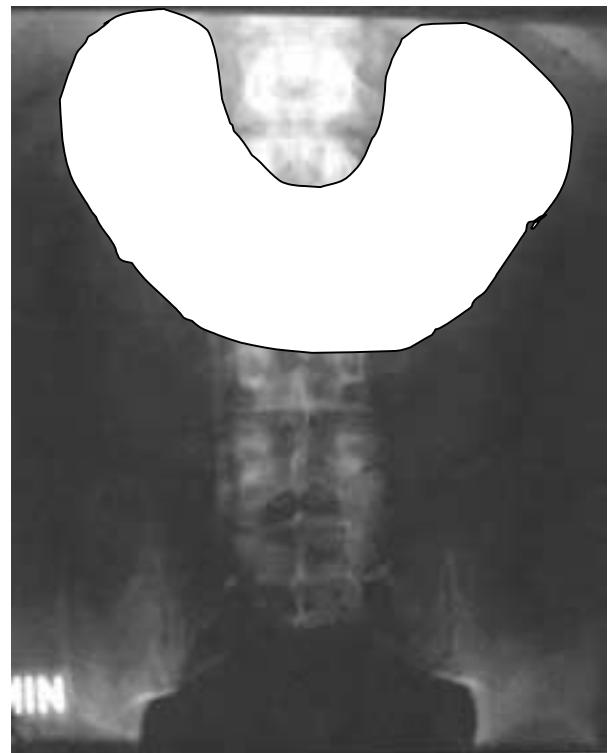


Figure #81. Although we don't have the KUB film of this patient with horseshoe kidneys, you can easily see the renal outlines, and the diagnosis can be made without the contrast study. Images courtesy of Columbia U. Dept. of Radiology via the Internet.

Lumps and bumps of the renal outlines are frequently normal findings due to developmental lobulations or columns of Bertin. Even the experienced radiologist will often be unsure of their significance however, and it frequently takes additional imaging to exclude pathology. Note the similarity between the patient with a "normal" lobulated kidney vs the patient with renal pathology in the next illustrations.

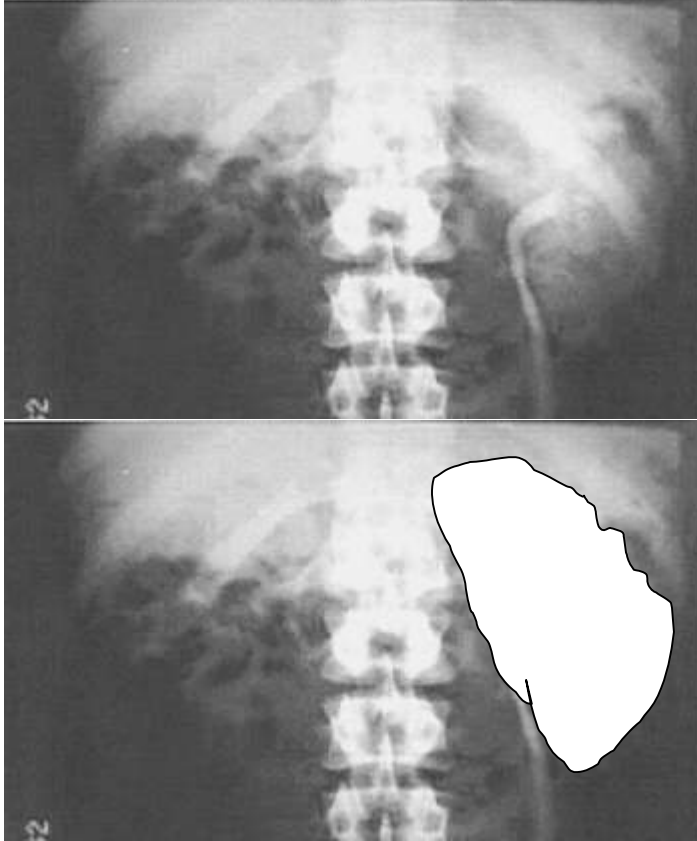


Figure # 82 (left). Contrast IVP study showing lobulated outline of the left kidney. The lobulations may be the result of columns of Bertin or possibly the result of cortical parenchymal loss due to infarcts or previous bouts of pyelonephritis. A good history would be necessary to evaluate their current importance, but the lobulations are likely of no clinical significance. We see them often on KUB films and IVP studies. By the way- the right kidney in this patient is in an ectopic location in the pelvis and not visible in the coned-down films to the left.

Figure # 83 (right). Nephrogram phase of a renal angiogram demonstrates the bumpy cortical outline of a patient's kidney that has acute pyelonephritis.



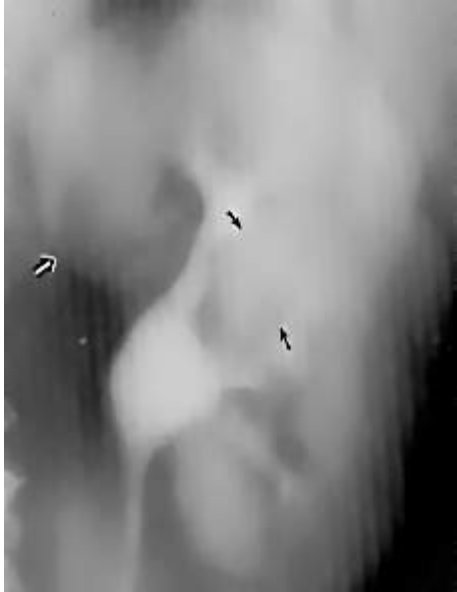


Figure # 84 (left). IVP tomographic study showing bumpy outlines of a kidney due to normal developmental lobulations or columns of Bertin. Black arrows point to normal islands of functioning renal tissue. Figures 83, 84 and 85 from the Radiologic Clinics of North America Apr. 1976. Articles by Drs. Hattery, Hartmann and Williamson.

Figure # 85 (right). Yellow arrow points to a bump on the left kidney of a patient that is more serious-this time a renal carcinoma as indicated by the neovascularity shown in the accompanying angiogram in Figure 85b (below).



The teaching point of the above illustrations is that if you are not sure of normalcy of the renal outlines, either on plain films or with IVP tomography, then get additional imaging such as ultrasound or CT!

The position of the kidneys is also important. Although the left kidney is closer to the diaphragm, i.e. higher, than the right, it can be a normal variant for it to be lower about 10% of the time. However, if it is seen to be in a lower position than the right kidney, that is a red flag to exclude displacement by either an enlarged spleen or some other retroperitoneal or intraperitoneal mass. Figure 86 below illustrates the point.

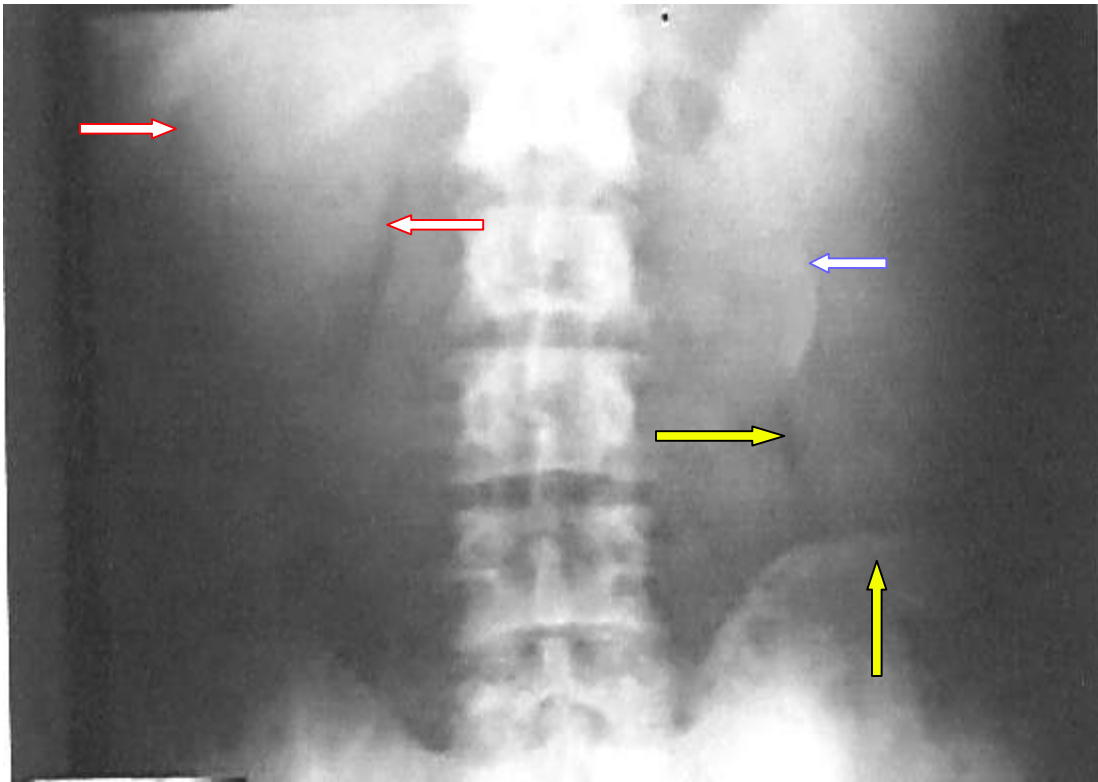


Figure # 86. Blue outlined arrow points to the lateral margin of the left kidney, which is seen to be in a lower position than the right kidney (red outlined arrows). This finding is a red flag to look for an enlarged spleen or other mass displacing the left kidney. Sure enough, the yellow arrows indicate the tip of enlarged spleen! Film courtesy of George Simon Collection via the Internet.

It's always easy to check for renal calcifications while your eye is on the kidneys, but if you don't stick to checklist system, it's easy to fixate on the obvious pathology and thus miss something more important. One of my colleagues, Dr. Norb O'keefe, former chairman of the University of North Dakota School of Medicine's Department of Radiology, used to have a sign on his desk that stated "**whatever it is, look at it last!**", to remind him not to fixate on the obvious.

The edge of the liver is also usually easily demarcated by the contrast of a water density organ bordered by peritoneal fat or gas filled bowel. Remember that Reidel's lobe can extend to below the iliac crest and does not indicate hepatomegally, although that is obviously one of the conditions to exclude when interpreting abdominal films. The liver edge can also be silhouetted out by ascitic fluid and an enlarged liver can displace bowel inferiorly and to the left.

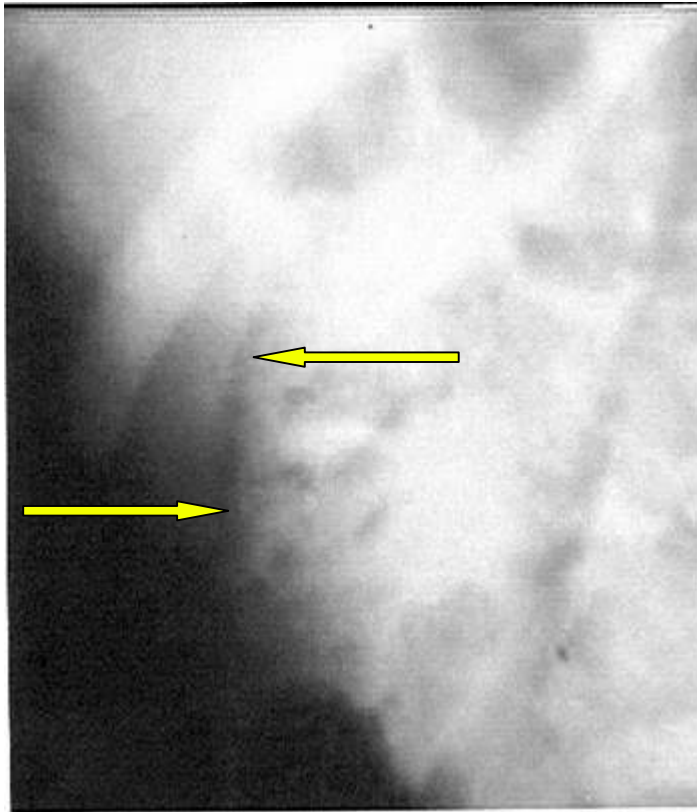
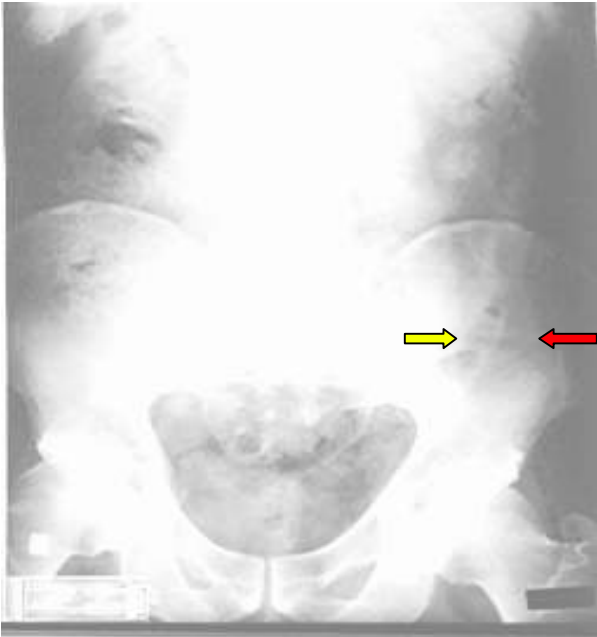


Figure # 87 (left) Yellow arrows indicate the normal fat line marking the edge of the liver. In this case the fat line is also abutting Gerota's fascia adjacent to the right kidney. If ascitic fluid is present the edge of the liver may disappear due to the silhouette sign. Film courtesy of George Simon Collection via the Internet.

Checking on the edge of the liver reminds us to evaluate the spleen as well. Note the splenomegaly and displaced left kidney in figure 86 on the previous page.

The preperitoneal fat lines (the fourth item on the checklist) are thin lines of fat that outline the peritoneal reflections as demonstrated in figure 88.

Figure # 88. We have deliberately manipulated brightness and contrast in this image to demonstrate the band of fat density (red arrow) along the lateral margins of the abdomen. Note that gas filled bowel (yellow arrow) abuts the preperitoneal fat line in this normal KUB film. When fluid such as ascities or blood is present in the peritoneal cavity, the bowel gas is usually displaced away from the fat line.



Gas or fecal filled bowel usually borders the fat lines, but if anything like fluid or blood comes between the bowel wall and the fat line, it is a good clue as to what is going on in the patient's belly because it causes the space between them to widen. This phenomenon is called by radiologists "widening of the flank stripe" or "displacement of the fat line". Note the widened flank stripe in figure 89 in a patient with ascities. Go back and compare to the normal KUB study on the previous page.

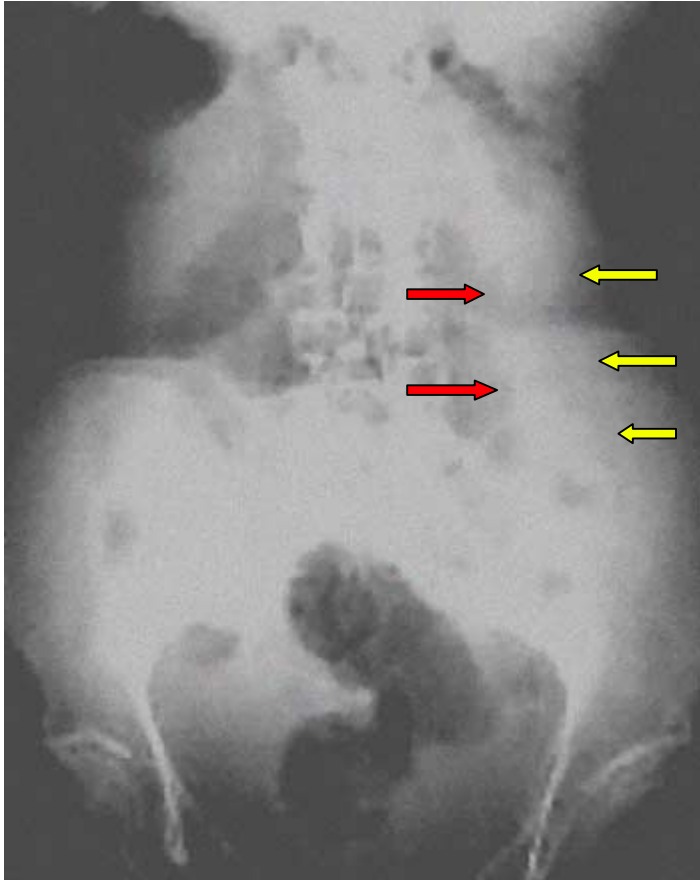


Figure # 89 (left). Notice the increased distance between the preperitoneal fat (yellow arrows) and the edge of gas-filled bowel (red arrows) in this patient with ascities.

Calcifications in the abdomen, the fifth item on the checklist, can be "Aunt Minnies" such as is seen in figure 90 in a patient with gallstones, or in figure 91 in a patient with a staghorn renal calculus.

Figure # 91 (right). Red outlined arrow points to classic "Aunt Minnie" of calcified gallstones in the right upper quadrant in this KUB study.





Figure # 91 (left). There is not much question about the diagnosis here. The red outlined arrow indicates a classic staghorn renal calculus in this “Aunt Minnie”.



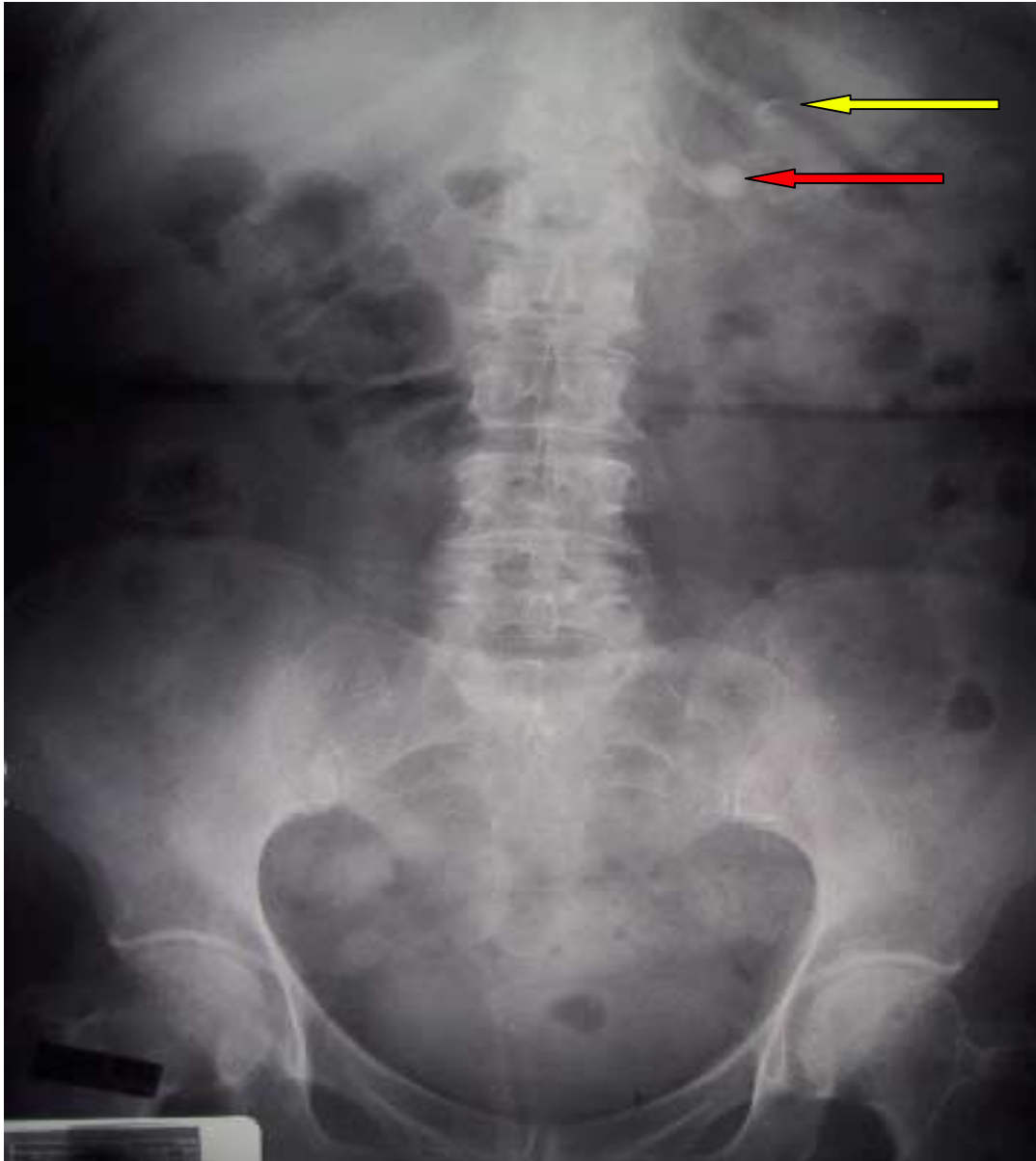
Figure # 92 (left). Black arrows point to thin lines of calcium deposit in this patient with abdominal aortic aneurysm. Look for aortic and other vascular calcifications as a part of your routine in evaluating all abdominal films. Films courtesy of an article by Drs. Jamie D. and Steven M. Santilli, American Family Physician, Sept. 15, 1997 via the Internet.

Splenic artery aneurysms or pancreatic calcifications are another couple of "Aunt Minnies". More frequently, however, the student will be called on to search for a ureteral stone in a patient with renal colic or flank pain. These can be difficult to separate from phleboliths in the pelvis and it may be necessary to utilize ultrasound to look for hydronephrosis or do an IVP to exclude renal lithiasis especially when the index of suspicion is high or there is microscopic hematuria.

Ureteral stones are such a common problem in the ER that we won't dwell on them here. Just drop down to your Radiology department to see a few good cases.

See figure 93 for typical pancreatic calcifications (the location gives them away).

Figure # 92a (below). **Yellow arrow points to an Aunt Minnie, a splenic artery aneurysm. The red arrow points to another Aunt Minnie. Radiopaque medication in the upper gut.**



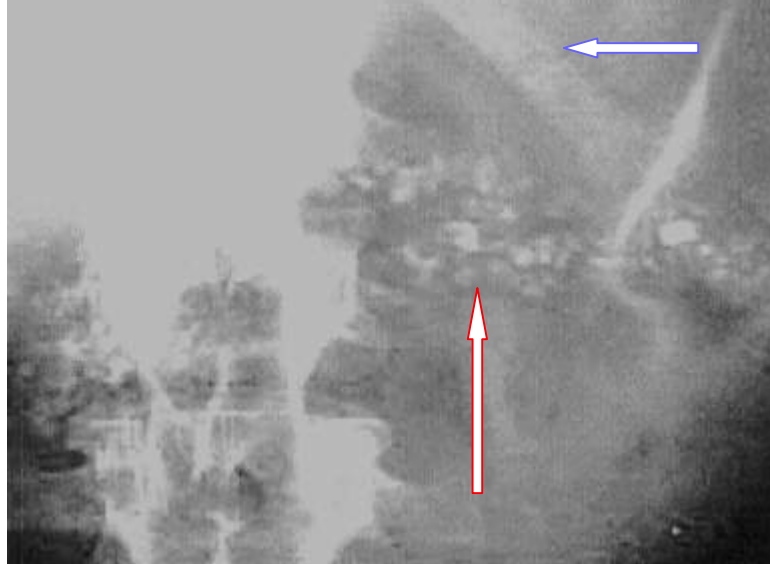


Figure # 93. Red outlined arrow points to large clusters of punctate calcifications in the location of the body of the pancreas consistent with chronic pancreatitis. The blue arrow points to the left twelfth rib. Courtesy of Bruce Brown, MD, U. of Iowa via the Internet.

The final item on the major checklist for the abdomen is the bony skeleton, and the same rule applies as it did for the chest, i.e. **LOOK AT EVERY BONE!** Just for practice see if you can spot the bony abnormality or abnormalities in figures 94-100 before reading the labeled answers.



Figure # 94 (left). Look at the vertebrae outlined by the gastric air bubble. (The rest of the digital reproduction is sub-optimal). What do you see? Refer to figure 95 on the next page.

Figure # 95 (right). The blue arrow indicates a markedly narrowed disc space at L3-4. The curved red outlined arrow shows a notch in the superior cortex of L-4, that may represent a Schmorl's node (more about that later). What would you do to clarify the issue? Answer: Get more views or additional imaging.

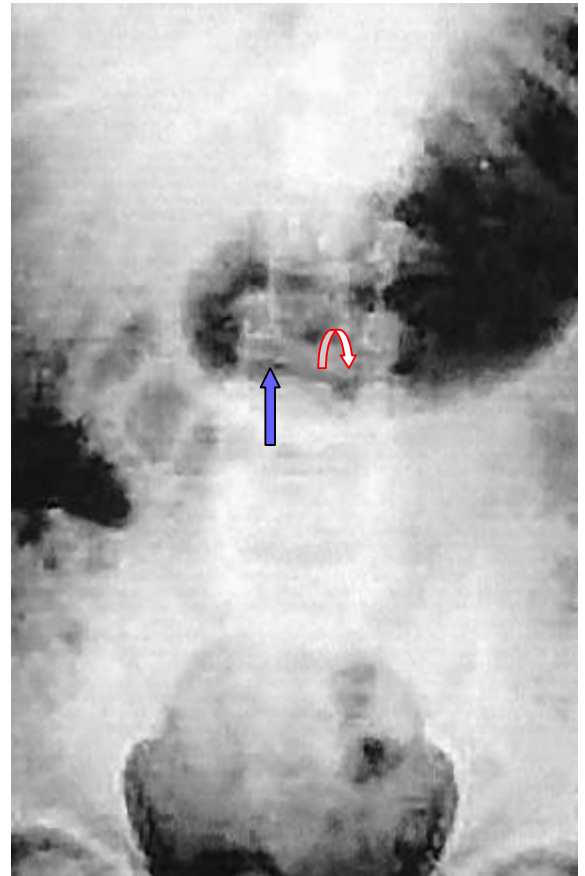


Figure # 96 (below). Transaxial and coronal CT images demonstrate cortical bone destruction (blue arrow). Note the loss of normal cortex (green arrows). The white arrows indicate abscess formation in both psoas muscles in this child with spinal tuberculosis. Films from www.childsdoc.org via the Internet.

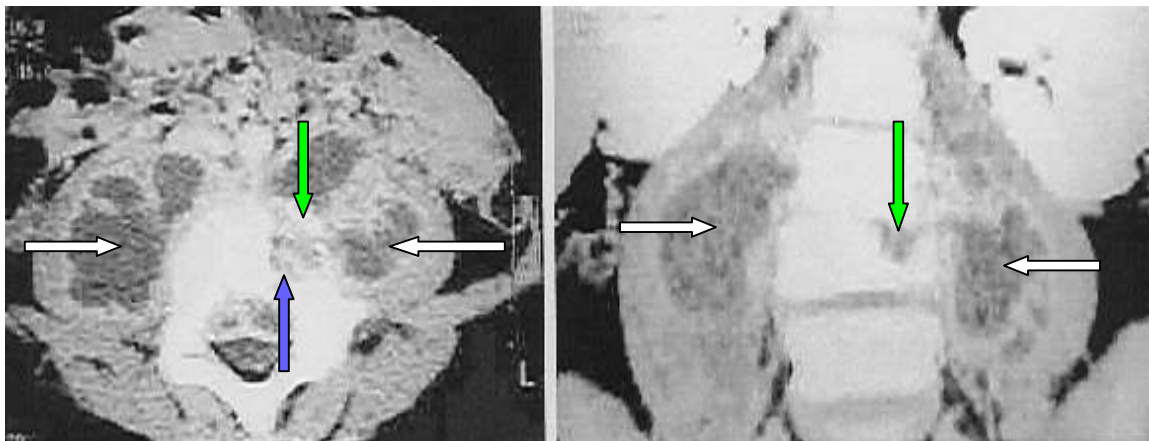




Figure # 97. This AP view of the pelvis is the same projection you would see in a full KUB study. Do the bones look normal? Refer to figure 98 to see if you are right. PS. Ignore the high contrast (white bone) in this reproduction and concentrate on cortical outlines.



Figure # 98 (left). Note the loss of definition of the posterior iliac crest (curved red outlined arrow) due to bone destruction in this patient with a plasmacytoma.



Figure # 99. Here's another case of bone abnormality picked up on a routine IVP examination. What do you see?

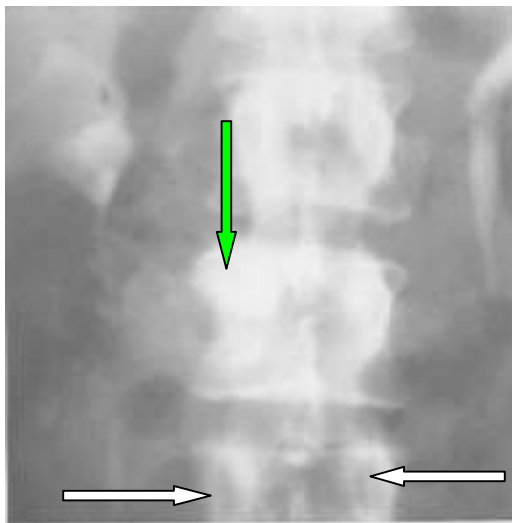


Figure # 100 (left). Note the normal appearing pedicles (white arrows) vs. the sclerotic pedicle (green arrow) on the vertebra one level higher in this patient with osteosarcoma of the vertebra.

One final reminder then, the system to remember for the abdomen is

GAS PATTERN

PSOAS & RENAL SHADOWS

LIVER & SPLEEN

PRE-PERITONEAL FAT LINES

CALCIFICATIONS

BONES

And, of course, you will also remember to check the patient's ID, left & right markers and the date, won't you?

CHAPTER FOUR

THE SKULL

With the advent of CT imaging plain view studies of the skull have become almost passé. I am reminded of the day my youngest son asked me "what was it like in the olden days Dad?" He was about 10 years old at the time. Well in the "olden days" of radiology I can remember as a resident sitting in front of a view box for hours on end with a real skull in my hands and the standard skull views in front of me just to learn the radiographic anatomy. I don't think it's necessary to spend a lot of time on that for the non-radiologist, but maybe a few tips are in order for those who will not have immediate access to a scanner, and who may have to screen cases by the old fashion methods.

The checklist for the skull includes:

1-SIZE AND SHAPE

2-BASILAR STRUCTURES

3-SINUSES AND MASTOIDS

4-SOFT TISSUES

5-CALVARIUM (for abnormal densities, lines, fractures)

The size and shape of the skull are important in kids in looking for premature closures of the sutures and in excluding hydrocephalus. Another one of the few measurements still valid to help you decide whether or not the skull size in an infant or child is normal is the cranial-facial index. Figure 101 gives the essentials.

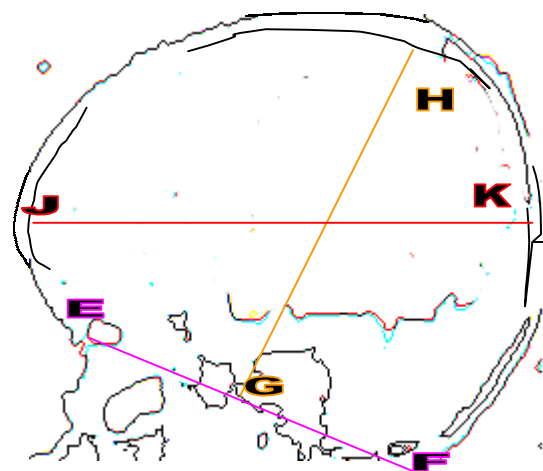
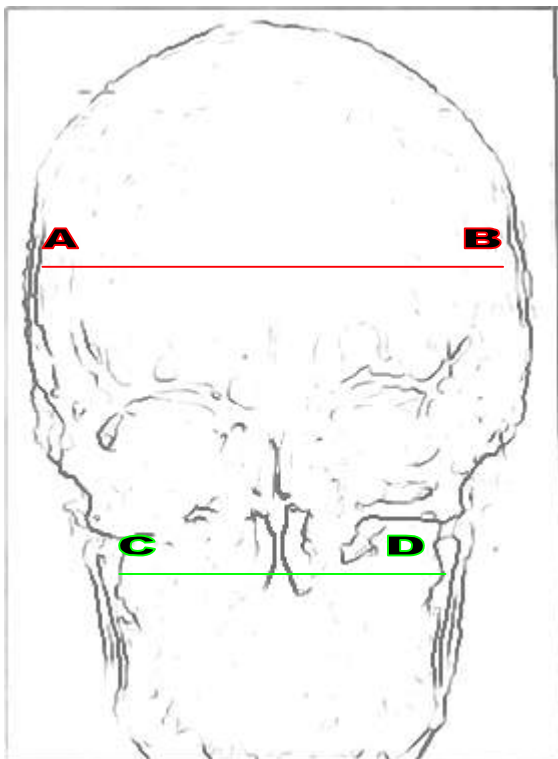


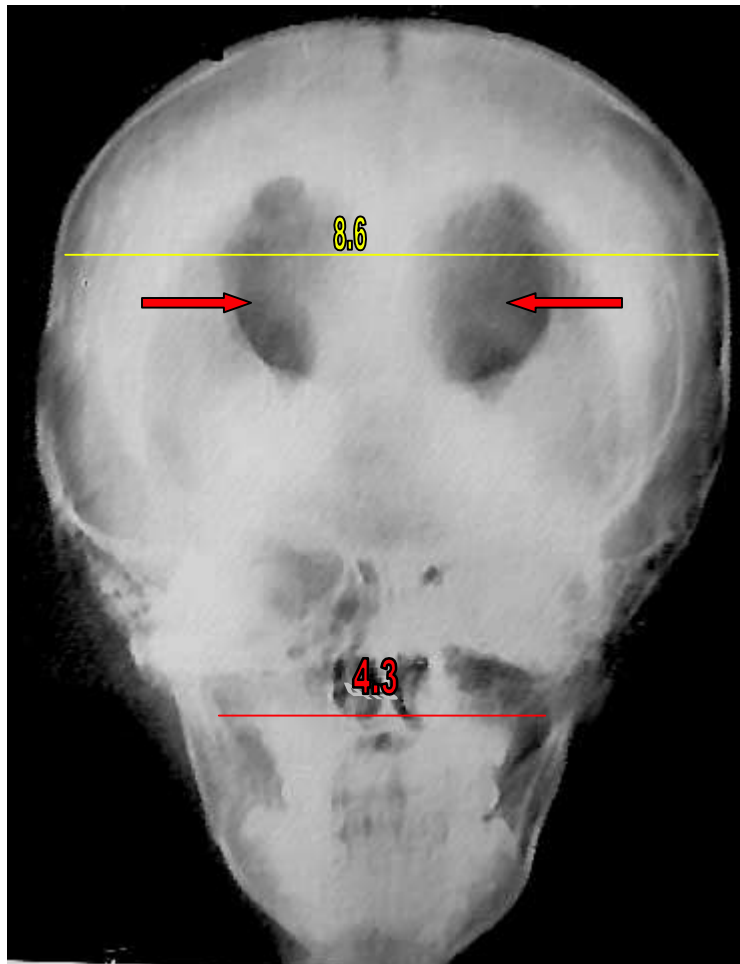
Figure # 101. (above and left). $AB+GH+JK$ divided by CD times 10 should give you a normal cranial-facial index of between 50 and 55. Measure the lines from the inner tables of the skull. The line CD is measured from the medial margins of the mandibular condyles. The line EF extends from the nasion to the opisthion, and the line GH is drawn at right angles from EF to the vertex of the skull. Anything over 55 is suspicious for hydrocephalus. Anything under 50 suggests premature closure of one or more of the sutures or some anomaly.

It's also true that an infant's head may be large with normal ventricles, or normal size with large ventricles (hydrocephalus), but these cases are unusual. The C-F index is a pretty good screen in borderline findings, when identification of abnormal head size is clinically not readily apparent.

Figures 102-105 show cases of hydrocephalus and premature closure of one of the sutures, which effects the shape of the skull.



Figure # 102 (left). There is no need for a cranial-facial index measurement in the case illustration here. Note the marked cranial-facial disproportion in this child with hydrocephalus!



Figures # 103 (left) and # 104 (next page) show a positive cranial-facial index in a child with hydrocephalus secondary to a tumor of the vermis of the cerebellum. The measurements are relative because of the reduced size of the radiographs, but remain valid since they are proportional to the original size and standard magnification present with tabletop films. The c-f index in this case measures just over 59. The dark areas (red arrows) represent air in the ventricles injected into the subarachnoid space via a lumbar puncture---an old fashioned diagnostic procedure called a pneumoencephalogram. These studies were hard on the patients, difficult to perform and difficult to interpret, but were the only way to see the ventricles prior to the invention of CT and MRI scanning. The c-f index measurements are intended for plain films of the skull at the radiologist's discretion (intuition?). We used them if the head looked a little bit large. The pediatricians or family practitioners using a tape measure picked up most cases of hydrocephalus, but occasionally we would catch an early unsuspected case.

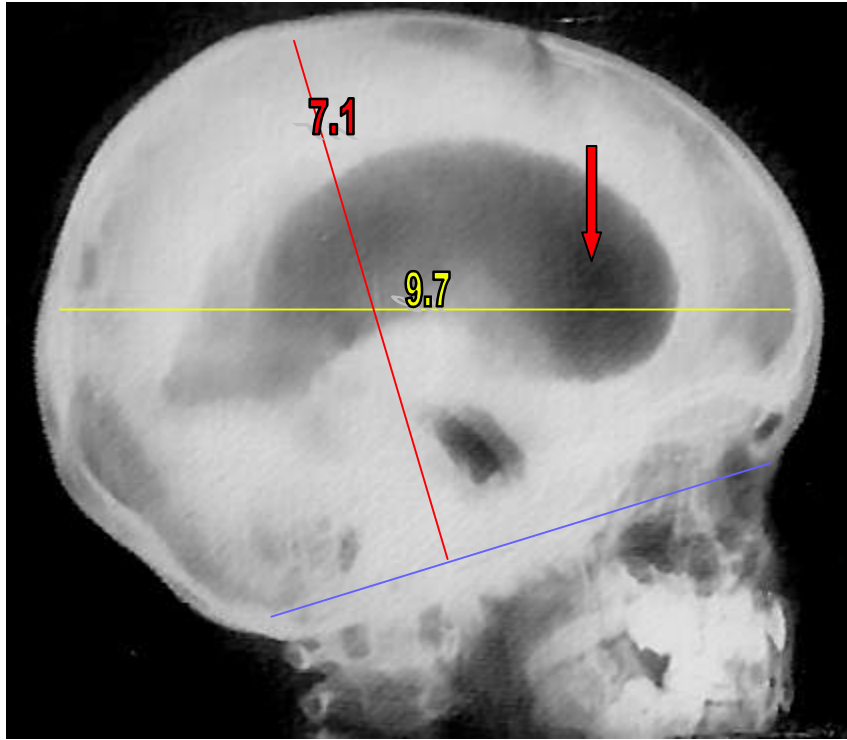


Figure # 104 (left). Using the numbers in figures 102 and 103: $8.6 + 7.1 + 9.7 = 25.4$. 25.4 divided by $4.3 = 5.9$ $\times 10 = 59$. (Red arrow shows air in the lateral ventricles.)

The c-f index is above 55!

Figure # 105 (right). White arrows point to a segmental area of premature closure of the sagittal suture in a child. Over half (55%) of premature closures involve the sagittal suture. Note the distortion of the orbits and sphenoid wings as a result. The coronal, sagittal, and lamdoid sutures ordinarily persist throughout childhood.

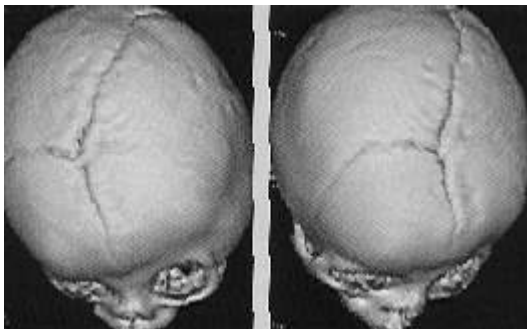
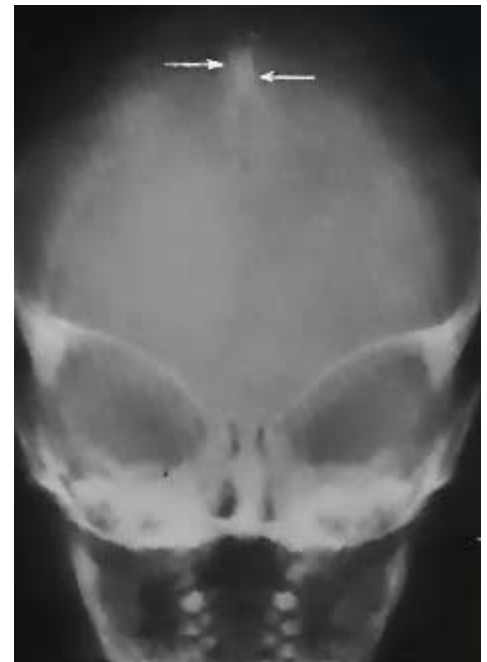


Figure # 105a (left). Multi-slice reformatted CT images make the diagnosis of a left unilateral coronal suture synostosis much easier. "The speed of MSCT enables the completion of most pediatric work, including 3-D imaging, without sedation" Courtesy Diagnostic Imaging supplement sponsored by an educational grant from GE Medical Systems. November 1999.

Evaluation of the basilar structures includes a look at the sella turcica and surrounding structures, region of the dorsum sella, optic chiasm area, the petrous portions of the temporal bones including the acoustic canals, the orbits and orbital foramen. The other basilar foramen including the foramen magnum, the jugular and others require a submental vertex view and are more the prerogative of the diagnostic or neuroradiologist.

If you are interested however remember ROS for foramens rotundum, ovale and spinosum (from anterior to posterior). The foramen lacerum through which the internal carotid artery passes is adjacent to the jugular.

The sella is probably best evaluated in a lateral view and although measurements can be made, a cursory look will usually define any gross abnormality as shown in figure 107 below.

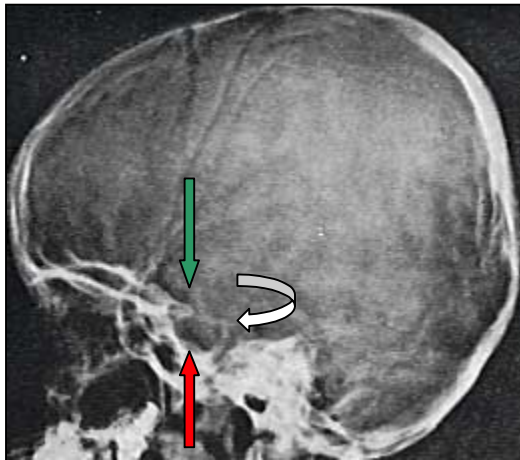


Figure # 106 (left).
Lateral view of a normal skull shows a normal size sella turcica (red arrow), anterior clinoids (green arrow) & posterior clinoids (white arrow).

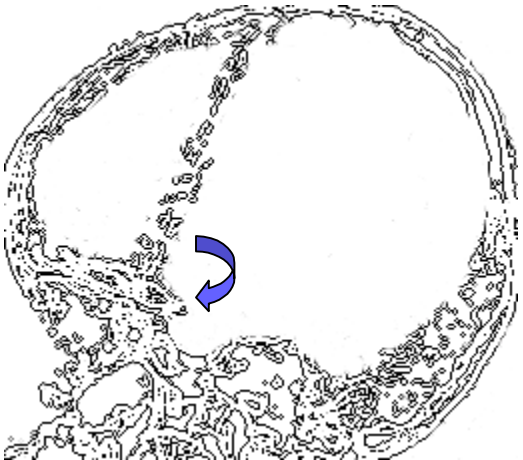


Figure # 107 (right). **Sketch of figure 106 now showing enlargement of sella, erosion of the anterior clinoids (blue arrow) and absence of the dorsum sellae and posterior clinoids, which is what would happen with an expanding intrasellar mass such as a chromophobe adenoma.**

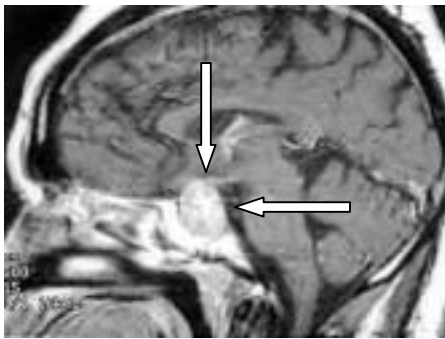


Figure # 107a (left) shows a MRI exam of a patient with an actual chromophobe adenoma (white arrows). You can see how the expanding lesion effects the bony structures of the sella.

The basilar structures also include the acoustic canals, and the student interpreter should make a definite effort to look for them. They are easily seen on plain films in the Towne's projection and also in a modified AP projection where the petrous ridges are seen projected through the orbits. They are, however, best seen by CT or MRI studies as illustrated in the next few images.

Note the normal acoustic canal on the right side (red arrows) as outlined in a Towne's projection of the skull in figure 108, as opposed to the expanded lucent area (black arrowheads) at the origin of the left acoustic canal. Here you are looking for asymmetry as shown in this patient with suppurative middle ear infection.

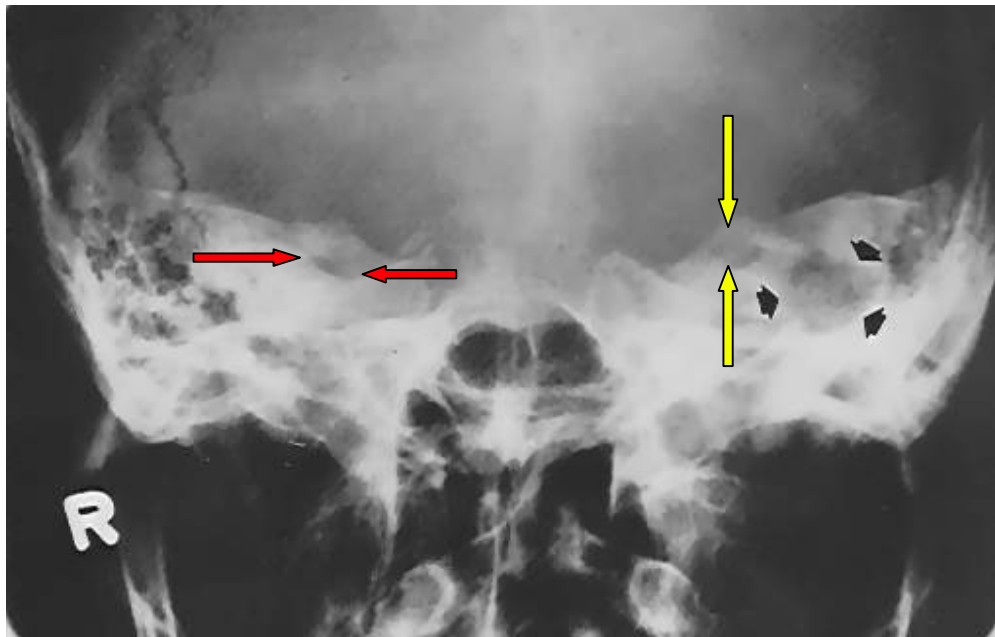


Figure # 108 (left). Normal acoustic canal on the right (red arrows). Acoustic meatus on the left is normal (yellow arrows), but the area of the labyrinth is expanded (black arrowheads). We have outlined the acoustic canals, meatuses, and the lytic area on the left in the next illustration

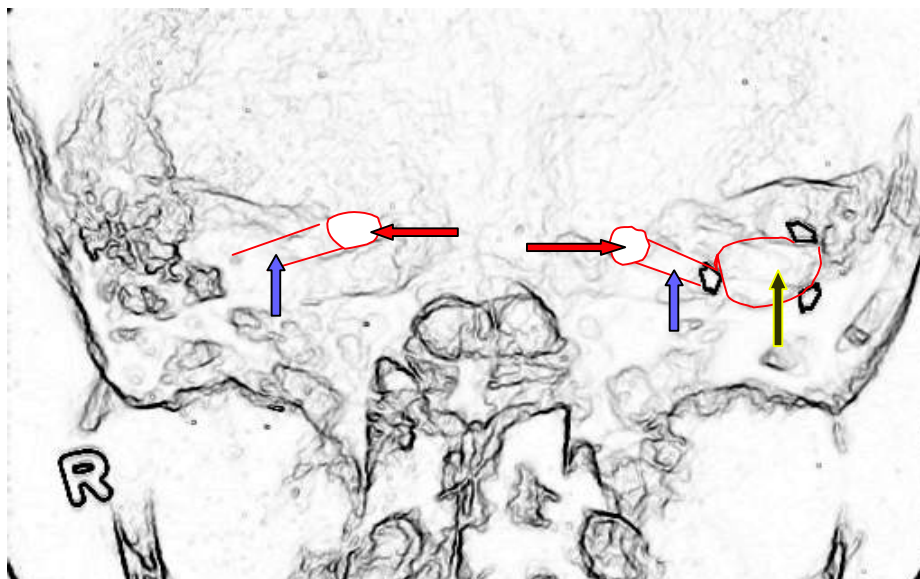


Figure # 109 (left). Red arrows point to the acoustic meatuses. Blue arrows indicate the acoustic canals and the black arrow and open arrowheads show the pathologic lytic area of suppurative labyrinthitis. Patients with an acoustic neuroma would usually show an expanded canal or meatus, Look for asymmetry!

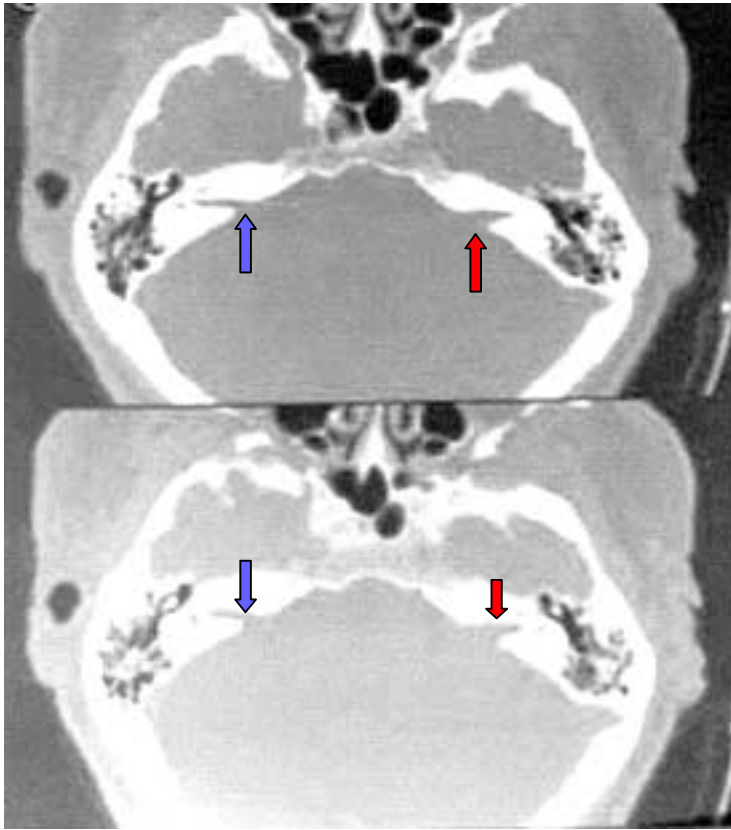
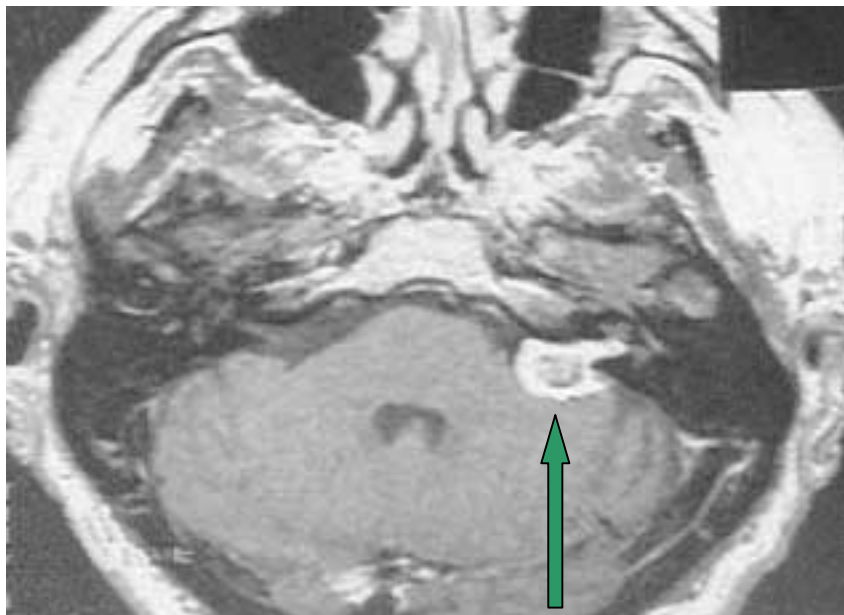


Figure # 110 (left).
CT study showing asymmetry of the acoustic canals.
Note the widened meatus on the left (red arrows)
compared to the normal on the right (blue arrows).

Figure # 111(below). The MRI study on this same patient
shows the cause of the expanded acoustic meatus, an
acoustic neuroma! (green arrow).



The sinuses are probably best evaluated by coronal CT images, but for our purposes the Water's view of the skull will suffice. In this projection a couple of tips include comparing the density of the frontal sinuses to the density of the orbits. They should be about the same in the normal individual. Also be sure to look at the thin lines of the floors of the maxillary sinuses. Note the subtle but real difference in the normal versus a patient with membrane thickening as demonstrated in figures 112-114. Of course its easy to spot the air fluid level.



Figure # 112 (left) Water's view of the paranasal sinuses. This particular image shows normal maxillary sinuses. Note the thin walls and roof of the sinuses (red arrows). Compare to the findings in image # 114.

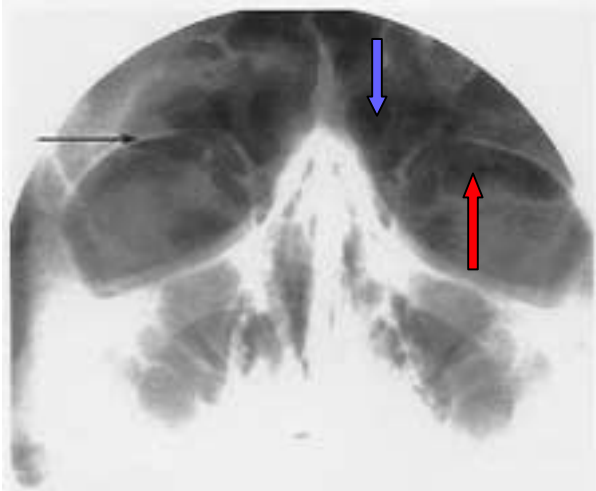


Figure # 113 (right). Normal Water's view of the sinuses. Black arrow points to orbital rim. Note the comparable densities of the frontal sinuses (blue arrow) to the upper part of the orbits (red arrow).

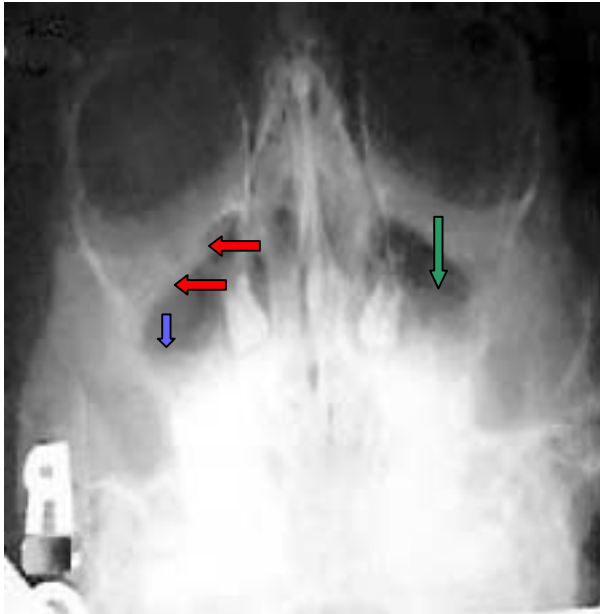


Figure # 114 (right). Water's view of a patient with acute maxillary sinusitis. Note the thickened membrane (red arrows) and the air-fluid level (blue arrow). The left maxillary sinus also shows polypoid thickening of the membrane of the floor of the sinus (green arrow). Be careful in this projection that the upper lip projected over the floor of the maxillary sinuses doesn't fool you!

Also remember that the maxillary sinuses are aerated in infancy and deciduous teeth sometimes obscure the floors. Careful analysis can usually separate normal from pathologic in this situation.

The mastoids are also best evaluated by high resolution CT, but screening for abnormal conditions can be helpful by a quick check of the Towne's and Waters's views. Note the loss of normal mastoid aeration in this patient with acute sclerosing mastoiditis shown in figure 115.

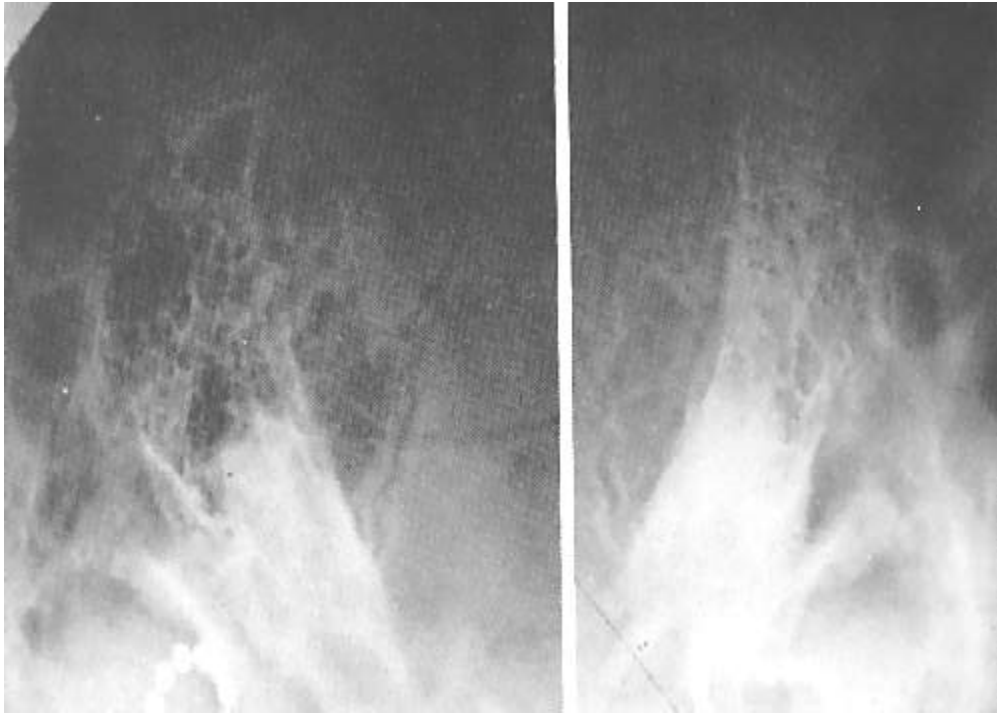


Figure # 115 (left). Close up views of the left and right mastoids in a patient with acute sclerosing mastoiditis. Note the relatively normal mastoid air cell outlines in the section to your left as you face the page, compared to the sclerotic cells on the right. If the acute infectious process progresses, there will be cell wall destruction and coalescence of lytic bone destruction as shown in the next illustration.

Figure # 116 (right). Black arrows outline an area of lytic bone destruction in a patient with acute coalescing mastoiditis in this close-up view of the mastoid area, (very similar to the case shown in figure 108).



Bright lighting the soft tissues surrounding the skull is useful to help locate sites of trauma such as is demonstrated in figure 117 in a newborn with cephalhematoma.

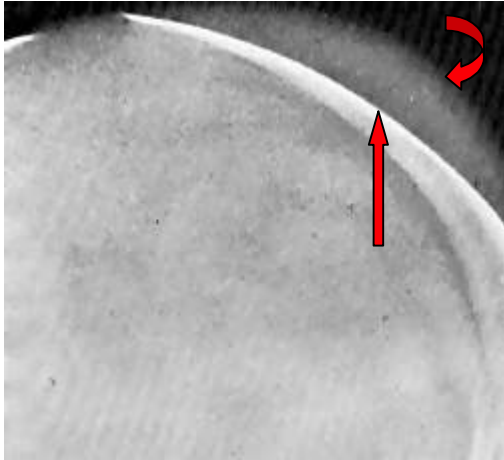


Figure # 117 (left). Close up of a Towne's view of the skull showing a cephalhematoma (red arrows) in a newborn.

Probably the most useful clues to screen for fractures of the skull include a look for lucent lines that are straight and that don't terminate in a venous lake, comparison with the opposite side of the skull for symmetrical lines (sutures), and bright lighting the scalp to look for soft tissue swelling or hematomas.

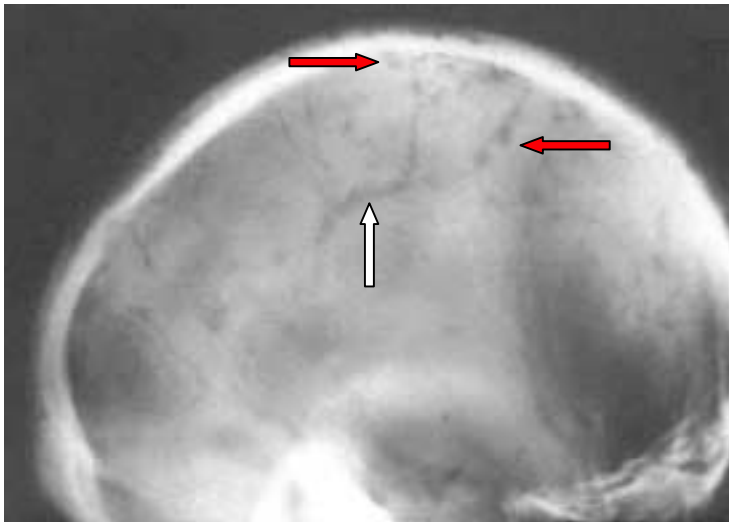
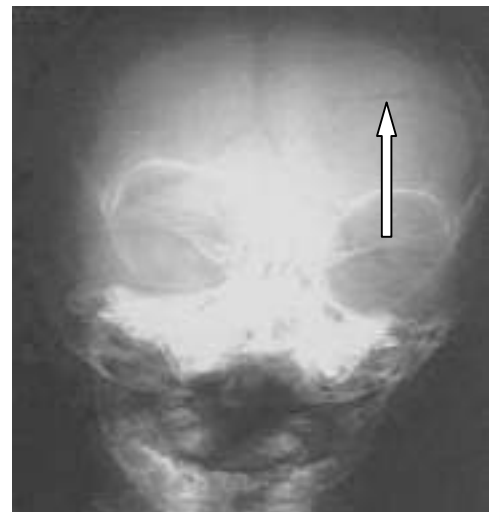


Figure # 118 (left). White arrow indicates a normal diploic vein in this lateral view of the skull. The red arrows point to normal venous lakes.

Figure # 119 (right). White arrow shows a transverse fracture, left side of the skull. Note the sharper edges compared to the diploic vein in the previous illustration. Also there is no apparent venous lake.



On occasion there will be a line of increased density when a skull fracture is depressed or there are overlapping edges. These findings are illustrated in figures 120-121.



Figure # 120 (left). White arrow points to a dense line indicating the overlapping edges of a depressed skull fracture caused by an iatrogenic event during forceps delivery.

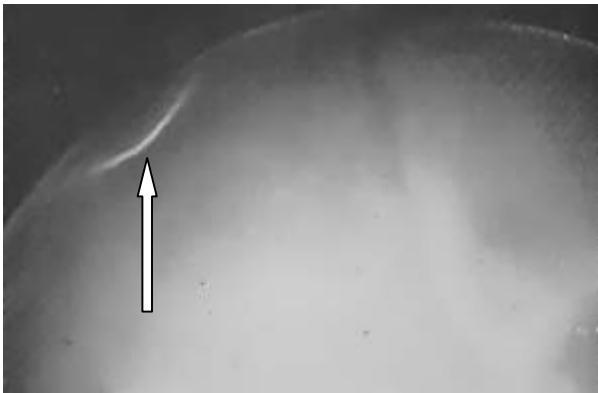


Figure # 121 (left). Another case of depressed skull fracture in a newborn as indicated by the white arrow.

Finally, there are a few Aunt Minnies to be learned in evaluation of the skull. Some of the common ones are shown in the following illustrations.

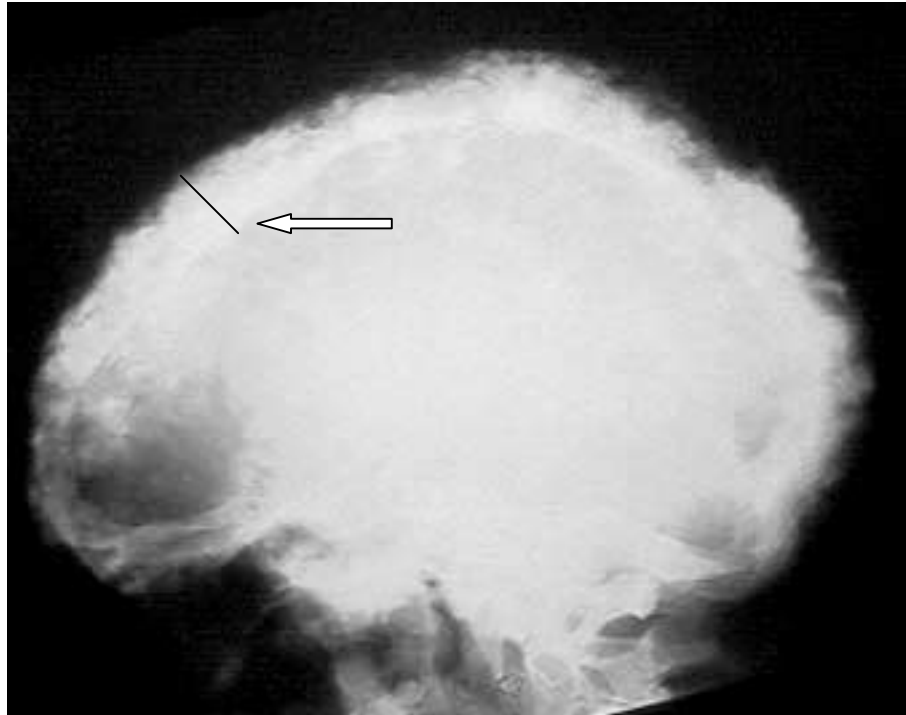


Figure # 122 (above). The four characteristics of Paget's disease (which you should memorize) on a radiograph of any bone are 1-Thickened cortex. 2-Course trabecular pattern. 3-Dense bone (therefore whiter on a film). 4- Soft bone (therefor sometimes deformed). Note the marked thickening of the cortex in the above figure as indicated by the white arrow and black line. Also note the increased density of the bone compared to the normal skull in figure 117. The coarsened trabecular pattern may require a magnifying glass to detect since there are few areas that have not progressed to coalescence of dense bone in this particular case.

The other (lytic) form of Paget's disease, osteoporosis circumscripta, is not necessarily an "Aunt Minnie". Note the difficulty of distinguishing osteoporosis circumscripta from metastatic bone disease in the next two figures.

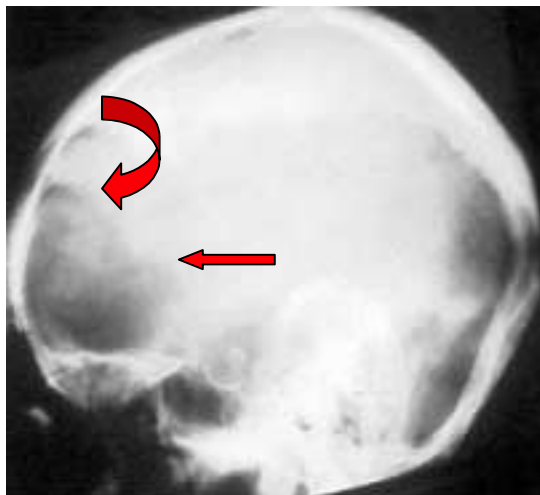
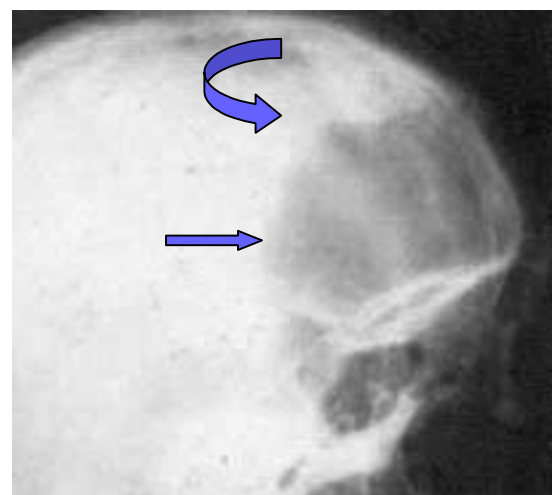
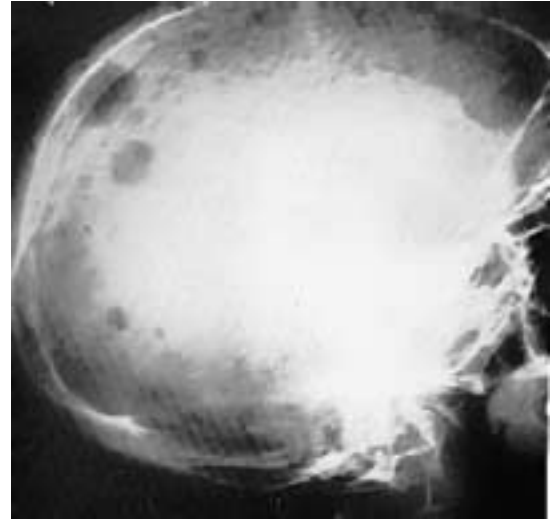


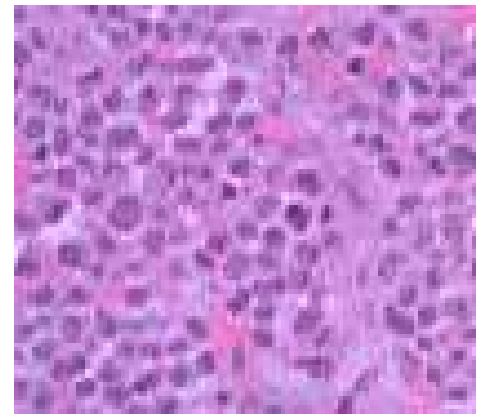
Figure # 123 (left). Lytic frontal bone area (red arrows) is due to osteoporosis circumscripta.
Figure # 124 (right). Lytic frontal bone area (blue arrows) is due to metastatic thyroid carcinoma!





Figures # 125 (above). Granted that multiple punched out areas of the skull as shown in the figures above do not constitute a 100% Aunt Minnie, but the differential includes multiple myeloma and should be your first choice in patients of the right age group. In fact, radiologists will often request a lateral view of the skull if a lytic bone lesion is seen elsewhere in the skeleton of patients over the age of 50. Results like these will usually clinch the diagnosis even before laboratory confirmation!

Figure # 126 (right). Photomicrograph at x40 of a patient with myeloma. The punched out lesions seen in the previous skull radiograph are caused by increased osteoclastic response that is stimulated by cytokines released by the sheets of plasma cells shown in the section to your right. Erosion begins in the intramedullary space and progresses through the cortex to cause the lytic lesions. Only patients with complete remissions experience any bony healing. Image courtesy of Bonetumor.org via the Internet.



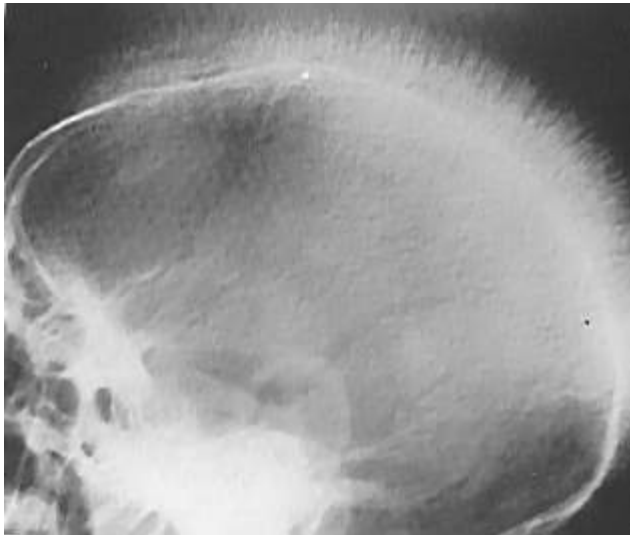
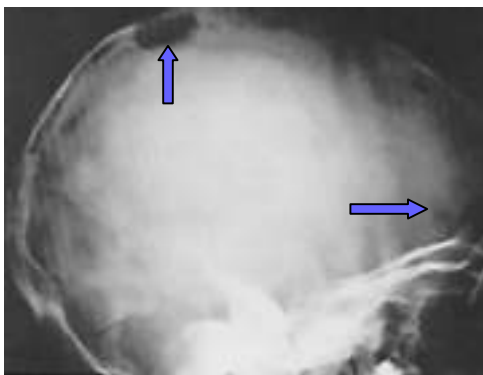


Figure # 129 (left). The hair-on-end appearance seen here is the result of widened diploic space due to hyperplastic marrow seen in certain kinds of anemia. With erythroid hyperplasia the marrow may perforate the outer table. Stimulation of the periosteum then causes new bone formation, which arranges parallel to the marrow vessels, which are perpendicular to the table. This results in the hair-on-end appearance seen here. This particular case represents sickle cell anemia, but thalassemia develops this picture more frequently. The appearance is an “Aunt Minnie” for erythroid hyperplasia.

Lytic, punched-out lesions of the skull in youngsters are almost “Aunt Minnies” as shown in the next two illustrations. If the lesion involves the outer table and has associated soft tissue localized swelling, then epidermoid cyst would be likely. Of course a rare metastatic lesion cannot be totally excluded, but would be unlikely in an asymptomatic patient. You won’t be confused by surgical defects (burr holes) once you’ve seen a few of them, but there are some other rare lesions that can mimic histiocytosis x. Check out the list in Felson’s and Reeder’s *Gamut’s* book.



Figures # 127 (left) and 128 (right) are examples of histiocytosis x. The lesion on the right (red arrow) represents eosinophilic granuloma. If there is more than one, think Hand-Schuller-Christian (blue arrows) or Letterer-Siwe disease.



Figure # 130 (right). Fibrous dysplasia is a complicated entity in which fibrous tissue replaces bone. It has no definite known etiology and can present in the skull as sclerotic or lytic forms. The dense basilar sclerosis seen here is typical of enchondral bone involvement. The disease generally affects youngsters.

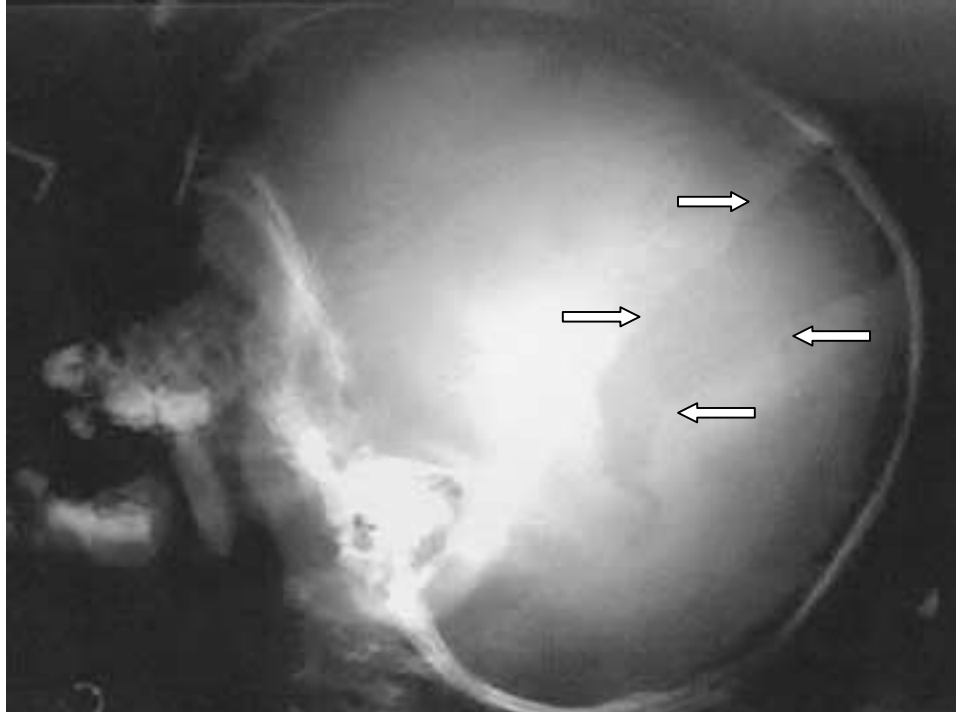


Figure # 131 (left). The broad area of relative lucency demonstrated here (arrows) is an Aunt Minnie for leptomenigeal cyst. The appearance results from a fracture in which the meninges get caught between the edges of the fracture preventing union. Thus diastasis occurs, the edges resorb and the space fills with fluid creating the cyst. Image courtesy of the U. of Utah via the internet.

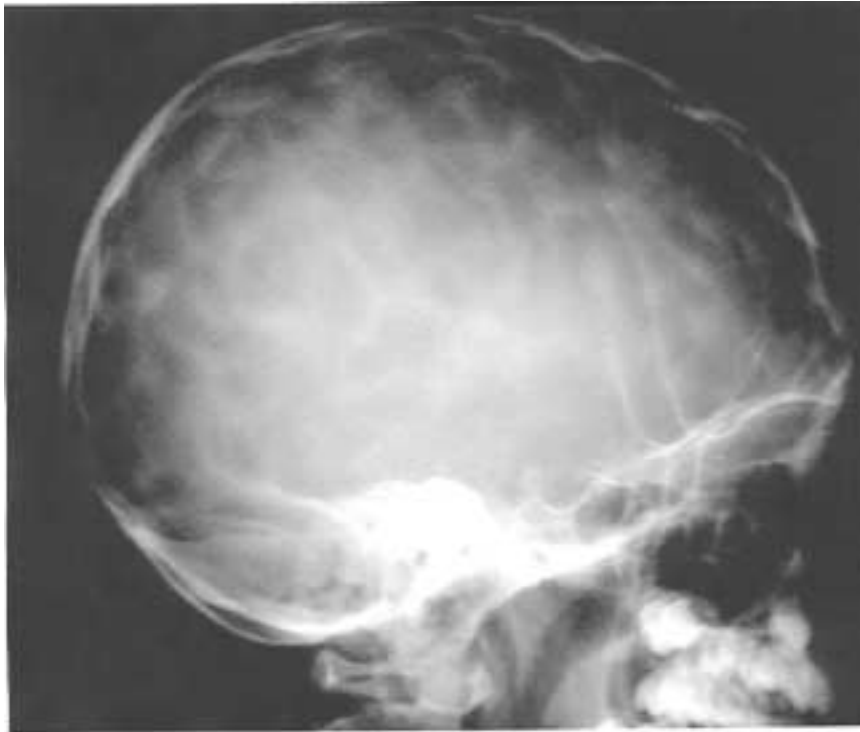


Figure # 132 (left). The hammered metal appearance of the calvarium seen here is an Aunt Minnie for exaggerated digital markings sometimes called lukenschadel. It represents a normal variant. It should not be confused with lacunar skull or craniolacunaria shown in figure 133 below.

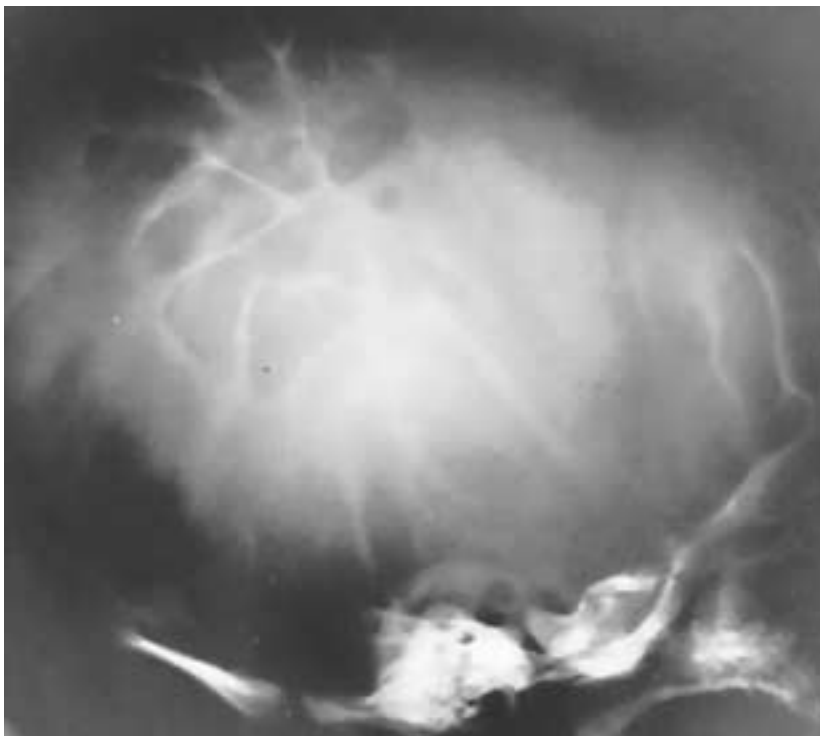


Figure # 133 (left). Example of craniolacunaria in a newborn. Note the similarity to the appearance of lukenschadel in the previous illustration. The difference is that this pattern is localized and may be associated with widened sutures, sellar demineralization or other signs of increased intracranial pressure. There may be absence of bone in the thinner (more lucent) areas. This appearance in a neonate is a sure Aunt Minnie for lacunar skull and is almost always associated with Arnold Chiari malformation, encephalocele, or spinal meningocele. Image credit Barton Lane, MD, Radiologic Clinics of North America, Vol.XII, no.2, August, 1974.

Here are some more “Aunt Minnies” taken from Keats which are normal findings with which you should be familiar.

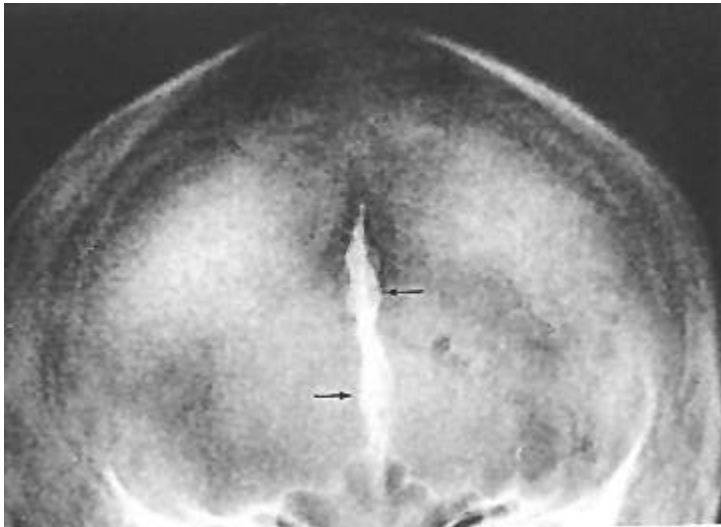


Figure # 134 (left). Small black arrows point to heavy calcification in the falx cerebri, a normal variant.

Figure # 135 (right). Calcification in the Choroid plexus of each lateral ventricle is another normal variant.



Figures # 136 and 136a (below). Black arrows indicate the presence of hyperostosis frontalis interna, another “Aunt Minnie” of no clinical significance in most cases.

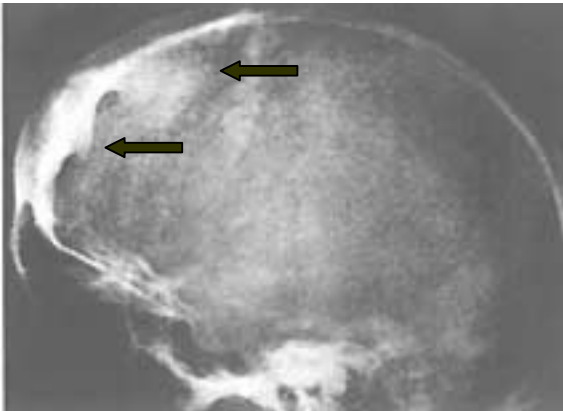




Figure # 137 (left). A persistent metopic suture is not an unusual finding. Note the saw-tooth serration and the location and you won't mistake it for a fracture.

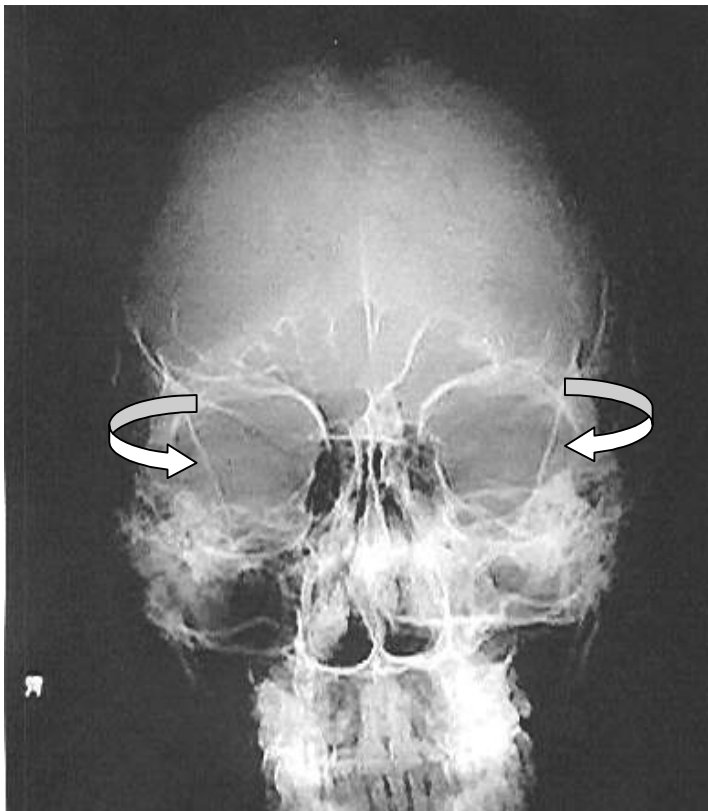


Figure # 138 (left). Did you ever wonder what these two oblique white lines (arrows) represent in an AP view of the skull? They are called the innominate lines, a fancy way of saying "no name" lines, and they represent the thin portions of the temporal bones seen on end.

A final review, then for your system in reading the skull is:

Size and shape

Basilar structures

Sinuses and mastoids

Soft tissues

Calvarium for densities, lines, fractures.

Get familiar with the normal appearance of the sella, the mastoids and sinuses, the acoustic canals, and the normal thickness of the calvarium cortex. There are some natural variations. Only by recognizing normal, will you feel confident in raising the question of abnormal! The interpretation of plain films of the skull is not easy, and diagnostic radiology consultation is indicated in all cases.

CHAPTER FIVE

THE SPINE

A system for evaluating the spine includes:

1-HEIGHTS OF THE VERTEBRAL BODIES AND INTERSPACES

2-BONE DENSITY

3-FACETS (the Scotty dog)

4-NEUROFORAMINA

5-ALIGNMENTS

facets

margins

spinous and transverse processes

6-SOFT TISSUES

Whether it is cervical, thoracic or lumbosacral spine films, the system is valid.

In evaluating the heights of the vertebral bodies, compare the vertebra above and below, and look for any cortical wrinkles. If a compression fracture is present you will need to compare any old available films to determine its age. You will also need to recognize typical Schmorl's nodes and limbus vertebrae, examples of which are shown in the figures below.



Figure # 139 (left). Black arrows point to typical Schmorl's nodes which indent the normal vertebral margins on either the inferior or superior surface. They can be considered a normal variant as a result of notochordal remnants, or some people have attributed them to trauma, where a portion of disc material is forced into the adjacent vertebral cortex. If the defect appears after a prior film shows none, then certainly a traumatic Schmorl's node can be diagnosed. Most, however, are of no clinical significance.

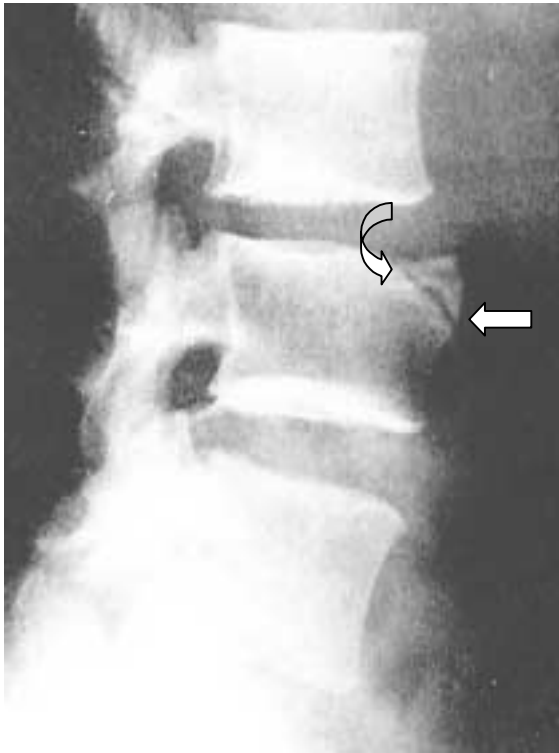


Figure # 140 (left). Ununited ring apophysis as indicated by the white arrows represents a limbus vertebra and should not be mistaken for a fracture

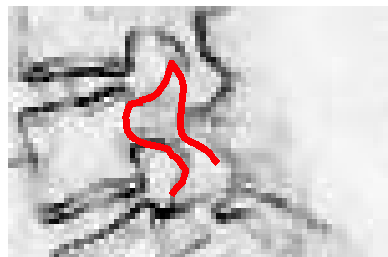
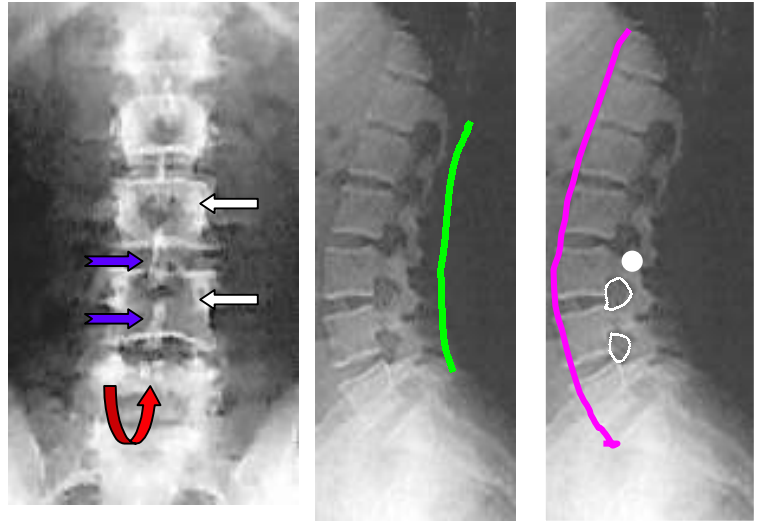


Figure # 141 (above) and # 142 (left). AP and lateral views of the L-S spine. Note that the heights of the vertebral bodies are equal throughout. The intervertebral disc spaces are also equal although they appear narrower cephalad. This is because the central ray of the x-ray beam is centered over the L3 vertebra (white octagon) and as it “fans” out causes some distortion of the image. Note also that the bone density of the visible vertebrae is even. The “Scotty Dog”, illustrated by the red line, is an important landmark. The dog’s neck represents the pars interarticularis, and the film interpreter should look for a defect or “collar” (spondylolysis) at all levels on each film. Neuroforamina are the spaces (outlined in white) above and below the Scotty dog. These spaces allow nerves to exit from the spinal cord and are better evaluated by CT or oblique views, but encroachments such as caused by osteophytes are easily seen. Note that the anterior vertebral margins align in a smooth curve (pink line). The posterior spinous processes do likewise, (green line) although not all are seen in this reproduction. One should also look at each facet in the AP view for integrity and alignment (white arrows) and the posterior spinous processes (blue arrows) which project over the next adjacent interspace. Occasionally one will detect a defect such as a spina bifida occulta indicated by the curved red arrow in figure 141 above by the white arrow in figure 143 left.



Figure # 143 (left). Gives you a better look at a spina bifida occulta of the 5th lumbar segment (white arrow).

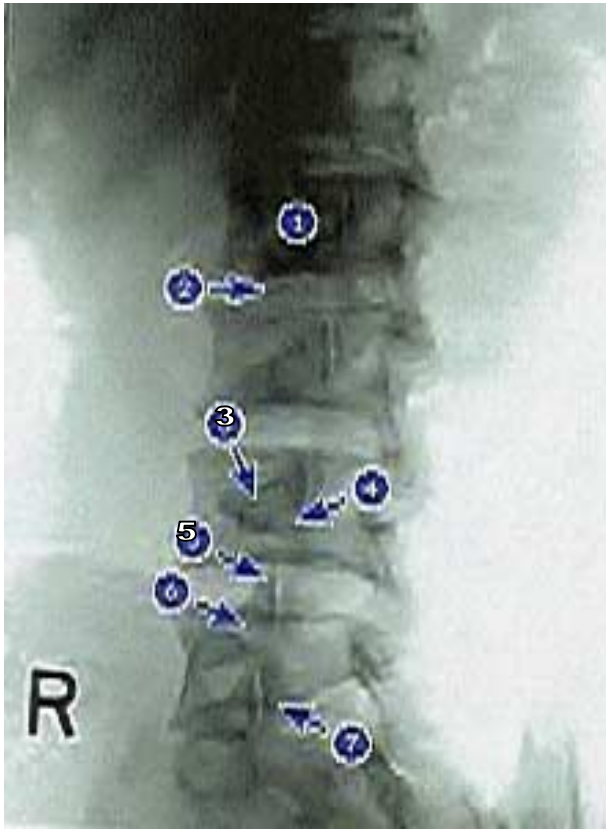
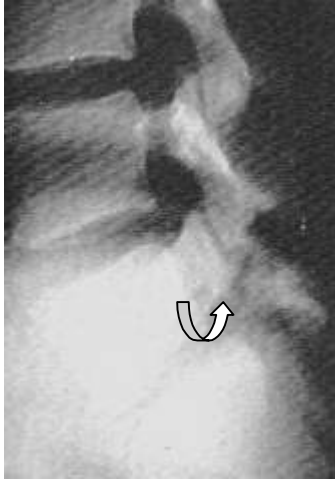


Figure # 144 (left). The oblique view of the lumbar spine demonstrates the "Scotty Dog" much better than the lateral view and is often ordered to evaluate the pars interarticularis.

- 1- Body of L-2 vertebra
- 2- Disc
- 3- Transverse process of L-4, the "nose"
- 4- Pars interarticularis of L-4, the "neck"
- 5- Superior articular process of L-5, the "ear"
- 6- Pedicle of L-5, The "eye" of the Scotty Dog.
- 7- Inferior articular process of L-5, the front leg of the dog.

If you see a collar (defect) across the dog's neck, it represents a spondylolysis. These defects may be the result of a birth defect, or trauma (un-united fracture). These can lead to an unstable back with subluxation of a vertebral body called spondylolesthesis. Illustration courtesy of RAOnline via the Internet.



Figures # 145 (left) and # 146 (sketch right) shows the classic collar on the Scotty Dog of a spondylolysis defect.

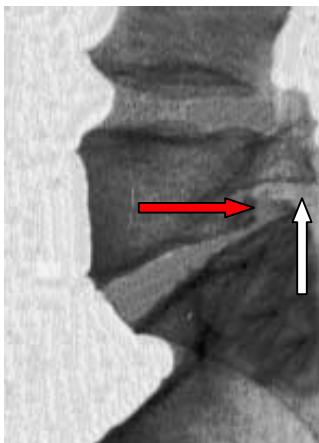
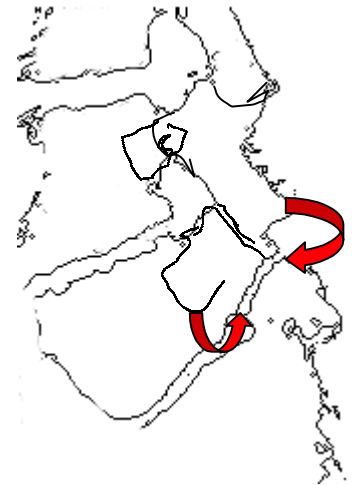


Figure # 147 (left and right). Stage I anterior spondylolesthesis of L-5 on the sacrum is demonstrated with an associated spondylolysis (white arrows). Note that the posterior margin of L-5 (red Arrows) has slid forward (anterior) on the sacrum (S). A stage II slip would be further subluxation to about 50% of the opposing surface and a stage IV would be almost complete displacement.

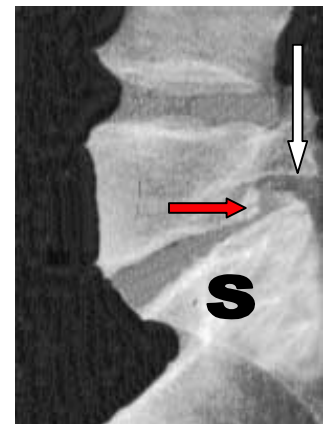




Figure # 148 (left). Don't get the idea that a defect in the pars interarticularis is necessary for a spondylolesthesis to occur. This myelogram demonstrates an anterior spondylolesthesis of L-4 on L-5 with an intact neural arch. The white arrow shows the posterior margin of L-4 and the red arrow the posterior margin of L-5. This slippage is usually found in women over the age of 45, commonly effects the L4-5 level and is related to degenerative change with hypertrophy of the apophyseal joints.

The intervertebral disc spaces can be difficult to evaluate if the patient has scoliosis or the patient is positioned less than optimally. One way to solve this dilemma is to mark the inferior edge of one vertebra and the superior edge of an adjacent vertebra with wax crayon, always using either the most superior or the most inferior margins of both apparently tilted vertebrae. You can then observe the height of the disc space readily and measure if necessary. This process is illustrated in figures 142-143.

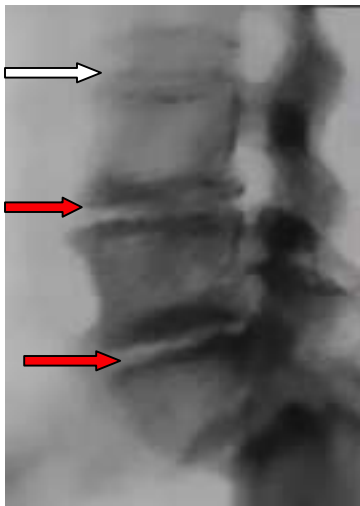


Figure # 149 (left) and 150 (right). Note how difficult it is to evaluate the disc space at L2-3 (white arrow) compared to the obvious narrowing of the disc spaces at L3-4 and L4-5 (red arrows). If you draw the lower margin of L2 (red lines) and the upper margins of L3 (green lines), and then measure top to top (blue arrow) as illustrated, you will see the disc space at L2-3 is relatively normal!



Recognition of bone density abnormalities comes with experience and familiarity with a particular radiology department's technique. One way to gain that experience rapidly is to guess the patient's age when looking at spine films and then confirm your estimate. After awhile you'll get pretty good at it. Bone mineral loss is reported by radiologists as osteopenia or osteoporosis and results in darker skeletal structures on the radiograph. Increased density, on the other hand, is termed eburnation or increased bone density and is usually described with other findings which will help the referring physician determine the cause.

Isolated areas of increased bone density in a male over the age of 60 are prime suspicion of metastatic carcinoma, particularly of the prostate. Of course this finding oft times has to be differentiated from Paget's disease which is relatively easy once you remember the four radiographic signs of Paget's which are:

- 1-thickened cortex**
- 2-coarse trabecular pattern**
- 3-deformity or enlargement (due to soft bone)**
- 4-increased density**

Sclerotic metastatic carcinoma of the prostate (or other primary site) does not result in thickened cortex or coarse trabeculae. Instead the trabeculae often become smudgy looking. Both can result in increased density of bone and deformities, the latter in metastatic ca often due to pathologic fractures. These points are demonstrated in the next illustrations.

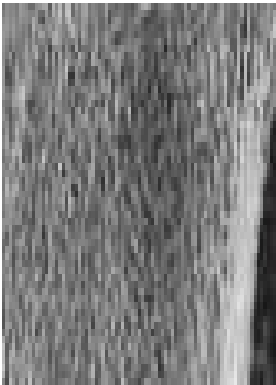


Figure # 151 (left). Magnified view of normal bone cortex and trabecular pattern.

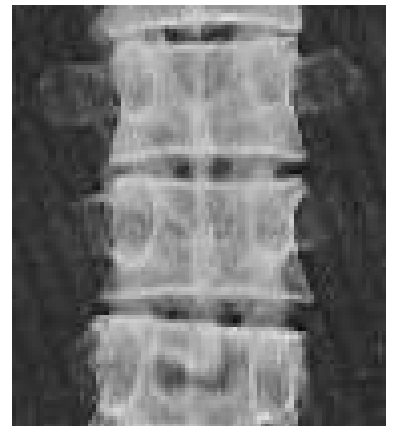


Figure # 152 (right). Normal vertebrae.



Figure # 153 (left). Magnified view of bone cortex and trabecular pattern in Paget's disease. Note coarsened trabeculae.

Figure # 154 (right). Note the dense thickened cortex of a vertebra with Paget's involvement. Compare to the normal above. This appearance is often said to resemble a picture frame. Image courtesy dirt museum via the Internet. Thanks to Dr. Ian Maddison, MA. BM. BCh. MRCP. FRCR. Reprinted with permission.





Figure # 155 (left). Magnified view of sclerotic bone metastasis. Note that the trabeculae are so smudged as to be non-recognizable.



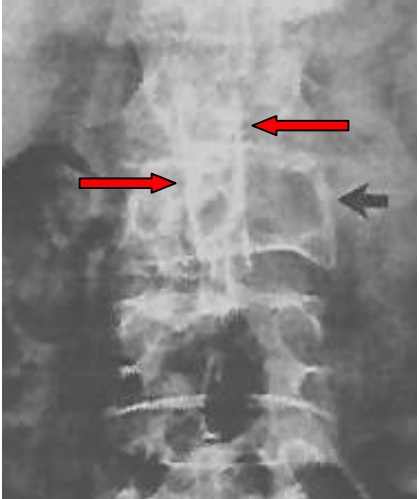
Figure # 156 (right). Sclerotic bone metastasis from a carcinoma of the colon. It could just as easily be from a prostatic primary. . Image courtesy dirt museum via the Internet, Ian Maddison.

Metastatic ca of the breast can result in either increased or decreased bone density depending on the host's defensive reaction and the cell type. Shown below are two cases illustrating this point.



Figure # 157 (left). Sclerotic metastasis to first three lumbar vertebrae from a carcinoma of the breast. Note increased density.

Figure # 158 (right). Lytic metastasis from carcinoma of the breast (black arrow). Note destruction of the pedicle. Also note calcification of the abdominal aorta (red arrows).



Step 4 in the system of the spine is evaluating the neuroforamina, and this is most important in the cervical spine in which they are well seen in oblique views. Encroachment by osteophytes is a common finding and explains the cause of many patients' parathesia symptoms. When associated with degenerative disc disease the findings are termed spondylosis (not to be confused with spondylolysis, the defect mentioned previously).

Figures 142 (previous) and 159 (next page) show normal neuroformina as opposed to a patient with cervical spondylosis.

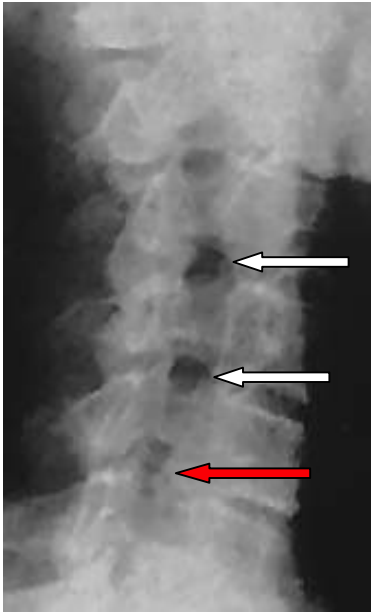


Figure # 159 (left). Oblique view of the cervical spine. **White arrows point to normal neuroforamina, as opposed to the encroachment by enostophytes as indicated by the red arrow. This is a common finding in patients with osteoarthritis and may be the cause of parathesias**

In the cervical spine, alignment evaluation is extremely important in evaluating trauma victims. The initial film is usually a cross-table lateral view. In this projection one should check the upper portion of the cervical spine in relation to the clivus, the extended line of which should intersect the odontoid in its posterior one third. Also the posterior and anterior vertebral margins should align fairly close in this view, as should the facets, pedicles and neuroformina in the oblique projections.

Remember that position and alignment of cervical vertebrae are maintained by ligaments, which may be stretched or fractured, and there may not be an associated bone injury.

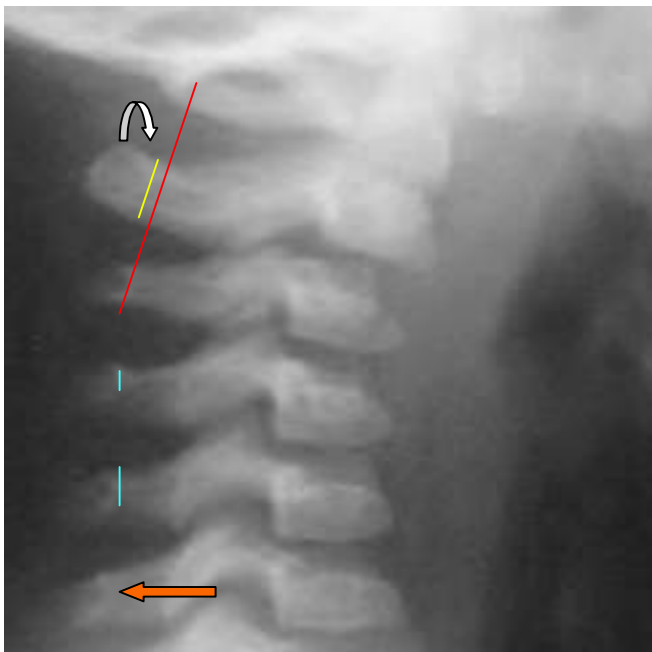
If flexion and extension views are provided, keep in mind there is a great deal of "normal" subluxation in children, whose ligaments are much more elastic than adults. In fact up to 40% of pediatric cervical spines will show a pseudosubluxation, most often at C2-3.



Figure # 160 (left) **Pseudosubluxation of the C- spine in a pediatric patient. Differentiating pseudosubluxation from the real thing, especially with a history of trauma can be difficult. The establishment of Swischuk's line as explained next may be a way out of this dilemma.** *Film courtesy of U. of Hawaii from a monograph by Loren G. Yamamoto, MD, MPH via the Internet.*

An excellent paper on the subject is available from Loren G. Yamamoto, MD, MPH, U. of Hawaii on the Internet. (www2.hawaii.edu/medicine/pediatrics/pemxray/vlc05.html.) Dr. Yamamoto's references include the original paper by LE Swischuk in *Radiology* **1977; 122: 759-763**.

Malalignment of C2-3 includes the common causes of pseudosubluxation and hangman's fracture. In order to resolve this problem, Dr. Swischuk defined a line drawn from the posterior arch of C-1 to the posterior arch of C-3. This line should be within one mm (some people say two mm's) anterior to the posterior arch of C-2. If it is greater than 2mm, a fracture of the arch of C-2 is likely.



*Figure # 161 (left). The red line represents Swischuk's line. The line should pass through or be no more than 1-2mm anterior to the posterior arch cortex of C-2 (yellow line). The turquoise lines indicate the position of the posterior arches of C-4 and C-5 so you get some idea of how to locate posterior arch margins. The arch is seen *en face* causing the denser oval appearance (red arrow).*

Sometimes in neck injuries like whiplash, all that can be seen is a loss of or straightening of the usual lordotic curvature. When the curvature reverses with angulation of the posterior vertebral margin, the injury is more severe and may involve an intervertebral disc or fracture. Frequently these findings can only be seen in an upright lateral view, which in my opinion, should be done if the patient's condition permits and the cross table view shows no abnormality.



Figure # 162 (left) and # 163 (right). Normal lordotic curve as indicated by the red line in figure 155. Note the loss of lordosis in figure 156 to your right. There is a hangman's fracture of C-2 (red arrow).



Since over 25% of cervical fractures involve C-1 C-2, it is good practice to include a coned down view of the odontoid in the a-p projection. ER personnel and trauma surgeons are familiar with the odontoid view, but should be aware of a couple of projection artifacts which are often interpreted as fractures. One is due to the gap between the two frontal maxillary incisors causing a vertically oriented pseudofracture. The inferior edge of these same incisors or sometimes the posterior arch of C-1 can also simulate a transverse fracture at the base of the odontoid.



Figure # 164 (left). Normal open mouth view of the odontoid. If the gap between the frontal incisors (red arrow in Figure # 165 right) superimposes the odontoid on the open mouth view, it causes the appearance of a vertically oriented fracture. Likewise, the inferior edge of these same incisors can fool you into thinking there is a transverse fracture across the odontoid (dens). Look for the teeth on every open mouth view and you won't be fooled!

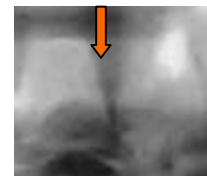


Figure # 166 (right radiograph negative). Here's an example of an incisor gap (white arrow) overlying the dens. I don't think many of you would be fooled because the linear lucency extends above the odontoid, but you can imagine how an inexperienced interpreter could get confused if the lucency was confined to the dens!



The odontoid view also gives you a good look at the alanto-atlas articulation and normal spacings. You will quickly learn to recognize anything out of the ordinary. Compare the normal odontoid view above with figure 167 on the next page and see if you can spot the abnormality before reading the answer.



Figure # 167 (left). Open mouth odontoid view of a trauma patient. Can you spot the abnormality? Clue: how do the lateral margins line up?

Figure # 168 (right). Note the lateral edges of C-1, the atlas, (red arrows) are lateral to the edges of C-2, the axis, white arrows). In addition there is a wide gap between the lateral masses of C-1 (blue arrow). This patient has a classical Jefferson fracture of the atlas. See lateral view next image.

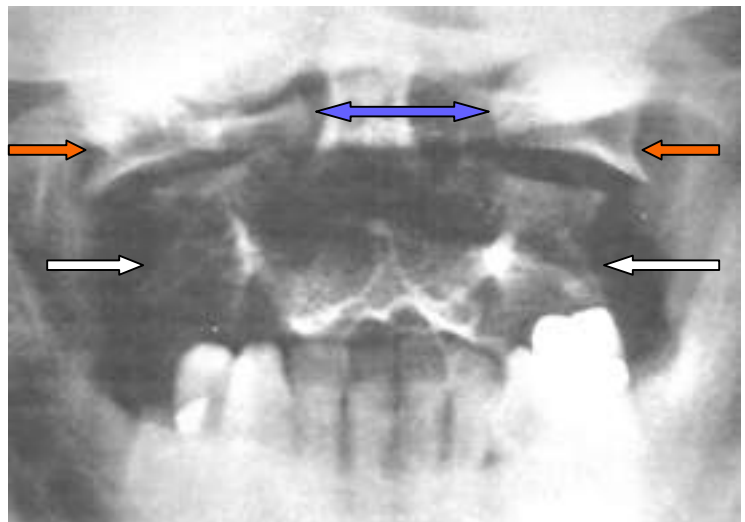


Figure # 169 (left). Small white arrow points to a Jefferson fracture of the atlas. Did you note the ET tube?

The spinous and transverse processes should also be carefully scrutinized during your alignment evaluation. In addition to the alignments look for fractures or defects. Failure of the posterior arch to fuse is a common congenital defect representing spina bifida occulta as shown in previous figures, but complete absence of the posterior spinous process or complete failure of the posterior arch to fuse can occur anywhere in the spine.

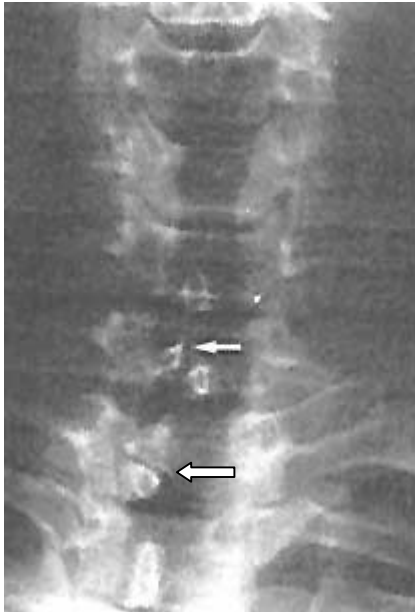


Figure # 170 (left). White arrows indicate another case of spina bifida occulta, this time involving two levels at the cervical dorsal junction (C-7 and T-1).

Don't be fooled by the Os ligamentum nuchae, a normal sesmoid in the neck, as shown in figure 171.

Figure # 171 (right) negative radiograph. Red arrow points to an os ligamentum nuchae which is a normal sesmoid sometimes seen in the neck. The position of the os nuchae in this case might be mistaken for an avulsion fracture of the posterior spinous process.

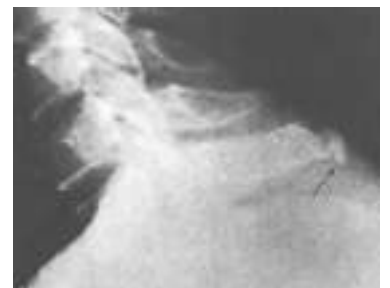


Figure # 172 (above). Small black arrow shows an un-united apophysis which can also be mistaken for a fracture.

Radiologists also look at all the information on the film, which includes the soft tissues. You don't want to miss a large aneurysm or other gross finding just because you were zeroed in on the bones! See if you can spot the soft tissue abnormalities in the following illustrations.



Figure # 173 (left). Can you spot the soft tissue abnormality in the radiograph to your left? Answer on the next page.

Figure # 174 (right). Ignoring the vertebrae which are not very well reproduced on this image, scrutinize the soft tissues for a specific abnormality and diagnosis. See next page for answer.





Figure # 175 (left) and #176 (right). The red arrow on the left shows a normal distance from the airway to the anterior vertebral line. The blue arrow shows displacement of the airway anteriorly by a retropharyngeal mass in this case representing an abscess.

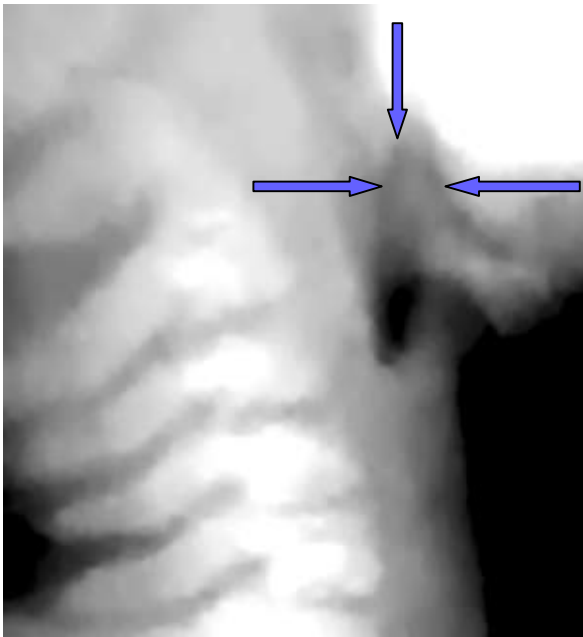
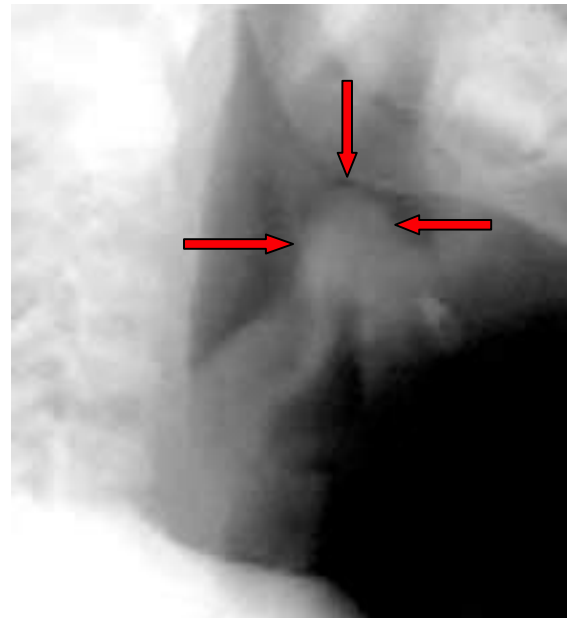


Figure # 177 (left) and # 178 (right). The blue arrows show the outline of a normal epiglottis contrasted by air in the hypopharynx. The red arrows show the “thumb-like” swelling of the epiglottis in a patient with acute epiglottitis, a medical emergency.



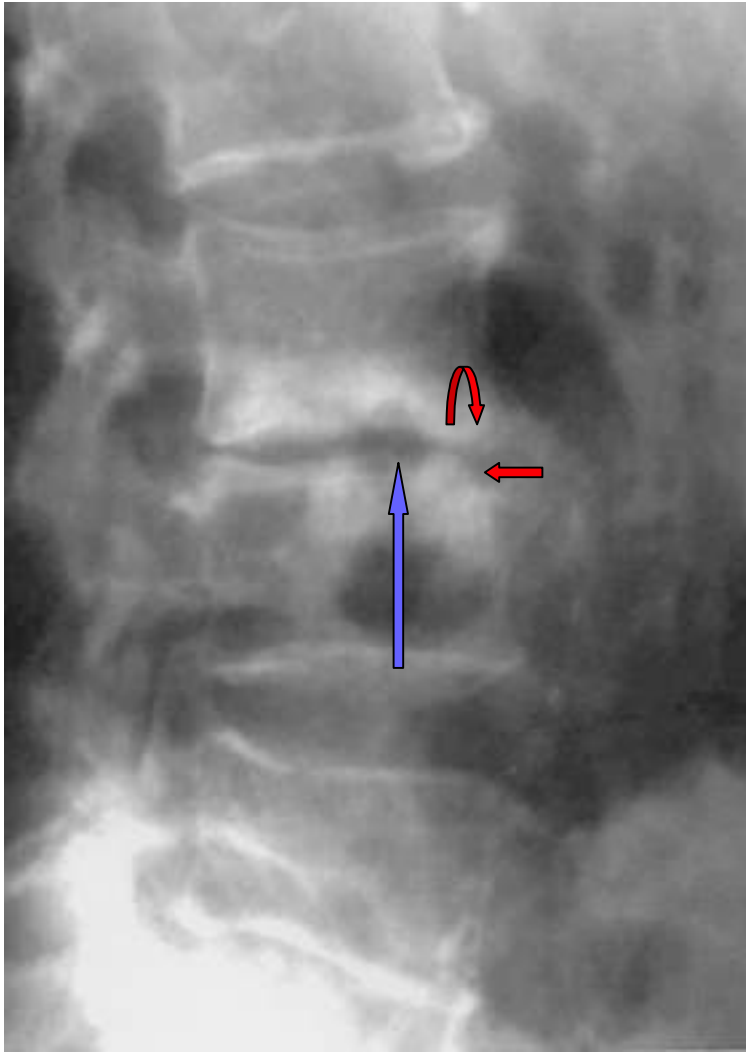
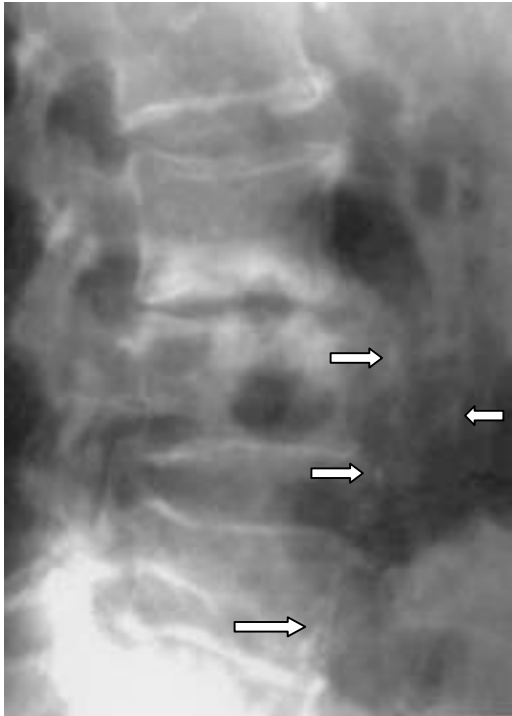


Figure # 179 (left). Besides the obvious narrowed disc (blue arrow) associated with eburnation (whitening) of the vertebral margins and reactive bone anteriorly (red arrows), there is also other (soft tissue) abnormality. What do you see?

Figure # 180 (right). Did you spot the calcifications in the abdominal aorta (white arrows)? These show a normal caliber aorta opposite L-4, however it is not unusual to see an aneurysm. Any aneurysm over 4cm in diameter is likely significant. By the way, did you make a diagnosis of discitis in this case? It's very suspicious!



Finally, the spine gives rise to a couple of Aunt Minnies besides the limbus vertebrae and Schmorl's nodes mentioned previously.

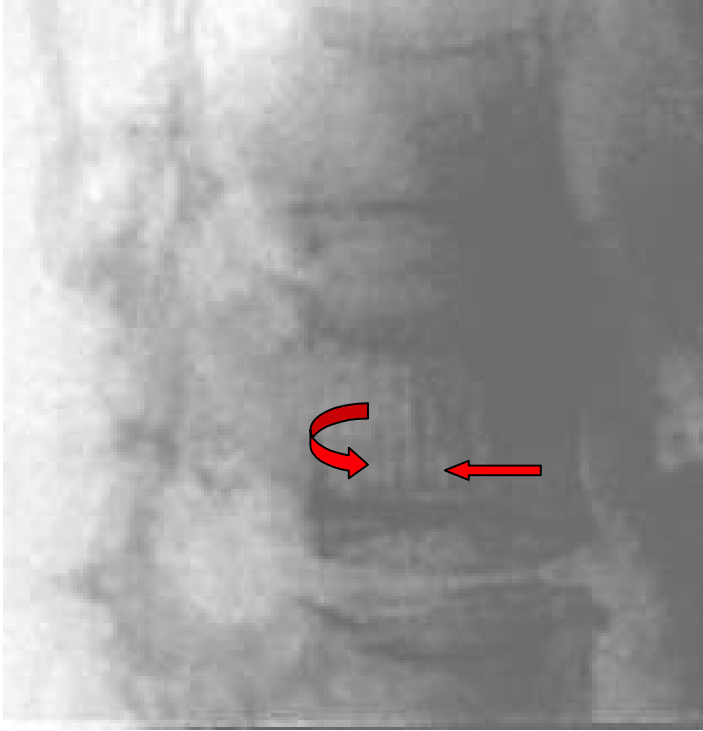


Figure # 181 (left). **The vertically oriented trabeculae (red arrows) in this lateral view of a vertebral column have been likened to Yankee pin stripes. The appearance is an “Aunt Minnie” for vertebral hemangioma.** Film courtesy of the X Ray Files www.radiology.co.uk/xrayfile/xray/cases/3/3-005/q.htm. Credit Scottish Radiological Society. Thanks to Dr. Andrew Downie.

Figure # 182 (right) **The most outstanding feature of ankylosing spondylitis (Marie-Strumpell disease) is the ossification of the spinal ligaments. The anterior longitudinal ligaments are affected first as shown here (white arrows). The appearance is an “Aunt Minnie” for this disease.**



A final review, then, for reading the spine is:

1-HEIGHTS OF THE VERTEBRAL BODIES AND INTERSPACES

2-BONE DENSITY

3-FACETS (the Scotty dog)

4-NEUROFORAMINA

5-ALIGNMENTS

facets

margins

spinous and transverse processes

6-SOFT TISSUES

CHAPTER SIX

PELVIS AND HIPS

A system for evaluating the pelvis and hips includes a look at the shape of the pelvis, the density of bone, the sacroiliac joints, the hip joints, and alignments of the natural ovals of the pelvis, as well as the symphysis pubis, sacrum and coccyx.

1-SHAPE

2-DENSITY

3-SI AND HIP JOINTS (includes fat lines about the hips)

4-OVALS

5-SYMPHYSIS PUBIS, SACRUM & COCCYX

The shape of the pelvis is important in order for you to become familiar with normal, which will immediately raise a red flag if you see an FLP, i.e. a funny looking pelvis. You then must play detective, which is the essence and fun of diagnostic radiology, to explain your observation.

One good exercise is to guess the age and sex of the patient before you look at the confirming data. You will soon become pretty good and usually be in the right decade on age, and almost always right on the sex of the patient.

The shape of the pelvis is abnormal in cases of achondroplasia, Mongolism and some other congenital syndromes. It becomes distorted in severe trauma including radical surgery, Paget's disease, primary and metastatic neoplasm, and with certain metabolic, neurogenic or degenerative problems such as acetabulae protrusio (Otto Pelvis), post poliomyelitis cases or severe degenerative arthritis.

Figure # 183 (right) AP (anterior-posterior) view of a normal pelvis. Some important landmarks include the ischial spines (outlined in red), and the obturator foramen (outlined in blue).

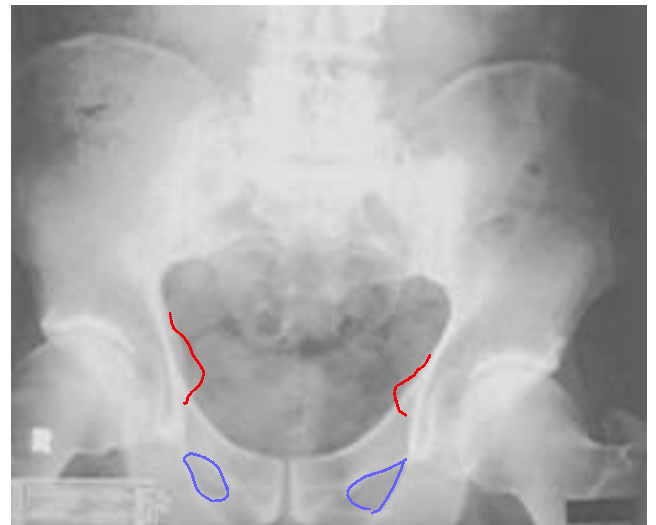


Figure # 184 (right). Better positioned AP view of the male pelvis (note soft tissue outline of the penis –red arrow). This image shows the obturator foramen better. In the system list for the pelvis the ovals we refer to include the obturator foramen, the pelvic inlet and gutters (outlined in yellow) and Shenton’s line(s) (outlined in blue). The small white arrow points to the right ischial tuberosity. The ischial tuberosities are the bones on which we sit.

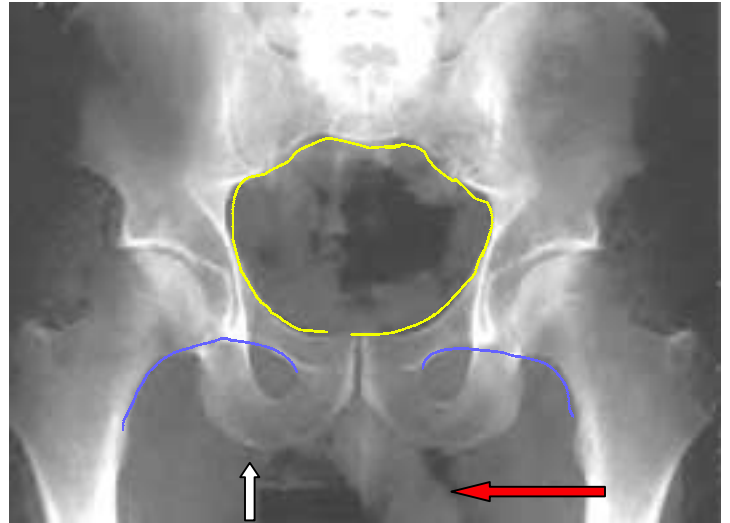


Figure # 185 (left). Take a good look at the shape (outlines) of this pelvis. What do you see? Ignore the high contrast of the spine and hips, which has been manipulated to better demonstrate other pathology.

Figure # 186 (right) is the labeled version of figure 185. Note the loss of normal cortex (density and outline) of the left posterior iliac crest (white arrow). Localized bone mineral loss as demonstrated here is almost always due to malignant neoplasm, in this case a plasmocytoma.



Figure # 187 (right) radiographic negative.
Here is a funny looking pelvis in a kid.
Note the lack of normal flare of the iliac wings which are squared off and vertically oriented. The acetabulae are also flat, lacking the normal angles. The diagnosis would not be a problem if you saw the long bones in this achondroplastic dwarf. Did you know dachshunds are canine achondroplastic dwarfs?



Figure # 188 (left). **It's easy to spot the disruption of the natural ovals of the pelvis in this patient with a fracture of the superior ramus of the left ischium. Note the distortion of Shenton's line. Refer to figure 184.**

Figure # 189 (right). **Ignoring the area of the SI joints, which are under exposed in this reproduction, check for density differences in the remainder of the pelvis and hips. What do you see? Answer on the next page.**



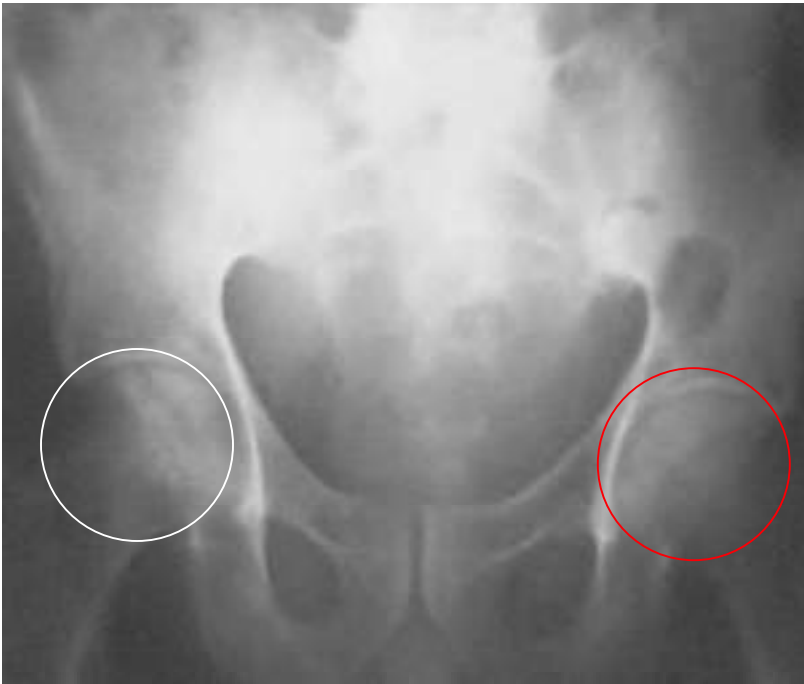


Figure # 190 (left). Compare the density of the right femoral head inside the white circle with that of the left inside the red circle. The increased density of the right hip is classic for avascular necrosis and can be considered an "Aunt Minnie" for that diagnosis. An earlier diagnosis can be made with MRI, which is probably the modality of choice in unexplained hip pain, after plain film radiography. MRI exams should be interpreted with plain films of the hips and pelvis because avascular necrosis is not the only cause of altered marrow signal in the hips.

Suspicion of avascular necrosis can be confirmed by MRI studies as noted in figure191 below.

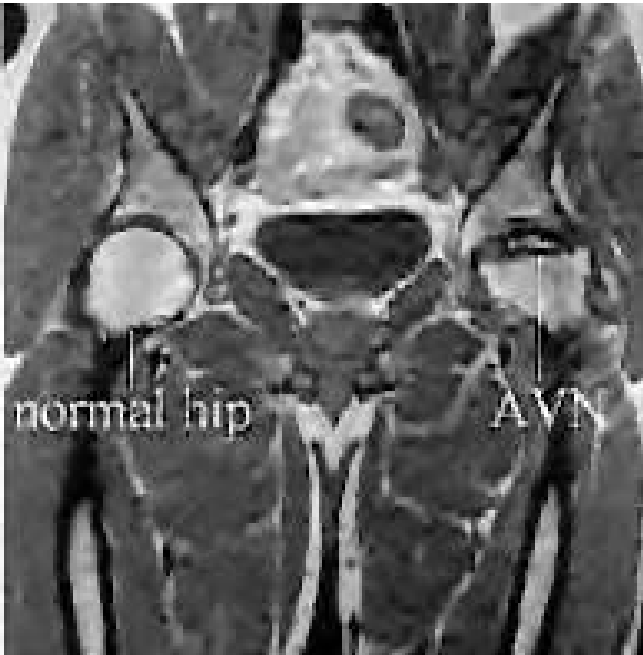


Figure 191 (left). Early Changes of avascular necrosis (AVN) are easily detected as alterations of the marrow signal seen in a normal femoral head. This case is more advanced with deformity of the femoral head already present. Image courtesy of Steven H. Brick, MD of Drs. Groover, Christie & Merritt, PC. via the Internet.



Figure # 191 A (left). When avascular necrosis occurs in an adolescent whose femoral epiphysis have not yet closed it is known as coxa plana or Legge-Perthe's disease. The radiographic negative to your left shows early flattening of the right epiphysis (red arrow) compared to the normal left side.

Figure # 191 B (right). This is the same patient as in 191A above as seen a few months later. Note the fragmentation of the right femoral epiphysis. The fat lines (red arrows) are easy to see in this radiographic negative. These fat deposits lie next to the joint capsule. Compare their positions and appearance to those of the normal left hip (blue arrows). Do you think there is distention of the capsule on the right? I do!

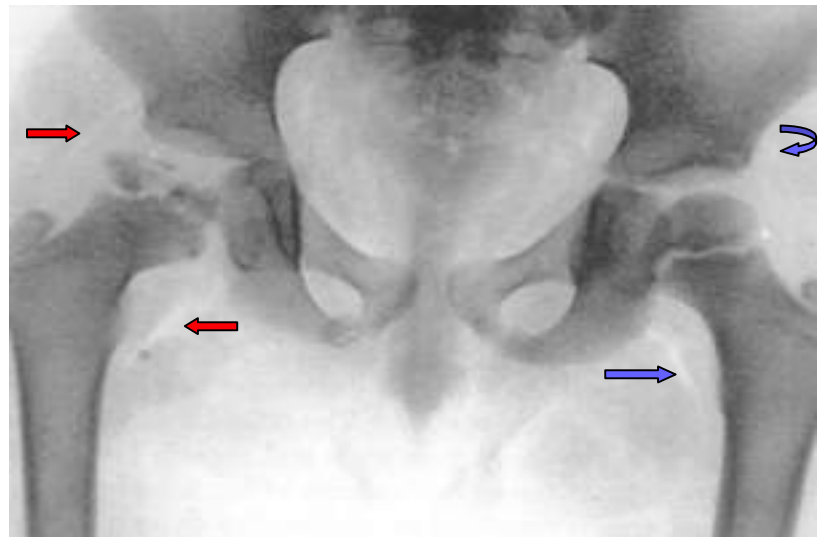


Figure # 191 C (left). Just to show you that all went well with the patient, this is a radiographic negative of the result of conservative management of this patient with Legge Perthe's disease!

Increased bone density occurs in Paget's disease, and metastatic ca of the prostate which we discussed earlier. Increased density of the femoral heads either unilateral or bilateral is a clue to loss of normal nutrition of bone such as occurs in avascular necrosis of the hips as shown in the previous figures 189 and 190.

The density of the pelvis varies with age, and although osteopenia or osteoporosis is common in the elderly, spotty or localized areas of **bone mineral loss** is a clue to something more serious, such as the leukemic infiltrate shown next in figure 192.

*Figure # 192 (right), Note the density difference between the symphysis (red arrow) and the rest of the pelvis in this patient with leukemia and leukemic invasion of bone. Film courtesy of the dirt museum via the Internet.
www.sbu.ac.uk/~dirt/museum/margaret/448-341-3320341.jpg*



Figure # 193 (left). Ignoring the overexposed areas of the posterior iliac crests in this reproduction, what catches your eye about the outlines of the pelvis in this young sprinter?*

**major clue!*

Figure # 194 (right) is the labeled version of figure 193. Did you identify the avulsion fracture of the left ischial tuberosity (white arrow)? This is a not uncommon injury in sprinters, particularly as they come out of the starting blocks and stress the hamstring muscles.

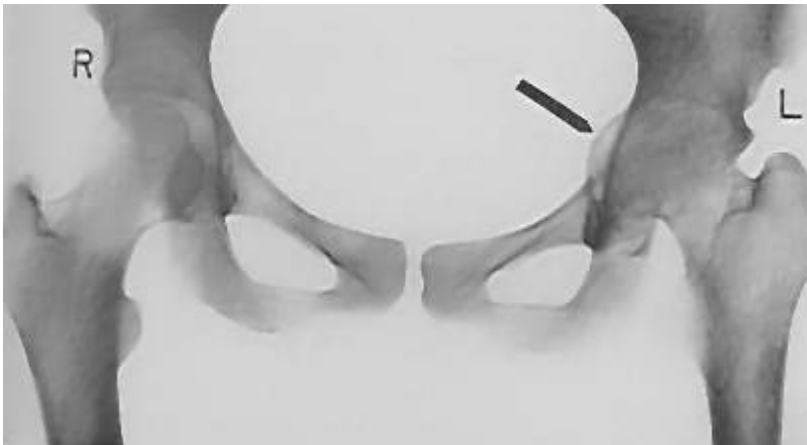


Figure # 195 (left) radiographic negative. Black pointer indicates intrapelvic protrusion of the acetabulum, a somewhat uncommon affliction of unclear etiology. This one happens to be in a 14-year-old girl. Bilateral acetabulae protrusio is common in Marfan's syndrome. Other cases are related to rheumatoid or pyogenic arthritis, osteoporosis, degenerative changes etc. Also known as Otto pelvis or (rarely) Arthrokatachysis. Courtesy of Children's Seashore House, Atlantic City, NJ.

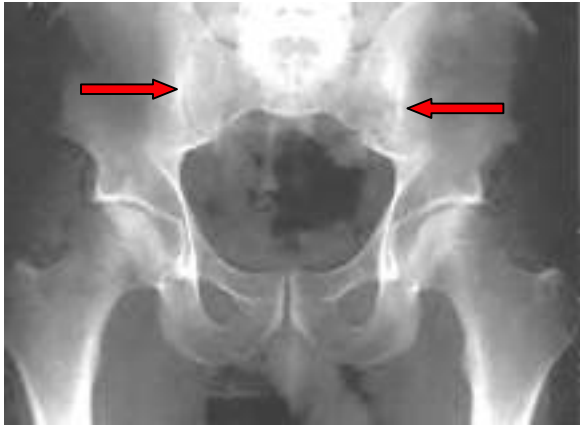
Studying the SI joints is necessary to exclude ankylosing spondylitis, and other diseases as shown in figures 196 and 197. The SI joints can also become disrupted in trauma.

Figure # 196 (right). Note the loss of normal definition of the SI joints in this patient with ankylosing spondylitis. Males predominate over females as much as 10/1 in some series, and most patients are serum negative for rheumatoid but HLA-B27 antigen positive (90%). The disease usually affects the joints symmetrically and the radiographic findings may precede symptoms.





Figure # 197 (left) shows obliteration of the right SI joint and surrounding eburnation (whitening) of a still open left SI joint in this patient with Reiter's syndrome. Compare to the normal SI joints (red arrows) in Figure # 198 (right).



The hip joints are also included in any study of the pelvis and it's also wise to include frog-leg lateral projections when feasible. Note the obvious slipped left femoral capital epiphysis in the child of figure 199. Not readily appreciated in the straight ap view, however, is the early slippage of the right side as well. This finding would be more easily detected by a frog-leg view of the pelvis. Figure 200 shows typical advanced degenerative osteoarthritis in a candidate for total hip replacement.



Figure # 199 (above). The advanced slippage of the left femoral capital epiphysis is obvious here (red arrows). What is not so obvious is the early slippage of the right femoral capital epiphysis, which would be easily detected by a frog-leg view (not available). Film courtesy of Loren G. Yamamoto, MD, MPH, and U. of Hawaii via the Internet.

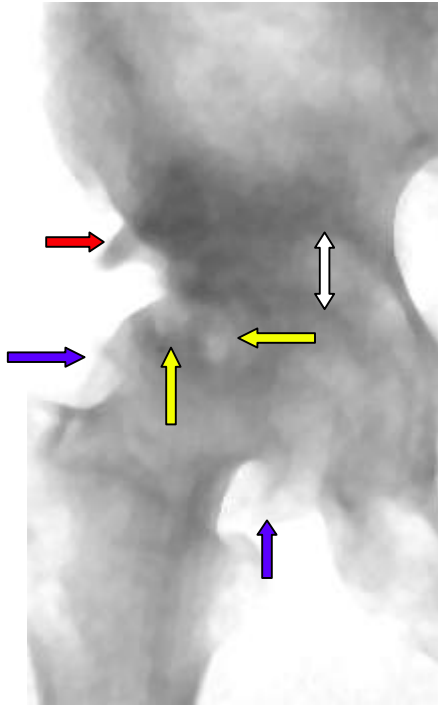


Figure # 200 (left). **Radiographic negative of a patient with advanced osteoarthritis of the right hip.** Note the large hypertrophic osteophytes on the femoral head (blue arrows) and lateral margin of the acetabulum (red arrow). There is also subcortical cystic change (yellow arrows) in the head of the femur. The joint space is not particularly narrow (white arrow), which is unusual with the other changes and which raises the question of a distended joint space due to fluid or pus. We can't see the periarticular fat lines in this reproduction which would help evaluate the joint space.



Figures # 201 and # 202 (left and right). **Red arrows point to the normal periarticular fat about the hips.** With fluid in the joint the fat lines may become bowed. It's part of your evaluation of the major joints to look for the periarticular fat and determine if it is normal or displaced. This part of major joint evaluation is invaluable for the elbow, knees, ankles etc., as we'll see later. Go back and review figure 191 b.

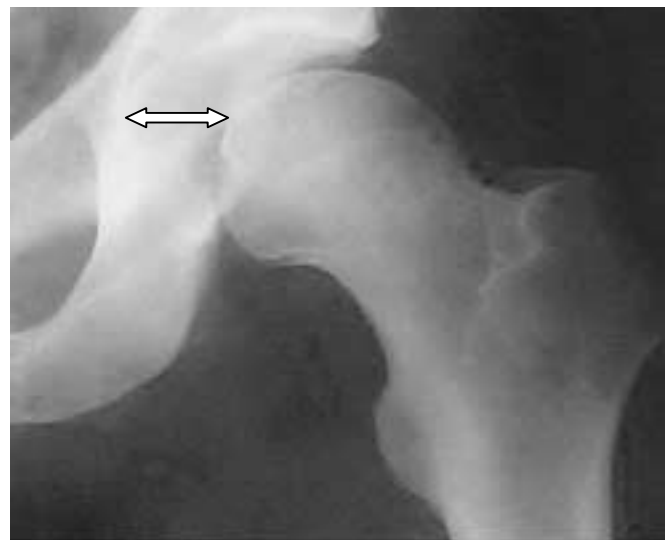


Analyzing the circles or more accurately, the ovals of the pelvis as demonstrated in figure 184, is crucial in evaluating trauma patients. I actually follow with my finger around the ovals to find subtle breaks in the cortex. Remember that if you find one break in the circle, there is likely another. In addition, in patients with clinical fractures, the fracture may not be appreciated by plain film radiography and it may be necessary to utilize high resolution or thin cut CT studies to confirm. See if you can spot a fracture in the radiograph below (figure 203).



Figure # 203 (left). This is an AP radiograph of the left hip following reduction of a traumatic dislocation. Can you identify a fracture? Is there any abnormality? Case courtesy of Michael L. Richardson, MD, U. of Washington via the Internet.

Figure # 204 (right). The same radiograph as # 203 above. No fracture is visible (at least to my eye), but there is noticeable widening of the joint space (white arrow). As Dr. Richardson so aptly points out in his on-line teaching file, "Any fracture of the pelvis that may involve the acetabulum should be studied by CT. The same holds for any dislocation of the hip" See CT study next page.



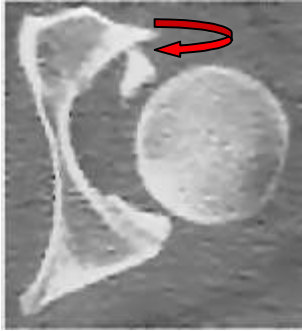


Figure # 205 (left) CT study of the hip in the case presented above shows a bone fragment (red arrow) in the joint space. Case courtesy of Michael L. Richardson, MD, U. of Washington via the Internet.

Finally, a look at the symphysis pubis, sacrum and coccyx completes your checklist for looking at the pelvis. Note a classic Aunt Minnie in this patient with osteitis pubis, which is a typical development after childbirth in some women.

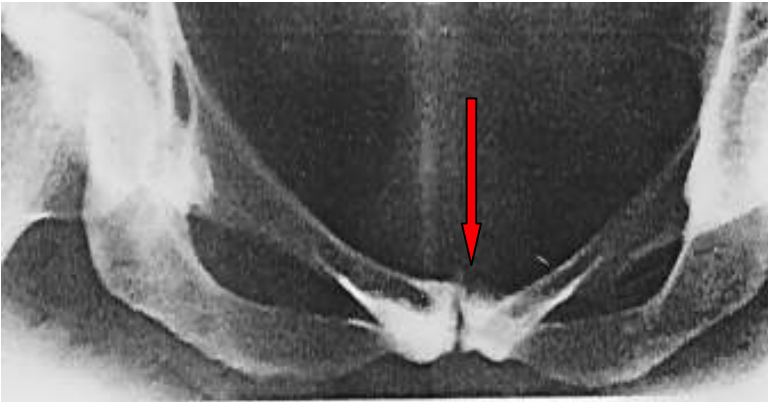
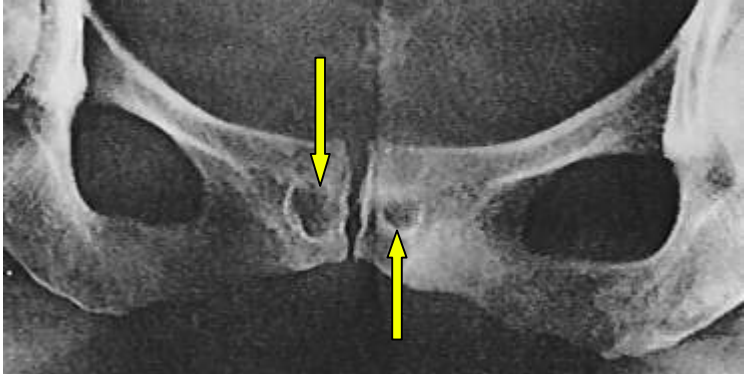


Figure # 206 (left). The symphysis here shows eburnation (whitening) typical of osteitis pubis, a post partum finding. (red arrow).

Figure # 207 (right). The sub cortical cysts in the symphysis illustrated by the yellow arrows represent another post partum “Aunt Minnie”.



The AP view of the sacrum in a pelvic film seldom shows pathology with the exceptions of trauma and some congenital anomalies. Occasionally a normal variant may raise a question if you have not seen it before, such as the prominent foramen show in the next illustration.

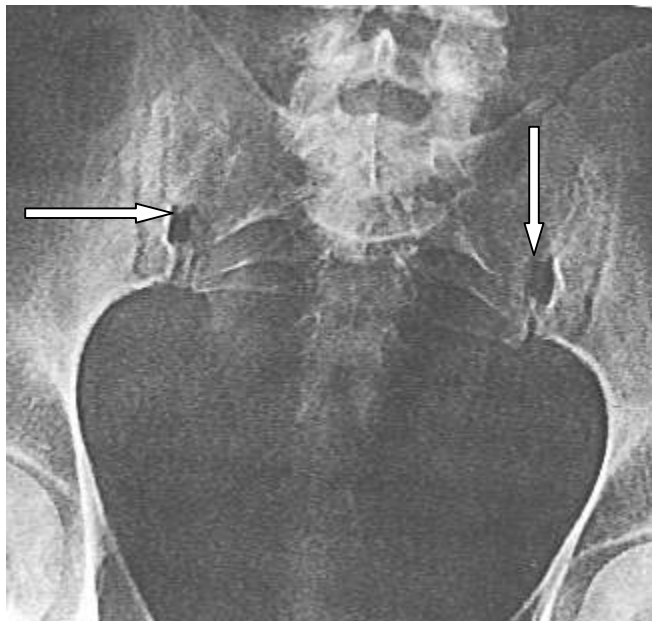


Figure # 207 (left). **The sacral foramina shown here (white arrows) are a prominent normal variant. The anterior sacral foramina transmit the first four sacral nerves, arteries and veins.**

The coccyx is best evaluated in the lateral view. The anteflexed position of the coccyx is a normal variant as shown here, and is not an indicator of traumatic dislocation or fracture by itself. Clinical correlation is required in cases of trauma. In childbirth an anteflexed coccyx will usually relocate (straighten) with vaginal delivery.

Figure # 208 (right). **The distal two segments of the coccyx shown here by the blue arrows are anteflexed, a normal variant.**



Let's see if you can put your new knowledge to work by evaluating the findings in the next image (Figure # 198 below). This is an AP radiograph of a 61-year-old male with hip pain. Film courtesy of Michael Richardson, U. of Washington via the *Internet*.



Figure # 198 (above).

For answers see next page.

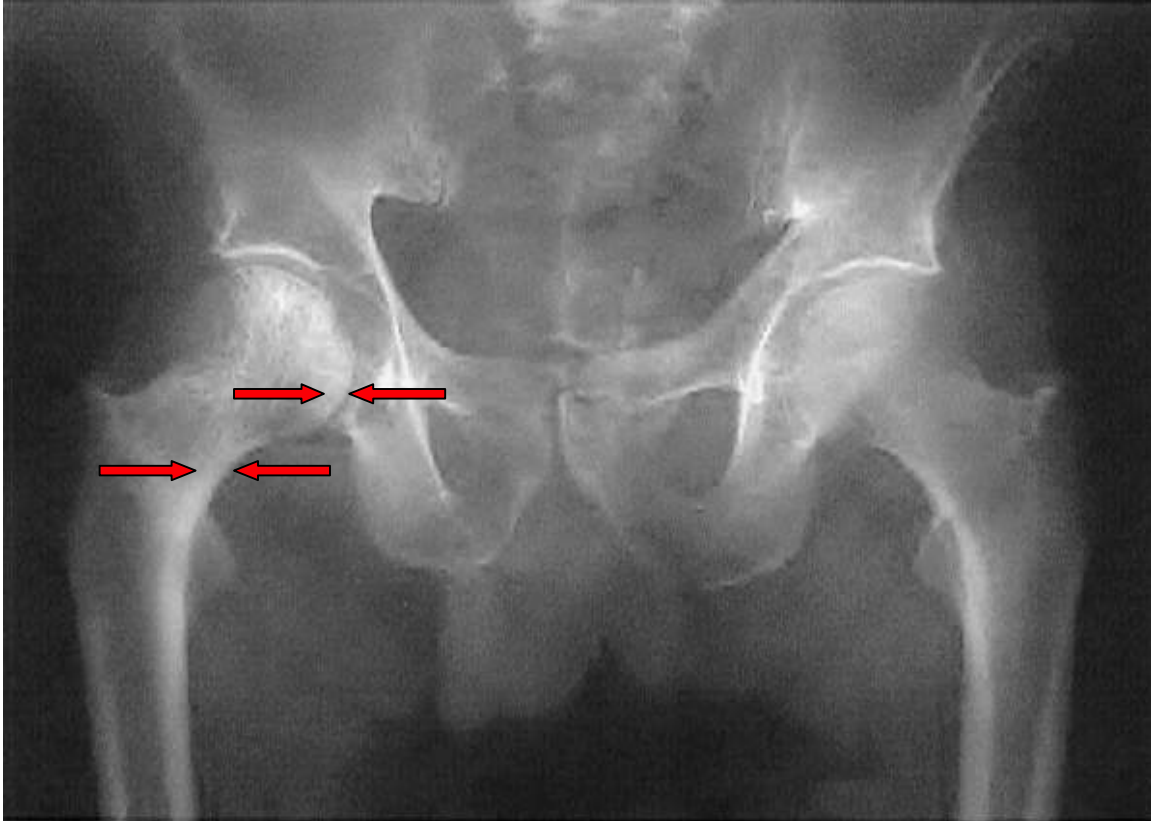


Figure # 199 (above) is the labeled version of figure 198. The findings include a coarsened trabecular pattern of the right hip, a slightly thickened cortex (red arrows) compared to the opposite hip, and increased density of the hip compared to the left side. Do these findings sound familiar? You are right! Three out of four signs of Paget's disease are present, which is enough to call the diagnosis!

CHAPTER SEVEN

THE ELBOW AND WRIST

We are including the elbow and wrist in the manuscript because they are frequently injured joints, which the primary care physician has to screen for serious injury often, and many times without immediate access to radiological consultation. I found when I was in family practice that the elbow, particularly in kids, was difficult to screen to my untrained eye. Once familiar with the anatomy and the secret of the flexor and extensor fat pads, however, the process is not so difficult. One also has to recognize the normal growth centers about the elbow and wrist joints. We will start with a system for the elbow.

- 1-FAT PADS**
- 2-RADIAL HEAD**
- 3-GROWTH CENTERS**
- 4-HUMERUS AND ULNA**

Displacement of the flexor fat pad of the elbow is a reliable sign of joint effusion, and in the case of trauma almost always indicates interarticular hemorrhage. If both the flexor and extensor fat pads are displaced the joint effusion is quite large as seen frequently in severe transcondylar fractures. Oft times the fat pad displacements are the *only* signs of fracture, and it behooves the attending physician to then immobilize the joint and obtain a follow up film in seven to ten days. Note the normal position of the *flexor* fat pad as seen in the lateral projection in figure 200.

Figure # 200 (right). Yellow arrow points to the normal position of the flexor fat pad of the elbow. Note its position adjacent to the anterior cortex of the distal humerus. You must look for this fat pad on every elbow examination because its displacement signifies fluid (such as hemorrhage) in the joint.

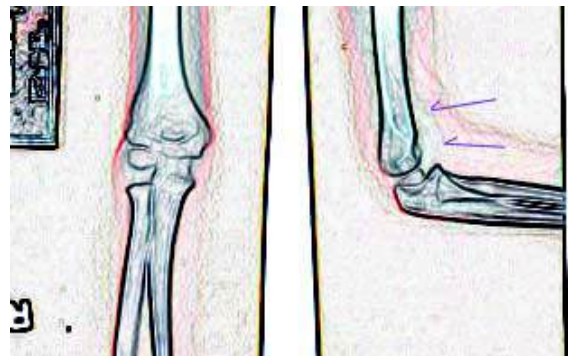


The *extensor* fat pad is usually not visible in a normal elbow joint. If you see it as shown in figure 201, it almost always indicates fluid or hemorrhage in the joint. Also note in figure 201 the anterior displacement of the flexor fat pad when compared to the normal position in figure 200.



Figure # 201 (left). Green arrow shows the extensor fat pad in this patient with an elbow injury. The yellow arrow shows an elevated flexor fat pad which is better seen on the original radiograph, but you can get an idea of what to look for by referring to another case with an accompanying edge-enhanced sketch below.

Figures # 202 (below left) and # 203 (below right). Another case of interarticular hemorrhage showing displaced fat pads (arrows).



The fat pads of the elbow should be the first things you look for when evaluating the joint. If they are displaced, chances are there is a fracture somewhere (in trauma cases). In these cases you should immobilize the joint and obtain follow up films in 7 to 10 days, which will often show evidence of a healing fracture such as periosteal new bone formation or early callus.

The radial head evaluation includes its position in relation to the ulna as well as a look for fractures. Even experienced radiologists or orthopedic surgeons may miss a dislocated radial head if they focus on an obvious fracture of the ulna. The combination of fracture of the shaft of the ulna and a dislocated radial head is known as a Monteggia fracture. The head of the radius should superimpose the ulna in all projections and a line drawn along the long axis of the radius should intersect the capitellum (refer back to the normal position in figure 200). Note its position in a patient with Monteggia's fracture in Figure 203.

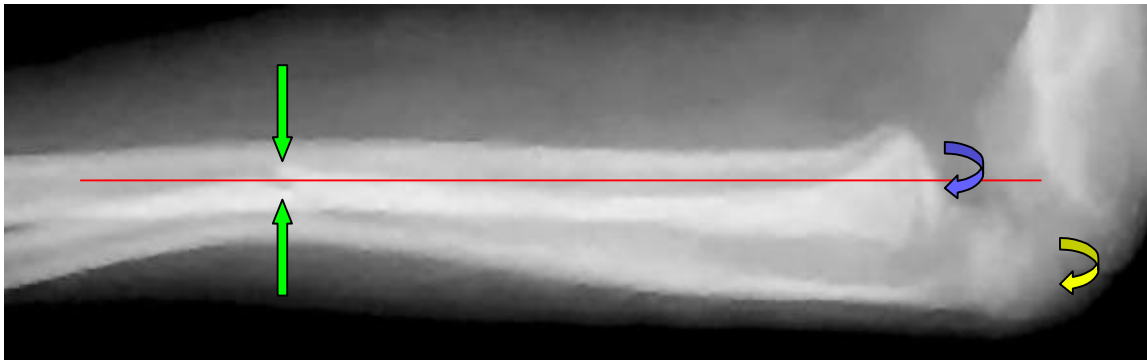


Figure # 203 (above). A line (red) drawn along the long axis of the radius misses the capitellum (yellow arrow) indicating a dislocated radial head (blue arrow) in this patient with a Monteggia's fracture (green arrows). Courtesy of Lynette L. Young, MD U. of Hawaii via the internet. www2.hawaii.edu/medicine/pediatrics

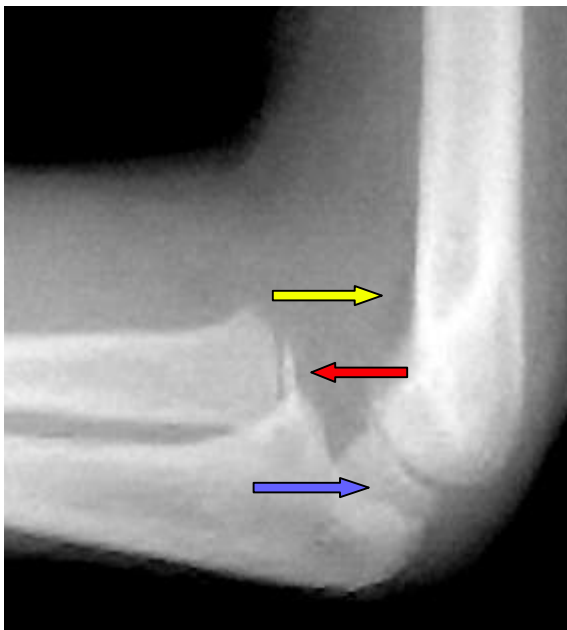


Figure # 204 (left). Here's another look at the elbow in the case of Monteggia's fracture above. Note the fat pad is adjacent to the bone (yellow arrow). The radial head, in this case the epiphysis (red arrow) does not point at the capitellum (blue arrow). Compare the position to the normal in figure 205. www2.hawaii.edu/medicine/pediatrics

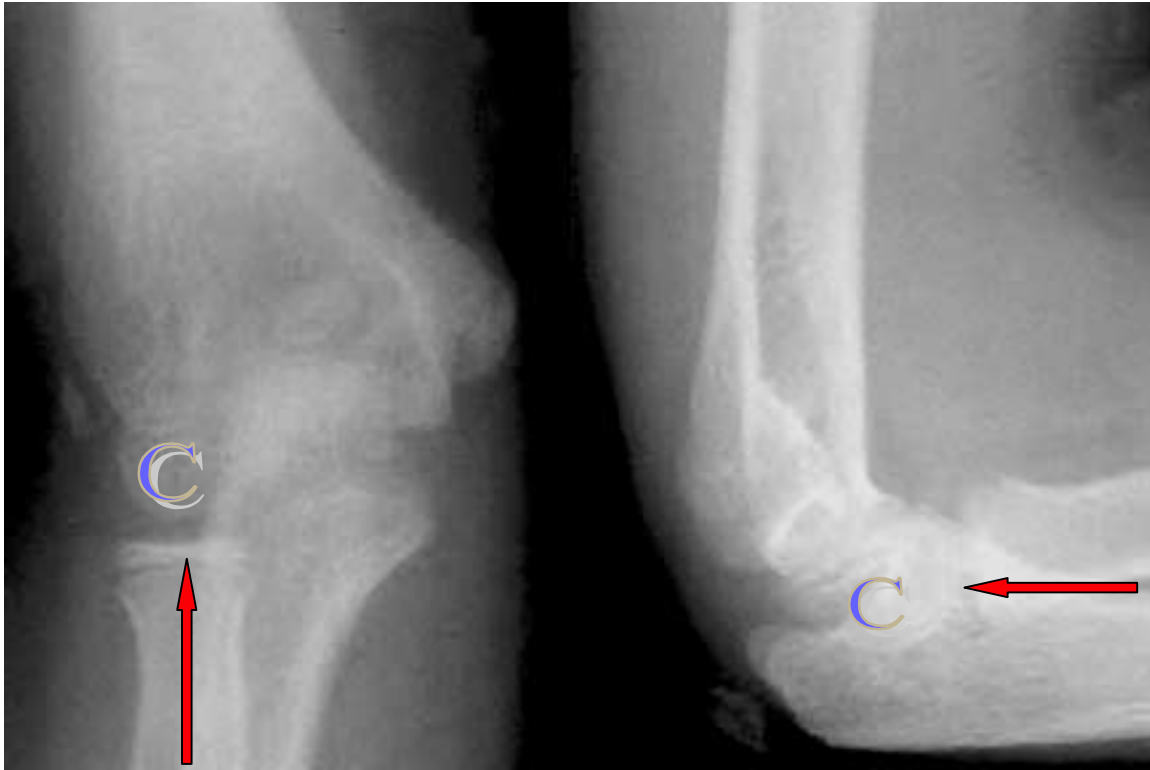


Figure # 205 (above). Normal elbow in a seven year old male. Note the alignment of the radial head (epiphysis) and shaft (long red arrows) with the capitellum (blue C). Also all of the growth centers of the elbow are visible in the radiographs above. Can you identify them? Radiographs courtesy of Alson S. Inaba, MD, author and Loren Yamamoto, MD, web page author, U of Hawaii via the Internet. www2.hawaii.edu/medicine/pediatrics

The growth centers of the elbow can be very confusing to the student. There are usually six and sometimes seven of them that appear at various ages. The capitellum (also spelled capitulum) and lateral part of the trochlea appear at 1 to 1 1/2 years of age and I for one am always getting them confused. One way to remember which side the capitellum is on is to think of the radial head as having a CAP. The lateral, also called the external, epicondyle is just above (cephalad) and lateral to the capitellum and appears at about age 14. It is the site of frequent inflammatory episodes called tennis elbow but the radiographs taken for this clinical diagnosis are usually negative. The medial, also called the internal, epicondyle appears at about age 8 or 9 (earlier in females).

Distal to the humerus are the growth centers of the proximal end of the olecranon (age1), the head of the radius (ages5-7), and occasionally, the radial tuberosity which appears at puberty. To make things even more confusing, ***the capitellum and trochlea fuse to form one epiphysis at ages 13-15***. The epicondyles usually fuse to the shaft of the humerus independently. Thus you can see it is necessary to have knowledge of these centers in order not to misinterpret one of them as a fracture. Of course one of the

oldest aids to the inexperienced eye is to take a radiograph of the normal side to compare. Note the position of the normal growth centers in figure 205 above and in the illustration in figure 206 below.

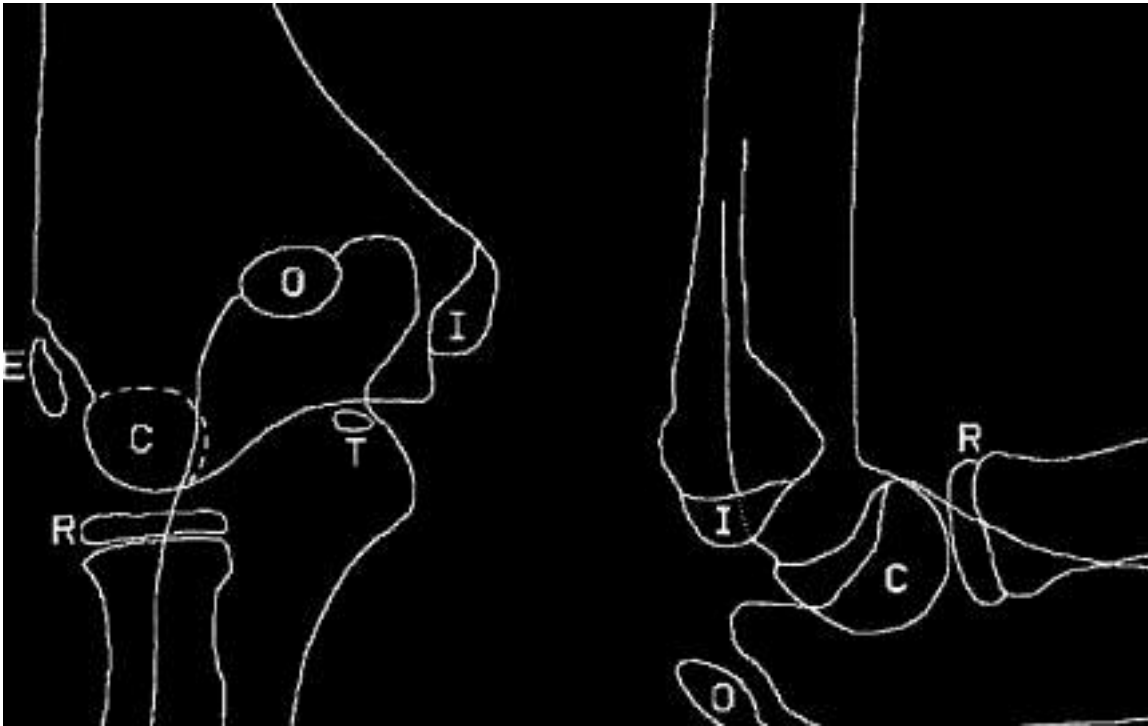


Figure # 206 (above). The normal growth centers of the elbow. They can be remembered in order of appearance by the mnemonic CRITOE.

Key: C-capitellum
R-radial head
I-internal epicondyle
T-trochlea
O-olecranon
E-external epicondyle

Illustration courtesy of Alson S. Inaba, MD, author and Loren Yamamoto, MD, web page author, U of Hawaii via the Internet www2.hawaii.edu/medicine/pediatrics

Occasionally one of the growth centers may be fractured or subluxated. This is not likely to happen without the secondary signs of interarticular hemorrhage discussed above (fat pad displacement), but even so it's always wise to splint the joint and obtain follow up films after a period of immobilization if there is any doubt clinically.

Evaluation of the hand and wrist usually does not cause problems to the untrained eye because fractures and dislocations are usually obvious. Occasionally, however, subtle lesions can be missed, and we will therefore give you a system to reduce the chance of a miss, leaving interpretation of more complex processes such as the arthritides to the radiologist, rheumatologist and orthopedic surgeons. Remember to always splint the affected part in cases of trauma, and you will have acted properly.

A system for looking at the bones of the hand and wrist includes: **Sam's Cortices**

- 1-Soft tissues**
- 2-Arcs**
- 3-Mnemonic**
- 4-Styloid processes**
- 5-Cortices**

Those not trained in trauma often ignore soft tissues, but radiologists will frequently look at soft tissue outlines first, if for nothing else to use as a clue to the site of injury. See if you can zero in on the site of injury in some of the following presentations.

The wrist has three curves, two of which are concave and one that is convex as seen in the AP projection. Refer to figure 207.

Figure # 207 (right). Look for the three arcs or curves of the wrist on your initial evaluation of the AP view. Any disruption of one of these arcs may signal a dislocation. The radial-carpal arc (red) should align the navicular, lunate, and triquetrum with the natural curve of the radius-articulating surface. The intercarpal curve is shown in blue, and the carpal-metacarpal arc in black.

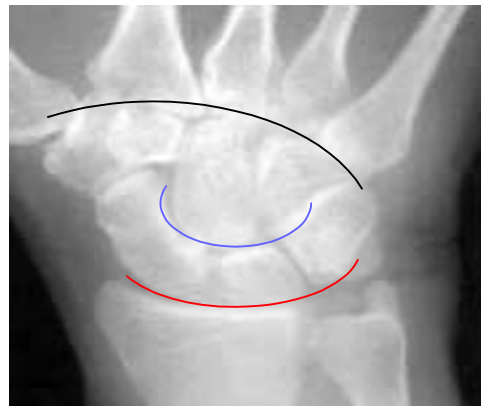
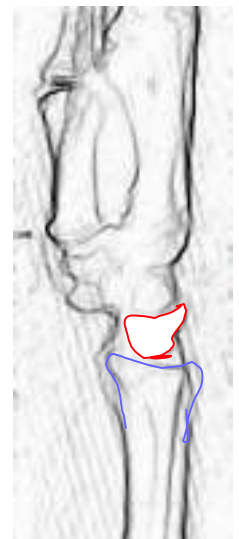


Figure # 208 (left). Lateral view of a normal wrist. Note the position of the lunate in relation to the articulating surface of the distal radius. See drawing in figure 209 (right).

Figure # 209 (right). The lunate, outlined in red, should always align with the distal articulating surface of the radius, outlined in blue.



Any break in the curves is a red flag for a subluxation or dislocation. In evaluating positions the curves are important as well as the position of the lunate in the lateral view. Note the position of the normal lunate in relation to the articulating surface of the radius in figures 208 and 209 on the previous page.

Now that you are aware of the normal arcs, how would you evaluate the wrist in the study (figure 210) below?

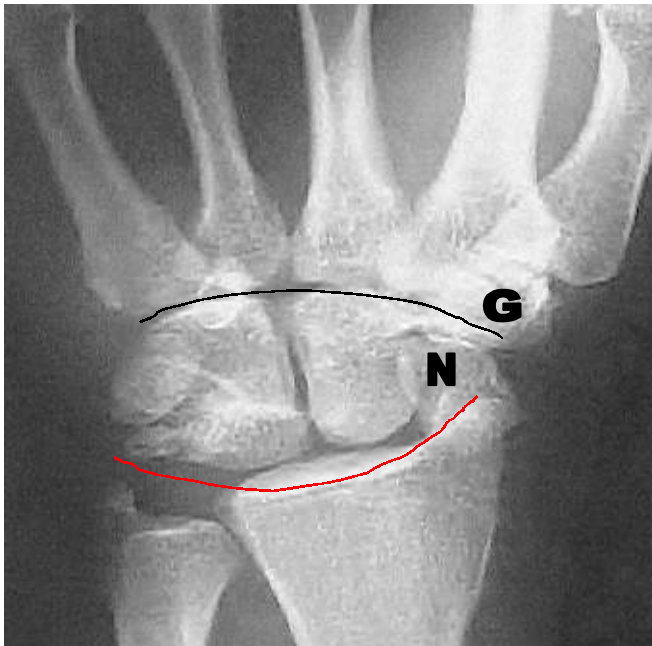


Figure # 210 (left). Note that you can draw the radial-carpal arc (red) and the carpal-metacarpal arc (black), but the intercarpal curve is not apparent. Also note the navicular (N) superimposes the radial styloid process in this AP view, and the greater multangular (G) is displaced distal to the black curve. This trauma patient has a trans-carpal dislocation as confirmed in the lateral view (figure 211) below.

Figure # 211 (right). Lateral view of the same patient. Note that although the lunate remains aligned with the distal radius, the remainder of the carpal bones are dislocated dorsally. Films courtesy of the EMBBS library via the Internet. www.embbs.com

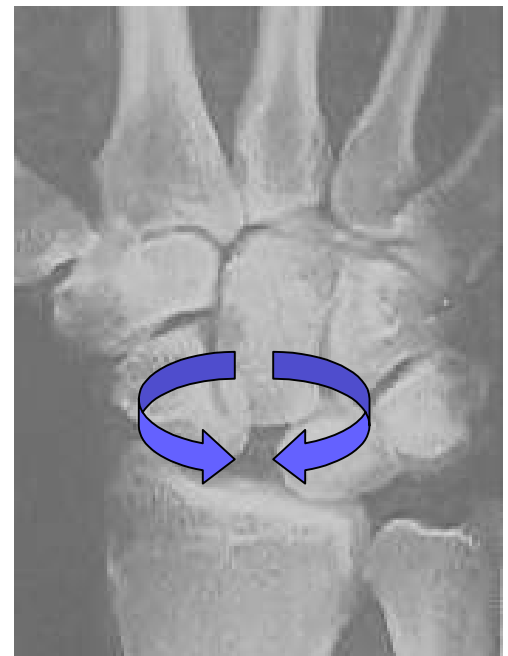


It is also easy to miss a subtle scaphoid-lunate dissociation, so I look specifically for widening of the space between the two. Note the normal relationship in figure 212.



Figure # 212 (left). Note the normal width of the navicular (also called the scaphoid) – lunate space (arrows). This is the same radiograph as seen in figure 207.

Figure # 213 (right). Note the widened space (blue arrows) between the scaphoid (navicular) and the lunate in this patient with a ruptured scaphoid-lunate ligament. The gap between these carpal bones is called the “Terry Thomas Sign” or “David Letterman Sign” after the famous gaps in their front teeth. Wrist arthrography (invasive) or MRI (non-invasive) can confirm the diagnosis.



Even after years of looking at small parts like the bones of the hand and wrist, I still take the time to look at each bone with a magnifying glass while reciting the famous (or is it infamous?) mnemonic, "never lower Tillie's panties, grandma might come home", to identify each of the carpal bones. For you youngster's who are not familiar with it, each first letter of the mnemonic stands for the first letter of one of the bones, i.e. Navicular, Lunate, Triquetrum (or triangular), Pisiform, Greater multangular, Multangular (lesser), Capitate (or cunate), and Hamate. This process forces me to evaluate each carpal bone for *position*, possible fractures etc. Therefore the third word in your system should be **mnemonic**.

One of the common fracture injuries is that of the carpal navicular, and if the ordering physician or PA is astute he or she will request a magnified view if there is tenderness in the anatomic snuffbox. Appreciate

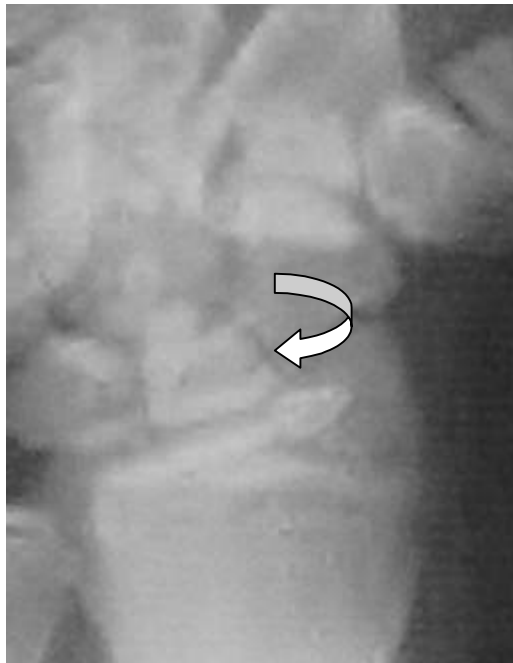


Figure # 214 (left). Even though this magnified view of the navicular did not reproduce well, it is still relatively easy to see the fracture line (arrow).

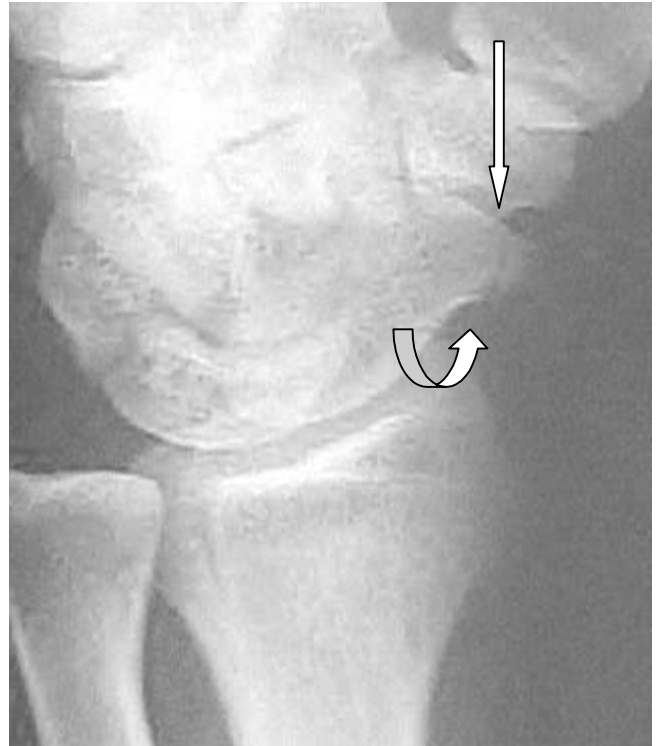


Figure # 215 (right). Here's another magnified view with the hand in ulnar deviation. This fracture (arrows) might not have been seen without special views.

how easy it is to diagnose a fracture of the navicular with a magnified view as shown in figure 214.

We target the radial and ulnar styloid processes specifically because fractures are so common in these locations. Sometimes all that can be discerned is a small wrinkle in the cortex which is why the cortices are included in the system. Also the cortices of the distal radius are subject to greenstick injuries known in the trade as torus fractures. These lesions are demonstrated in figures 216 and 217. The torus fracture



Figure # 216 (left) Looking at the styloid processes, in this case the ulnar styloid, often yields a fracture diagnosis as shown here (arrow). Let's see how sharp you are; what else is wrong with this wrist? Confession: I didn't see it either, but there is a lunate dislocation, which would be easily seen in a lateral view not available here. See U.Wisconsin athletic injury site on the WEB. The additional views were not reproducible.

in figure 217 can be classified as an Aunt Minnie.

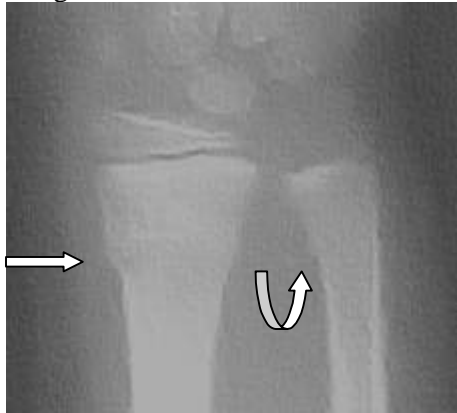


Figure # 217 (left). **The torus fractures of the radius and ulna demonstrated here by the wrinkles in the cortex (arrows) are “Aunt Minnies”. You should never miss one.**

Finally the cortical evaluation includes all of the other small bones visible on the film to make sure we are not missing an obvious fracture such as the boxer's fracture as shown in figure 218.



Figure # 218 (left). **Radiographic negative of a Boxer's fracture of the fifth metacarpal (red arrow). Be sure to look at all of the information (bones, soft tissue) on any given film.**

Here are a few “Aunt Minnies” for the elbow and wrist:

Figure # 219 (right). **Note that the ulna is elongated and dorsally subluxated. This is an Aunt Minnie known as Madelung's deformity (ulna plus). There is also an ulna minus deformity, where the ulna is short. See figure 220 next page.**





Figure # 220 (left). A short ulna or ulna minus deformity is a variation of Madelung's deformity as shown here.

Figure # 221 (right). Here's a kind of neat Aunt Minnie. The beak-like bony structure (arrow) extending from the anterior cortex of the distal humerus is called a supracondylar process. It is a vestigial structure analogous to a rooster's spur. The brachial artery often divides around this structure. It usually does not have any clinical implications.



Finally, a word or few about the Salter-Harris classification of fractures through the epiphysis and physis is in order. An excellent discussion of the classification and ways to remember it is presented on the Internet by Drs. Loren G. Yamamoto, Stanley M.K. Chung, and Alson S. Inaba at the U. of Hawaii site. The classification can be summarized by the illustration they present in figure 222 below. We present it here because you will see these fractures classified in radiology reports and it behooves you to know what is meant by the classification reported.

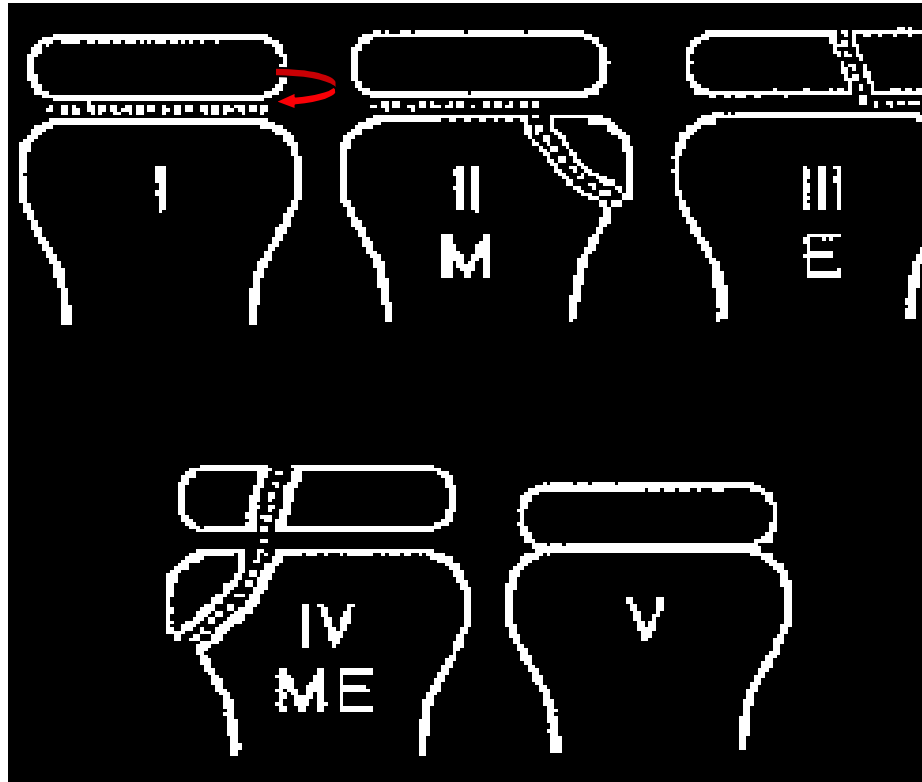


Figure # 222 (right). Salter-Harris classification of fractures is shown here courtesy of Drs. Chung, Inaba, and Yamamoto as noted above. The curved red arrow points to a dotted line indicating a fracture through the physis, classified as a Salter-Harris type I. The physis may or may not be widened, and therefore the injury may or may not be visible on the radiograph initially. The type II lesion shows an obvious fracture through the metaphysis, but again the physis may or may not be widened. Likewise for the physis in a type III fracture through the epiphyseal plate. A type IV fracture is usually associated with a widened physis. A type V injury is rare, where the physis is jammed or compacted into the metaphysis. There are often displaced fragments in the type II, III, and IV injuries. www2.hawaii.edu/medicine/pediatrics

CHAPTER EIGHT

ANKLES AND FEET

Evaluation of the ankles and feet does not require a great deal of detail since the principles are similar to other small parts studies, which we have already discussed. Thus we will limit our discussion to a few salient points. A system to memorize might include:

1-Soft tissues

2-Ankle mortise width

3-Base of the 5th metatarsal

4-cortices

Mnemonic: (Soft tissue ABC's)

The soft tissue evaluation frequently includes use of the bright light because of the technical difficulties of displaying all parts in good exposure. It also includes a specific look for a positive teardrop sign, which is another displaced fat pad as seen in the lateral view. The "teardrop" is actually a small bursa, which fills with fluid or hemorrhage following injury much the same as the fat pad signs in the elbow. Note the normal position of the anterior fat pad of the ankle as seen in figure 223, and the replacement of fat density by water density in the form of a teardrop as seen in an injured patient in figure 224.

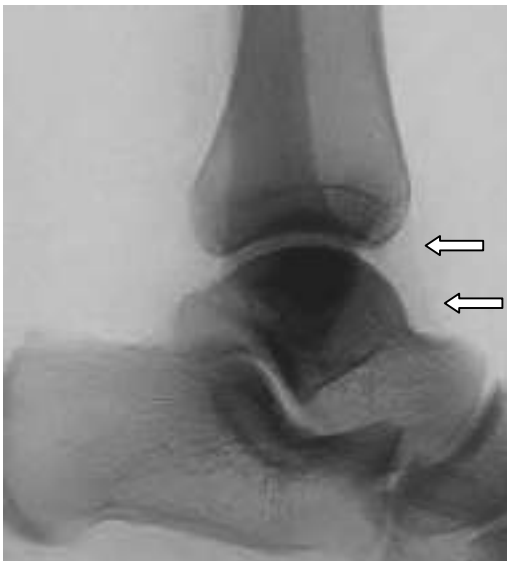


Figure # 223 (left). Note the normal position of the anterior fat pad of the ankle as demonstrated by the arrows in this radiographic negative. Figure #223a (below) shows the area of the fat pad and the location to look for it as outlined in white.





Figures #'s 224 (left) and 224a (below). It takes a little imagination on these reproductions to see the positive teardrop sign of an injured ankle. It's usually much easier on well exposed films, but many times you will have to use the bright light. Do it!



All injured ankles require evaluation of the mortise joint width because disruption of the supporting ligaments is a severe injury sometimes requiring surgical intervention, even if a fracture is not associated. Occasionally stress views are necessary to demonstrate a widened joint. Compare the normal width of the mortise joint in relation to the medial and lateral malleoli in figures 225 and 225a to the widened joint due to a ruptured deltoid ligament.



Figures # 225 and 225a (left & right). The AP (anterior-posterior) view on the left is an adolescent's ankle. The red arrows indicate the normal width of the mortise joint in the AP view. The oblique or mortise view on the right gives a better perspective of the ankle mortise joint and the normal width as indicated by the blue arrows in this adult patient.





Figure # 226 (left). Note the widening of the medial portion of the mortise joint (red arrow) due to a rupture of at least a part of the deltoid ligament.

The base of the fifth metatarsal is the most frequently fractured bone in the foot, so we have learned over the years to look specifically in this area in all cases of trauma to the foot or ankle. To the untrained eye the apophysis at the base of the fifth can be confused with a fracture. However, it's really very easy to tell the difference simply by knowing that the growth center line is parallel to the shaft of the fifth metatarsal and practically all fractures of the fifth are in a transverse plane as demonstrated in figures 227-229.



Figure # 227 (left). The growth center of the proximal fifth metatarsal (red arrow) is oriented near parallel to the proximal cortex (blue and green lines). Whereas a fracture at the base of the fifth is usually oriented transversely as shown by the blue arrow in Figure # 228 (right).





Figure # 229 (left). Note the transverse or horizontal orientation of the fracture at the base of the fifth metatarsal (yellow arrow) as opposed to the vertical orientation of the apophysis as seen in figure 227 on the previous page. Case courtesy of Wheelless Textbook of Orthopedics on line. www.medmedia.com

Occasionally there may be soft tissue swelling over the apophysis at the base of the fifth metatarsal along with a question of possible separation or avulsion. In this case it is not possible to differentiate an avulsion fracture of the apophysis from a soft tissue injury until a follow up radiograph shows healing periosteal new bone. Obviously the prudent thing to do is to treat the patient as if it were fractured until a follow up film either proves or disproves the case.



Figure # 230 (left). Sometimes the apophysis appears to be separated from the proximal cortex at the base of the fifth metatarsal (yellow arrow). Don't mistake this for an avulsion fracture. Avulsions can occur at this location but they are rare and almost always associated with soft tissue swelling and clinical point tenderness. Note that there is no soft tissue swelling here.

There are also other sesmoids or ununited apophyseal growth centers in the region of the ankle or foot that sometimes cause confusion. These have been well demonstrated in the reference texts listed in the first chapter of this book. However it is worth mentioning that sesmoids and growth centers have a smooth, rounded cortex, where as avulsion fractures usually have sharp edges. A case in point is demonstrated in this next case as shown in figure 231.

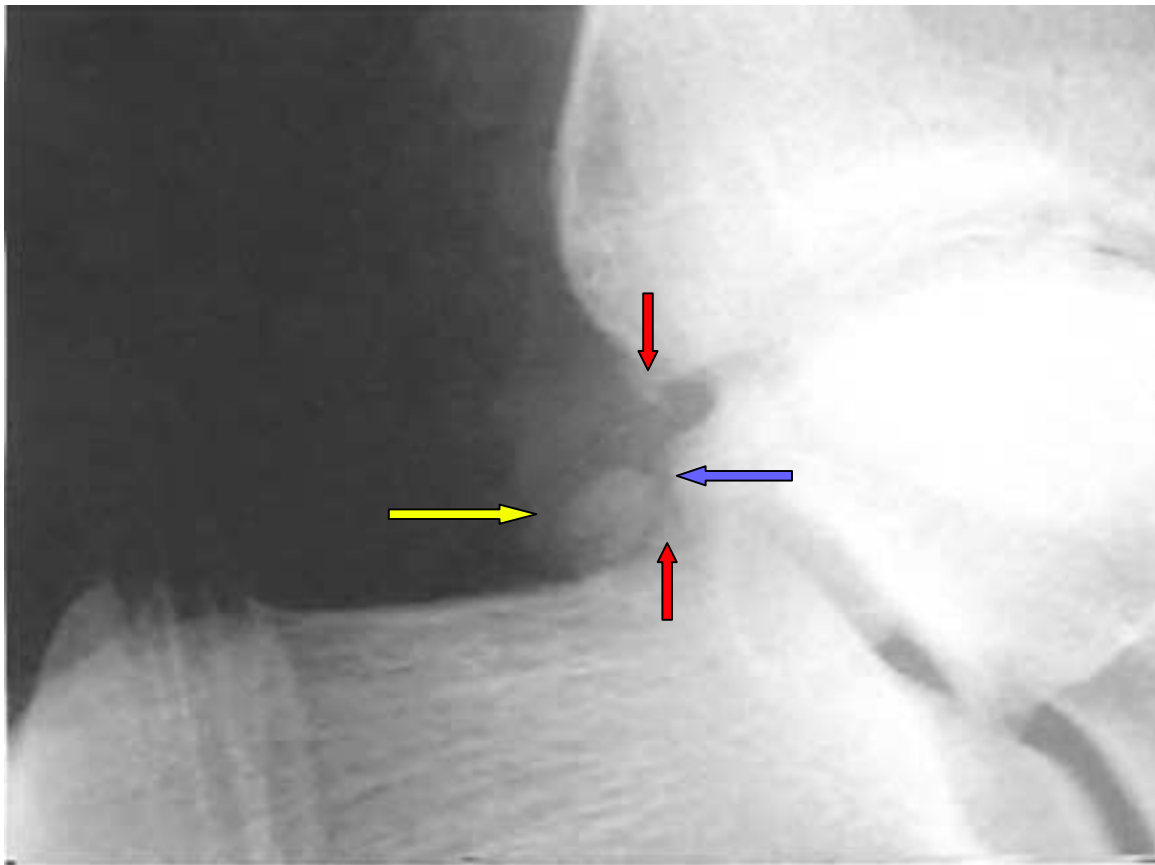


Figure # 231 (above). There is indeed a fracture demonstrated in the above radiograph. Can you spot it? The yellow arrow points to the os trigonum, a normal sesmoid seen in about 50% of the population. Some have postulated that the os trigonum represents an ununited apophysis of the posterior process of the talus. Note the smooth rounded edges typical of a sesmoid bone. Also note the ragged edge of the posterior process of the talus (blue arrow). This area is likely the origin of the two small avulsion fragments (red arrows) demonstrated in this patient with a Sheppard's fracture, i.e. a fracture of the lateral tubercle of the posterior process of the talus (also called the astragalus). Case courtesy of *Wheeless Textbook of Orthopedics on line.*
www.medmedia.com

Finally, as in all small parts evaluation, look at the cortices of each bone before declaring the study negative in your mind, and it is always prudent to await the consulting radiologist's report before telling the patient your interpretation. Lord knows even experienced physicians including we radiologists miss

things once in awhile! Two or three pairs of eyes are always better than one, and remember that you have the advantage of the patient who the radiologist seldom sees face to face, so be sure to provide that third side of the diagnostic triangle-history!

END

GLOSSARY

Adenopathy Enlarged lymph nodes.

AP Anterior to posterior

Cardiomegally enlarged heart

CAT SCAN or CT SCAN Computed axial tomography scan or computed tomography scan.

CHF Congestive heart failure

COPD Chronic obstructive pulmonary disease (emphysema).

CT Ratio Cardiac thoracic ratio. Transverse measurements on a chest radiograph.

CT Stands for computed tomography.

Eburnation: Whitening of bone.

Gamuts A list of differential diagnoses.

Hot Light A small spotlight brighter than an ordinary view box.

KUB Stands for kidney, ureters, bladder, a plain film of the abdomen .

PA Posterior to anterior

SI Joints: sacroiliac joints

Silhouette Sign The border disappears between two water density tissues that touch.

Target The anode in an x-ray tube. The source of x-rays produced.

Target-film distance The distance from the anode in an x-ray tube to the film cassette.

TE Fistula Tracheo-esophageal fistula, an abnormal connection, usually a birth defect.

REFERENCES

1. *Atlas of Normal Variants That May Simulate Disease*, 4th Edit. Theo. E. Keats, MD. YearBook Medical Publishers, Inc. Chicago, London, Boca Raton.
2. *Borderlands of the Normal and Early Pathologic in Skeletal Roentgenology*, 3rd Edit. Prof. Dr. E.A. Zimmer, Translated by Stefan P. Wilk, MD. Grune & Straton, New York, London.
3. *Reeder and Felson's Gamuts in Radiology*, 3rd Edit. M. Reeder, Springer-Verlag 1993, NY, Berlin, Heidelberg, London, Paris, Tokyo, Barcelona, Budapest.
4. *The Radiologic Clinics of North America, Symposium on the Spine*, A.R. Sandrock, MD, Guest editor, Vol. XV, no.2, Aug 1977, W.B. Saunders Co., Philadelphia, London, Toronto.
5. *The Radiologic Clinics of North America, Symposium on Trauma*, Solomon S. Schwartz, MD, Guest Editor, Vol. XI, no. 3, Dec. 1973, W.B. Saunders Co., Philadelphia, London, Toronto.
6. *Paul and Juhl's Essentials of Radiologic Imaging*, 6th Edit. John H. Juhl, MD; Andrew B. Cunningham, MD, editors, JB Lipponcott Co. Philadelphia.
7. *Normal Radiographic Anatomy*, 2nd Edit. Isadore Meschan, MD, with assistance of R.M.F. Farrer-Meschan, MD, (Melbome), W.B. Saunders Co., Philadelphia.
8. *Handbook of Orthopedic Surgery*, 5th Edit. Alfred R. Shands, Jr., MD, In collaboration with Richard B. Raney, MD, C.V. Mosby Co. St. Louis.
9. *WWW and Internet Sources* are documented in the text.

INDEX

Abdomen, guarding: 60
Abdomen, localizing signs: 53
Abdomen: 53
Acetabulae protrusio: 112
Acetabulum, fracture of: 115,116
Achondroplasia: 108
Acoustic canals: 76,77
Acoustic meatus: 77
Acoustic neuroma: 77,78
Adenopathy, hilar: 39
Adenopathy, mediastinal: 39
Aerophagia: 53
Air bronchogram: 9,10
Air fluid levels, gut: 55
Alveolar pneumonia: 9,10,11
Alveolar: 6
Aneurysm, abdominal aorta: 67
Aneurysm, splenic artery: 67
Aneurysm, thoracic aorta: 44
Ankylosing spondylitis: 104,112
Anteflexion of coccyx: 117
Anterior clinoids: 76
Aorta, coarctation of: 49,50
Aorta, thoracic: 44
Aortic valve prosthesis: 34
Apophysis, fifth metatarsal: 134
Appendicitis: 55
Arc, carpal-metacarpal: 125
Arc, intercarpal: 125
Arc, radial-carpal: 125
Arnold Chiari malformation: 87
Artifacts, odontoid: 98
Arthrokatadysis: 112
Asbestosis: 46
Ascitic fluid: 65
Astragulus: see talus
Atrial enlargement: 30,31
Atrial septal defect: 30
Aunt Minnie, definition: 15
Avascular necrosis, hip: 108,109
Azygous lobe fissure: 16,17
Azygous vein: 38
Bertin, columns of: 62,63

Bochdalek's hernia: 46
Bone metastasis, lytic: 95
Bone metastasis, sclerotic: 95
Bone mineral loss: 93
Bone, trabeculae: 94
Boxer's fracture: 129
Bronchiectasis: 12
Bronchogenic carcinoma: 37
Bronchovascular markings: 7,12
Calcification abdominal aorta: 103
Calcification in aortic aneurysm: 67
Calcification of diaphragm: 46,48
Calcification, mitral valve: 33
Calcification, pancreas: 67,68
Calcification, pericardial: 33
Calcification, skull: 88
Calcified gallstones: 66
Calcified granuloma: 45
Calculus, renal: 66
Capitellum: 123,124
Carcinoma, bronchogenic: 37
Carcinoma, prostate: 94
Carcinoma, renal: 63
Carcinoma, renal: 63
Carcinoma, Thymus: 40
Carcinoma, thyroid metastatic: 83
Cardiac chambers: 28-34
Cardiac coelomic cyst: 35
Cardiac fat pad: 35
Carpal dislocation: 126
Carpal-metacarpal arc: 125
Central ray: 91
Cephalhematoma: 81
Cholecystitis: 56,60
Choroid plexus: 88
Chromophobe adenoma: 76
Chylothorax: 27
Clinoids: 76
Coarctation of aorta: 50
Coccyx: 117
Computed Tomography: 13
COPD: 18-22
Cranial sutures, synostosis of (premature closure): 75
Cranial-facial index: 73-75
Crescent sign: 58,59
Crus of diaphragm: 47
CT ratio: 28
CT: see computed tomography
Cyanotic congenital heart disease: 32
Cyst, Cardiac Coelomic: 35
Cytokines: 84

David Letterman sign: 127
Densities, radiographic: 1
Diaphragm, calcification of: 46
Diaphragm, crus: 47
Diaphragm: 44-46
Disc spaces: 93
Dislocation of lunate: 128
Dislocation of wrist: 126
Diverticulum, esophageal: 45
Dorsum sella: 76
Ebstein's anomaly: 32
Effusion, ankle: 133
Effusion, lobar: 13,14, pleural: 14,15; loculated 26
Elbow, growth centers: 124
Emphysema: 18-22
Emphysematous cholecystitis: 56
Empyema: 26
Encephalocele: 87
Eosinophilic granuloma: 85
Epicondyles, of humerus: 124
Epiglottis: 102
Facets: 91
Falx cerebri: 88
Fascia, Gerota's: 60,61
Fat pad, cardiac: 35
Fat pad, of ankle: 132,133
Fat pads, elbow: 120-122
Fat pads, hips: 110,114
Fecaliths of appendix: 55
Femoral epiphysis: 113
Fibrous dysplasia: 86
Fluoroscopy: 13
Foramina, sacral: 117
Fracture of talus: 136
Fracture of ulnar styloid: 128
Fracture vs. epiphysis, foot: 134-136
Fracture, Boxer's: 129
Fracture, fifth metacarpal: 129
Fracture, fifth metatarsal: 134,135
Fracture, ischial tuberosity: 111,112
Fracture, ischium: 108
Fracture, Monteggia's: 122
Fracture, Sheppard's: 136
Fracture, skull: 81
Fracture, ulna: 122
Fractures, C-1, C-2: 98,99
Fractures, Torus of radius & ulna: 129
Free air: 57,58
Gallstones: 66
Gas pattern: 53-59
Gas, biliary duct: 56

Gerota's fascia: 60,61,65
Granuloma, calcified: 45
Growth centers, elbow: 123,124
Guarding, of abdomen: 60
Hamman-Rich: 12
Hand-Schuller-Christian disease: 85
Haustral markings: 53,54,57
Heart: 28-36
Hemangioma, of vertebrae: 104
Hemorrhage, retroperitoneal: 60
Hernia, Bochdalek: 46
Hernia, diaphragmatic: 46
Hernia, hiatal: 41
Hernia, Morgagni: 46
Hiatal hernia: 41
Hilar adenopathy: 39
Hip, effusion: 115
Hip, fat pads: 110,114
Hip, osteoarthritis: 114
Hip, Paget's disease: 119
Histiocytosis x: 12
Histiocytosis x: 85
HLA-B27 antigen: 112
Honeycomb lung: 11
Horseshoe kidneys: 61
Hydrocephalus: 74,75
Hydropneumothorax: 27
Hyperostosis frontalis interna: 88
Innominate lines, skull: 89
Intercarpal arc: 125
Interlobar effusion: see effusion
Interstices: 6
Interstitial pneumonia: 8,9,10,
Interstitial: 6
Intussuception: 58,59
Ischial spines: 105
Ischial tuberosities: 106,111,112
Jefferson fracture: 99
Kidneys: 53, 61-65
Lacunar skull: 87
Left atrial enlargement 30,31
Legge-Perthe's disease: 110
Leptomeningeal cyst: 86
Letterer-Siwe disease: 85
Leukemia, of bone: 111
Limbus vertebrae: 91
Lobar effusion: 13,14,15
Lordotic curve: 97
Lukenschadel: 87
Lunate dislocation: 128
Lunate: 125,126

Lymphoma: 39
Madelung's deformity: 129
Marfan's syndrome: 112
Marie-Strumpell disease: see ankylosing spondylitis
Mastoids: 80
McBernie's point: 55
Mediastinal adenopathy: 39
Mediastinum compartments: 36
Meningomyelocele: 87
Metastasis, bone 50-52
Metopic suture: 89
Miliary: 11,12
Mitral valve prosthesis: 34
Mitral valve stenosis: 43
Mitral valve: 33
Monteggia's fracture: 122
Morgagni hernia: 46
Mortise joint: 132-134
Multiple myeloma: 84
Myeloma: see multiple myeloma
Navicular, fracture of, wrist: 128
Navicular, wrist: 127
Navicular: 127 also see scaphoid
Neovascularity: 63
Neurofibromatosis: 19
Neuroforamina, encroachment: 96
Neuroforamina, sacral: 117
Neuroforamina: 91,92,95
Nodules, pulmonary: 13,29
Obstructive emphysema: 22,23
Obturator foramen: 106
Odontoid, artifacts: 98
Odontoid, view: 98
Olecronon: 124
Optic chiasm: 76
Orbits: 79
Os ligamentum nuchae: 100
Os trigonum: 136
Osteitis pubis: 116
Osteoarthritis, hip: 114
Osteoclastic response: 84
Osteopenia: 93
Osteoporosis circumscripta: 83
Osteoporosis: 93
Osteosarcoma: 71
Otto pelvis: 112
PACS introduction
Paget's disease, hip: 119
Paget's disease, signs of: 94,119
Paget's disease, skull: 83
Paget's disease, spine: 94

Paranasal sinuses: 79
Pars interarticularis: 92
Pectus Excavatum: 36
Pelvic inlet: 107
Pelvis and hips: 106-118
Perforated viscus: 56-58
Pericardial calcification: 33
Plasmacytoma: 70,107
Pleural based densities: 25,26
Pleural effusion: see effusion
Pneumoconiosis: 12
Pneumoperitoneum: 58
Pneumothorax: 24,25: hydropneumothorax: 27
Posterior clinoids: 76
Preperitoneal fat lines: 53,65
Pseudosubluxation: 96
Pseudotumor: 13
Psoas abscess: 69
Psoas muscles: 53,60
Pulmonary hypertension: 21
Pulmonary nodules: see nodules
Pulmonary stenosis: 32
Radial head, dislocation of: 122
Radial-carpal arc: 125
Radiograph definition of: 1
Reidel's lobe, liver: 64
Reiter's syndrome: 113
Renal calculus: 66
Renal carcinoma: 63
Renal carcinoma: 63
Renal lithiasis: 67
Renal shadows: see kidneys
Reticulonodular: 12
Retroperitoneum: 60
Retropharyngeal mass: 101,102
Rib notching: 49,50
Rib, metastasis: 50, 51
Right ventricular hypertrophy: 32
Sail Sign: 17
Salter-Harris classification of fractures: 131
Sarcoidosis: 12
Scaphoid, fracture of: 128
Scaphoid-lunate dissociation: 127
Schmorl's node: 69,90
Sella turcica: 76
Sentinel loop: 53
Sesmoid, neck: 100
Shenton's lines: 107
Sheppard's fracture: 136
SI joints: 113
Sickle cell anemia: 85

Silhouette sign: 9,14
Silhouetting: 13,14
Silicosis: 12
Sinuses, paranasal: 79
Sinusitis: 79
Skull fracture: 81,82
Skull, basilar structures: 76
Skull, hair-on-end appearance: 85
Skull, lacunar: 87
Skull: 73-89
Slipped femoral capital epiphysis: 113
Spina bifida occulta: 91,100
Spine, anatomy: 92
Spine, scotty dog: 91,92
Spine: 90-105
Spondylolesthesis: 92,93
Spondylolysis: 91
Spondylosis: 95,96
Staghorn calculus: 66,67
Stenosis, mitral valve: 43
Supracondylar process, of humerus: 130
Swischuk's line: 96,97
Symphysis pubis, post partum cysts of: 116
Synostosis, cranial sutures: 75
System, diagnostic, ankle and feet: 132
System, diagnostic, for abdomen: 53
System, diagnostic, for chest: 52
System, diagnostic, for skull: 73,89
System, diagnostic, of elbow: 120
System, diagnostic, of wrist: 125
System, diagnostic, pelvis and hips: 106
System, diagnostic, spine: 90,105
System, diagnostic of ankle: 132
Talus, fracture of: 136
Target sign: 58,59
TE fistula: 42
Tear drop sign: 133
Teleradiology introduction
Teratoma: 38
Terry Thomas sign: 127
Tetrology of Fallot: 32
Thalassemia: 85
Thoracic aorta: 44
Thymus, carcinoma of: 40
Thymus: 17, 40
Thyroid carcinoma, metastatic: 83
Tomography: 13
Torus fractures: 129
Towne's view: 80
Trabecular pattern: 94,95
Trochlea: 123,124

Tuberculosis: 12
Ulna minus deformity: 130
Ulna plus deformity: 129
Ulnar styloid fracture: 128
Ununited apophysis, spine: 91,100
Venous lakes: 81
Ventricular septal defect: 32
Ventriculogram: 74
Vertebrae, anatomy: 92
Vertebrae, posterior arch: 97
Vertebral hemangioma: 104
Von Recklinghausen's disease: 19
Water's view: 79